Chemoenzymatic Synthesis of Heparan Sulfate

Renpeng Liu

A dissertation submitted to the faculty of the University of North Carolina at Chapel Hill in partial fulfillment of the requirements for the degree of Doctor of Philosophy in the Eshelman School of Pharmacy (Medicinal Chemistry and Natural Product)

Chapel Hill
2010

Approved by

Jian Liu, Ph.D.

Qisheng Zhang, Ph.D.

Harold Kohn, Ph.D.

Michael Jarstfer, Ph.D.

Marcey Waters, Ph.D.

ABSTRACT

Renpeng Liu: Chemoenzymatic synthesis of heparan sulfate

(Under the direction of Jian Liu, Ph.D.)

Heparan sulfate (HS) participates in a variety of biological functions and has been exploited for its ability to be utilized as a HS-based drug. Chemical synthesis of HS remains extremely challenging. Previous research has proven the feasibility of using a HS enzyme-based approach to synthesize HS structures with unique biological activities. Our central hypothesis is that all subsequent modifications following *N*-sulfation during HS biosynthesis are governed by the number and position of the GlcNS residue. In this dissertation, a fluorous affinity tag-assisted chemoenzymatic synthesis technique has been developed to build a HS octasaccharide library with defined *N*-sulfo glucosamine (GlcNS) positions. The HS backbone was synthesized by heparosan biosynthetic enzymes. *N*-acetyl glucosaminyl transferase from *E.coli* K5 (KfiA) was used to transfer either GlcNAc or GlcNTFA (*N*-trifluoroacetylglucosamine) residues to the growing chain. Heparosan synthase from *pasteurella* (PmHS2) was used to transfer the GlcUA residues. A selective de-trifluoroacetylation was performed because under these conditions, the GlcNTFA is labile and will be converted to glucosamine ($GlcNH_2$) while the GlcNAc residue remains intact. The resultant $GlcNH_2$ is then converted to a GlcNS residue by *N*-sulfotransferase (NST). *N*-sulfo-6-*O*-sulfo HS backbones with different 6-*O*-sulfation patterns and different sizes were

also prepared. Furthermore, we prepared oligosaccharide capable of binding to antithrombin (AT), which correlates to HS anticoagulant activity. In this study, an AT-binding dodecasaccharide was prepared and its structure was proven. The continuation of this dissertation will allow us to not only investigate enzymatic approaches to synthesize HS-based anticoagulant drugs, but also develop a general method for synthesizing structurally defined HS oligosaccharides that could aid in the discovery of novel HS-based therapeutic agents.

ACKNOWLEDGEMENTS

First and foremost, I would like to thank my advisor, Dr. Jian Liu, for his support, enthusiasm, motivation, and guidance. He has been instrumental in my success as a Ph.D. student and gives me confidence that I will carry with me throughout the rest of my academic career. I would also like to thank the other members of my doctoral committee, Drs. Harold Kohn, Qisheng Zhang, Marcey Waters, and Michael Jarstfer for their constructive advice.

My labmates, especially Dr. Yongmei Xu and Dr. Miao Chen, also deserve my gratitude for always giving me guidance when called upon no matter how trivial the problems were. I wish to extend my thanks to all my other labmates, Dr. Michael Duncan, Dr. Ronald Copeland, Dr. Jinghua Chen, Dr. Ding Xu, Dr. Tanya Burch, Dr. Kai Li, Dr. Juzhen Sheng, Dr. Xianxuan Zhou, Courtney Jones, Sherket Peterson, Elizabeth Pempe, Heather Bethea, Ryan Bullis, Justin Roberts, Lan Yu, Xinan Lu and Truong Quang Pham. They provided hands-on assistance and friendly discussion on my project which made me feel like we are a big family.

Furthermore, I would like to say thank you to Dr. Arlene Bridges for her assistance in MS and LC-MS, Dr. Robert Linhardt for providing me UDP-GlcNTFA in large quantities, Dr. Qian Shi for her assistance in my preparations of fluorous-tagged disaccharides, as well as Dr. Dan Cline and Dr. Ole Hindsgaul for their assistance in solid phase synthesis.

Finally, I wish to thank my wife, Qin Li for her love, support and encouragement

throughout my Ph.D. career. I also thank my parents, Chifu Liu and Tianyu Chang, and my sister, Zhimin Liu for their support in my life, especially during difficult times. My parents-in-law, Yuanjun Li and Meiying Ding also deserve my gratitude for their support during my Ph.D. period. I am truly grateful for everything - thank you.

TABLE OF CONTENTS

LIST OF TABLES

Table

LIST OF FIGURES

Figure

ABBREVIATIONS

2OST	uronosyl 2-O-sulfotransferase
3OST	glycosaminyl 3-O-sulfotransferase
6OST	glycosaminyl 6-O-sulfotranferase
ADP	adenosine diphosphate
AMP	adenosine monophosphate
AnMan	2, 5-anhydromannitol
AST-IV	arylsulfotransferase-IV
AT	antithrombin
ATP	adenosine triphosphate
C_5-epi	glucoronyl C_5-epimerase
calcd	calculated
CS	chondroitin sulfate
DS	dermatan sulfate
ECM	extracellular matrix
equiv.	equivalent
ESI	electrospray mass spectroscopy
FGF(R)	fibroblast growth factor(receptor)
GAG	glycosaminoglycan
Gal	galactose
GalNAc	*N*-acetylated galactosamine
GalTI/II	galactosyltransferase I/II
gB	herpes simplex virus -1 glycoprotein B

gC	herpes simplex virus -1 glycoprotein C
gD	herpes simplex virus -1 glycoprotein D
Glc	glucose
GlcNS	*N*-sulfated glucosamine
$GlcNH_2$	*N*-unsubstituted glucosamine
GlcNAc	*N*-acetylatedglucosamine
GlcNAcTI/II	HS GlcNAc transferase I/II
GlcUA	glucuronic acid
GlcUATI/II	HS glucuronosyltransferase
HA	hyaluronic acid
HIT	heparin induced thrombocytopenia
HCV	hepatitis virus C
HIV	human immunodeficiency virus
HS	heparan sulfate
HSPG	heparan sulfate proteoglycan
HSV	herpes simplex virus
IdoUA	iduronic acid
IdoUA2S	2-*O*-sulfated iduronic acid
KS	keratan sulfate
LB	luria-bertani
MALDI	matrix-assisted laser desorption/ionization
MS	mass spectrometry
NDST	*N*-deacetylase/*N*-sulfotransferase

PAP	3’-phosphoadenosine 5’-phosphate
PAPS	3’-phosphoadenosine 5’-phosphosulfate
PNP	*p*-nitrophenol
PNPS	*p*-nitrophenyl sulfate
PF4	platelet factor 4
ST	sulfotransferase
UDP	uridine diphosphate
UTP	uridine triphosphate
VEGF(R)	vascular endothelial growth factor (receptor)
XT	xylosyltransferase
Xyl	xylose
ΔUA	deoxy-α-L-threo-hex-enopyranosyluronic acid
k	kilo
L	liter(s)
M	moles per liter
m/z	mass to charge ratio (MS)
μ	micro

Chapter I. INTRODUCTION

Section 1. Structure of heparan sulfate

Heparan sulfate (HS) is a highly sulfated polysaccharide that represents a unique class of natural products. Heparin is a special type of HS synthesized within mast cells. It was discovered in 1918 (1) and has been widely used as an anticoagulant drug for decades. HS/heparin consists of 50 to 100 disaccharide units carrying sulfo groups. HS has an average molecular weight of about 30 kDa ranging from 5 to 50 kDa while heparin has an average molecular weight of 12 kDa ranging from 5-40 kDa (2-4). HS/heparin belongs to the glycosaminoglycan family. Depending on the structures of the disaccharide repeating units, glycosaminoglycans are classified as HS, heparin, chondroitin sulfate (CS), dermatan sulfate (DS), keratan sulfate (KS) and hyaluronic acid (HA). HS and heparin consist of highly sulfated repeating disaccharide units of 1→4 linked glucosamine (GlcN) and glucuronic (GlcUA)/iduronic acid (IdoUA) (Figure 1). CS and DS consist of sulfated repeating disaccharide units of 1→3 linked *N*-acetylgalactosamine (GalNAc) and GlcUA/IdoUA, and KS consists of sulfated repeating disaccharide units of 1→3 linked galactose (Gal) and *N*-acetylglucosamine (GlcNAc). HA consists of repeating disaccharide units of 1→3-linked GlcNAc and GlcUA and has no sulfo groups.

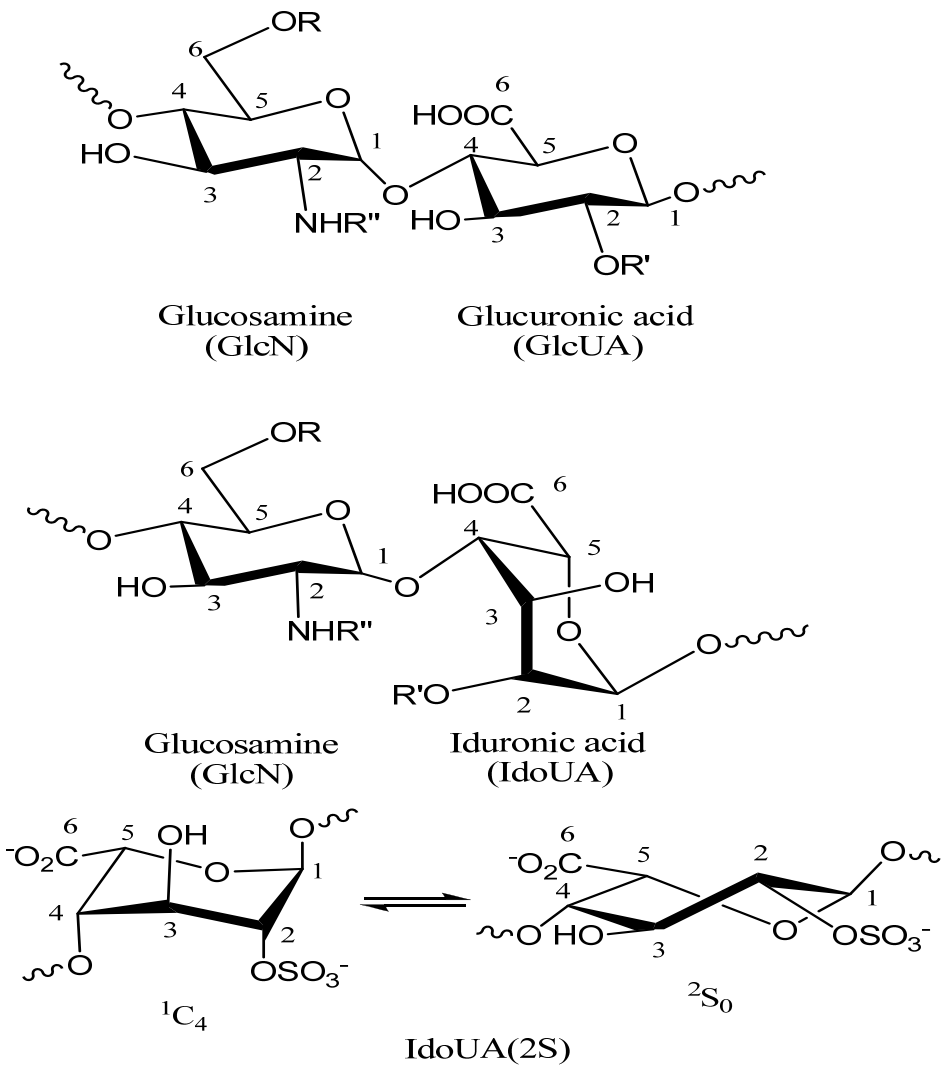

Fig 1. Disaccharide repeating units of HS and heparin. Sulfation (R= -SO_3) at Carbon 6 (known as 6-*O*-sulfated glucosamine, GlcN6S) of glucosamine is common. Sulfation (R'= -SO_3) at Carbon 2 of iduronic acid (known as 2-*O*-sulfated iduronic acid, IdoUA2S) is common. Sulfation at Carbon 3 of glucosamine (known as 3-*O*-sulfated glucosamine, GlcN3S) is rare. Both *N*-acetylated (R''=acetyl, GlcNAc) and *N*-sulfated (R''= -SO_3, GlcNS) are common. *N*-unsubstituted glucosamine (R''= -H, $GlcNH_2$) is a low abundant component. IdoUA (2S) is presented in both $^1C_4$ and $^2S_0$ conformation. Both conformations are presented (13).

HS is widely expressed on the cell surface and within the extracellular matrix on HS proteoglycans (HSPGs, which contain a core protein and polysaccharide side chains). HSPGs are involved in numerous biological processes, including blood coagulation, wound healing, embryonic development, and regulation of tumor growth, as well as assisting viral and bacterial infections (5-13). HS polysaccharides play an essential role in HSPGs functions. The wide ranges of biological functions of HS attract considerable interest in exploiting HS-based anticoagulant, antiviral and anticancer drugs.

The majority of glucosamine residues are either *N*-acetylated (GlcNAc) or *N*-sulfated (GlcNS) (14-16). However, up to 7% of the glucosamine residues in HS are present as *N*-unsubstituted glucosamine ($GlcNH_2$) which may play an important biological role (17). For example, it is known that the $GlcNH_2$ unit is involved in the binding of herpes simplex virus 1's (HSV-1) glycoprotein D (gD) (11, 18). The 6-*O*-sulfo glucosamine (GlcN6S) and 2-*O*-sulfo iduronic acid (IdoUA2S) units are common sulfated monosaccharides, and these units play critical roles in binding to fibroblast growth factors (FGFs), fibroblast growth factor receptors (FGFRs) (19) and platelet factor 4 (PF4) (20). 3-*O*-sulfo glucosamine is a rare component of HS and plays an important role in binding to antithrombin (AT) (3) as well as binding to HSV-1 gD (21). The distribution of different sulfo groups determines the biological function of HS. Although the overall structures of heparin and HS are similar; heparin has a higher content of IdoUA and more sulfo groups per disaccharide unit (3, 4). HS contains 0.6 sulfo groups per disaccharide unit, and 40% uronic acid of HS is iduronic, while heparin contains 2.6 sulfo groups per disaccharide unit and 90% uronic acid of heparin is iduronic (3, 4). In fact, heparin has the most negative charge of all glycosaminoglycans.

Section 2. Biological function of heparan sulfate

Anticoagulant activity

Heparin has remained the main anticoagulant drug on the market since it was introduced in the 1930s (2). The coagulation cascade consists of a series of proteases and their precursors. The anticoagulant action of heparin is due to the activation of the serine protease inhibitor AT. The AT/heparin complex inhibits the activity of factor Xa and thrombin (or named as factor IIa), two key proteases in controlling the blood coagulation cascade (Figure 2). The advantages of heparin as an anticoagulant drug include the following: heparin is the only drug can inhibit both factor Xa and thrombin activities, heparin has a fast anticoagulant response, and excessive anticoagulant activity can be reversed by protamine (3).

Heparin is an exclusive product of mast cells, and is released during degranulation of mast cells. Therefore, HS, rather than heparin, is considered to be the "natural anticoagulant" in humans. Pharmaceutical grade heparin is derived from slaughtered domesticated animal tissues such as the porcine intestines. The purity of heparin heavily depends on the quality of the pig resource (13). It is estimated that 30-40 tons of heparin are prepared each year worldwide from 400 to 700 million pigs (22). The majority is from China.

Heparin's complex structure causes many of the unwanted side effects of heparin, including hemorrhaging and heparin-induced thrombocytopenia (HIT) (23). Furthermore, since heparin supply chain is long, it could be contaminated by human factors. Most recently, a contaminated heparin drug made by Scientific Protein Labs (SPL) caused severe side effects including life-threatening anaphylactic reactions resulting in abnormally low blood pressure, difficultly breathing and occasional vomiting (13, 24). Hundreds of patients

worldwide have suffered the severe reactions linked to this contaminated heparin and this accident has led to 81 deaths. This accident resulted in a major heparin recall in the USA, countries of the European Union and Japan. Oversulfated chondroitin sulfate (OSCS) was identified as the contaminant in heparin (25, 26), and it is believed to have been intensionally added for illegal profits. This tragic event suggested that the heparin supply chain is vulnerable. Thus, a synthetic heparin that can be manufactured in a confined facility remains a high priority. The cofined facility can increase the purity and decrease the chances of contamination.

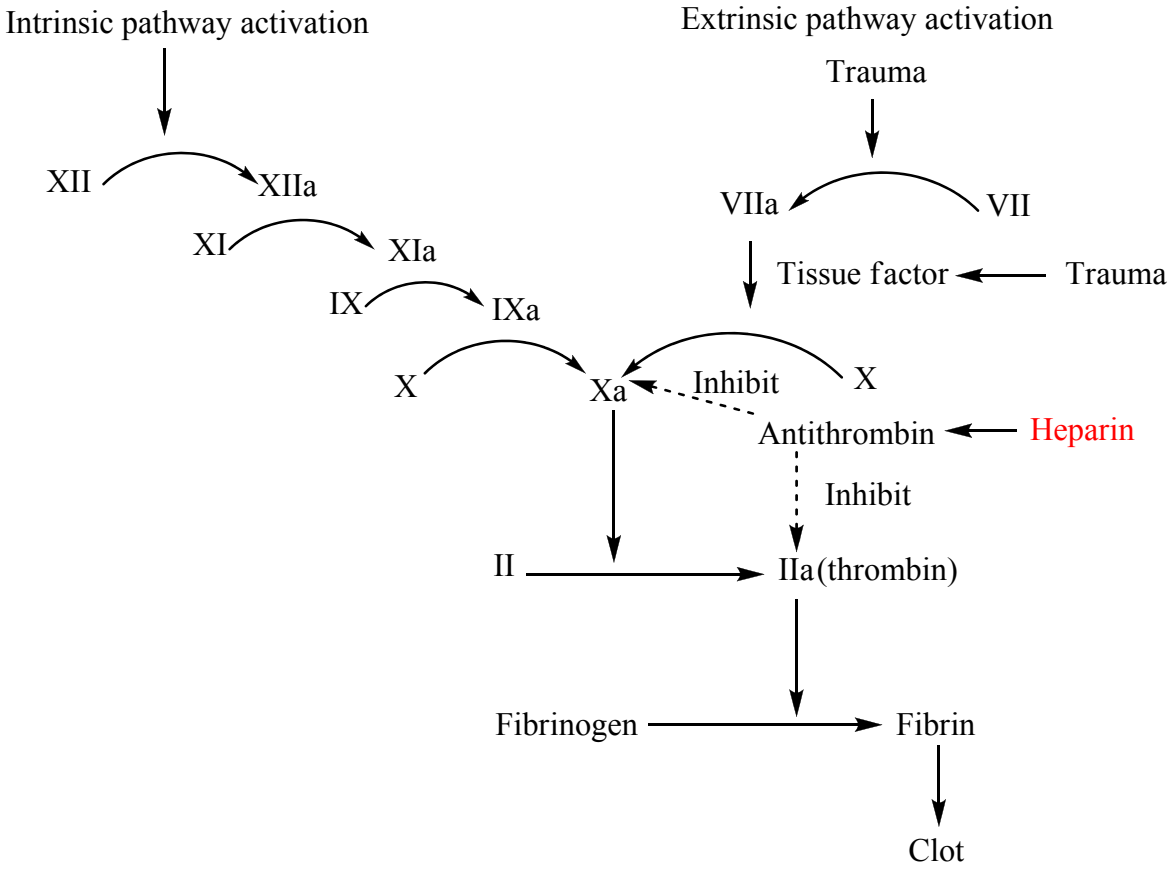

Fig 2. Coagulation cascade. The anticoagulant action of heparin is due to the activation of the serine protease inhibitor antithrombin (AT).

Assisting virus infection

In order to establish an infection, a virus must first make close contact with the host cell. Since HSPGs are widely expressed on the human cell surface, it is not surprising that HS could function as docking and/or receptor sites for different viruses to attach to and/or invade host cell. HSV-1, human immunodeficiency virus (HIV) and hepatitis virus C (HCV) are known to utilize HS to establish the infection (11). Therefore, the mechanism of HS-involvement in viral interaction with host cells has attracted considerable interest from both scientific and pharmaceutical communities.

The involvements of HS in HSV-1 and HIV infections are the most thoroughly studied. HSV-1 is a widespread virus which can cause facial mucocutanous lesions, keratitis, and occasionally, life-threatening encephalitis. The involvement of cell surface HS in HSV-1 infection was discovered in 1989 (27). It is believed that HSV-1 first attaches to target cells through an interaction between its viral envelope glycoprotein C (gC), or in some cases of glycoprotein B (gB) and HS on the surface of host cells (11, 21). Structural analysis of HS involvement in gC binding indicated that a saccharide sequence containing IdoUA2S and GlcNS(or Ac)6S is required for this interaction. Once contact is established, the binding of viral envelope protein gD and the cell surface entry receptors triggers fusion between viral particles and their target cells, permitting the viral particles to penetrate the target cell membrane (21). Studies indicated that the 3-*O*-sulfo glucosamine of HS plays an important role in binding to HSV-1 gD. It is important to note that the 3OST1-modified HS does not bind to gD while 3OST3 and 3OST5-modified HS binds to gD, suggesting that 3-*O*-sulfated HS involved in the HSV-1 infection contains a specific 3-*O*-sulfation pattern (11, 28-30).

Several lines of research revealed that HS may play multiple roles in assisting HIV infection (11). First, it has been known for a long time that HS interacts with HIV envelop's glycoprotein gp120, the key viral protein for cell entry, and that this interaction facilitates the binding of HIV to host cells (31). HS binding to gp120 has been localized on the V3 loop. A V3 loop is a major epitope of gp120 which carriess variable positive charges. Although the V3 loop is not involved in the initial gp120-CD4 binding, it plays an essential role in subsequent steps that lead to membrane fusion for viral entry (4, 32 and 33). Recent studies showed other domains, including the cryptic and CD4-induced coreceptor binding surface, contribute to gp120-HS binding (34). Structural selectivity studies of heparin involved in the binding of gp120 and CD4 have been carried out. These studies showed *O*-sulfation, especially 6-*O*-sulfation, and *N*-substitution (*N*-sulfation or acetylation) are both essential for binding. Also, the minimum size of gp-120 binding heparin is a decasaccharide (4, 35). In addition to the role of facilitating initial binding of HIV to the target cell, HS promotes the spreading of HIV. A recent study shows HIV relies on HS to attach to the surface of sperm and these HIV viruses are transmitted to physiological target cells of HIV, such as dendritic cells, T cells and macrophages (36). Finally, HS facilitates the internalization of HIV transactivator protein, Tat, an etiologic agent of AIDS. Tat is released from HIV infected cells, and internalized Tat causes damage to the cells and tissues (11, 37-39). It is found that Tat binds to heparin or HS, and minimum size of the Tat binding domain is a hexasaccharide. The binding affinity increases with increasing oligosaccharide size, and about eighteen saccharide residues are required to match the full affinity of heparin (4, 11 and 40). Therefore, HS and heparin could be a potential multi-target agent in the therapy and prevention of HIV infection.

Stimulating cell proliferation

The FGFs are a family of growth factors involved in angiogenesis, wound healing, and embryonic development (4, 19). A total of 22 different isoforms of FGF have been reported (41). FGFs are key players in proliferation and differentiation of a wide variety of cells and tissues. The FGF signaling pathway is initiated by the binding of FGF to its receptor on the cell surface, triggering the dimerization of FGFR and downstream phosphorylation/activation of enzymes (42). It is well known that FGFs are heparin-binding proteins and interactions with cell-surface associated HS proteoglycans have been shown to be essential for FGF signal transduction. The FGF, FGFR and HS interaction has been elucidated by crystal structures. The crystal structure of a dimeric ternary complex of 2:2:2 FGF-2, a heparin decasaccharide and FGFR-1 demonstrated that heparin makes contact with both FGF-2 and FGFR-1 in each FGF-FGFR complex to stabilize FGF-FGFR binding. The FGFR-1 of the adjacent FGF-FGFR complex also makes contact with heparin to promote FGFR dimerization (4, 43). In contrast, the crystal structure of a complex of 2:2:1 FGF-1, FGFR-2 and a heparin decasacchride indicated a different dimerization pattern. In this complex, the heparin molecule links to two FGF-1 ligands into a dimer. The 2:1 FGF-1 heparin complex acts as a bridge between the two FGFR-2 ligands (4, 44).

Inflammation

Inflammation is a complex biological process in response of vascular tissues reaction to harmful stimuli such as irritants, pathogen infection and tissue injury. Inflammation is a protective attempt by the organism to remove injurious substances as well as initiate the

healing process for the tissue. Inflammation is a multi-step process involving chemokine generation at the infected tissue (45). Chemokines are a group of small proteins with a variety of biological functions including selective recruitment and activation of cells during inflammation. Chemokines migrate into the luminal side of the endothelial cells and bind to leukocytes within the blood vessel. This leukocyte-chemokine interaction triggers leukocyte extravasation and migration towards the infected tissue. The roles of heparin and HS involved in regulating inflammatory responses have been noticed recently (46). It has been shown that chemokines are heparin binding proteins (47); the HS and chemokine interactions have been determined to be essential for the presence of chemokines on the luminal surface of endothelial cells (47). HS also binds to cell adhesion molecules (such as L- and P-selectins), as well as, growth factors and growth factor receptors to regulate leukocyte migration through the blood vessel wall (48, 49). Although the mechanism is not fully understood, it is generally accepted that the sulfation patterns of HS direct the interactions of L-selectin and chemokines (50, 51). For example, the heparin carrying 6-*O*-sulfo groups exhibit anti-inflammatory effects by blocking the binding of HS and L- and P-selectins (52). Therefore, developing HS-based anti-inflammatory agents attracts a lot of interest.

Tumor growth, metastasis and heparanase

Clinical studies have clearly demonstrated the benefits of treating cancer patients with heparin, especially LMW heparin. Tumor cells release procoagulant molecules to activate factors X and VII. The interaction between immune and malignant cells activates platelets, factor XII, and factor X, leading to thrombin production and thrombosis. Thus, the anticoagulant properties of heparin are useful against thrombosis in cancer (22). Clinical

studies also indicate that heparin's antiangiogenic and antimetastatic properties may also contribute to its anticancer activity. For example, studies have found that the administration of LMW heparin has improved the survival rate of the patients with small cell lung cancer from 29.5% to 51.3%, while another commonly used anticoagulant drug, warfarin, did not exhibit the anticancer activity (22, 53 and 54). However, clinical evidence for heparin use as an antimetastatic and antiangiogenesis agent is not conclusive and anticoagulant side effect limits the anticancer application of HS (55).

Heparanase is an endo-β-D glucuronidase that cleaves HS into fragments ranging from 10 to 20 saccharide units (56-59) (Figure 3). Heparanase is highly conserved and so far only a single form has been found. Heparanase is involved in several physiological and pathological processes, such as wound healing, embryonic development and HS cleavage. Heparanase is attributed to cancer by two aspects: firstly, heparanase degrades the HS in the extracellular matrix, facilitating cell invasion and metastasis; secondly, by degrading HS, heparanase is involved in stimulating angiogenesis through the release of HS-bound growth factors such as vascular endothelial growth factor (VEGF) and FGFs. Therefore, the role of heparanase in tumorigenesis makes it an attractive anti-cancer target (60). Progen Pharmaceuticals has developed phosphomannopentose sulfate (PI-88), a mixture of highly sulfated monophosphorylated mannose oligosaccharides to inhibit heparanase activity (Figure 3). PI-88 also competes with HS for binding to growth factors such as FGF-1 and FGF-2, consequently reducing their ability to stimulate tumor angiogenesis. Unfortunately, although phase II studies of PI-88 in patients with numerous cancers showed promising results, Progen Pharmaceuticals recently terminated the phase III trial of PI-88 for several

reasons such as modest results to treat malignancies, lack of a global distributor, and its immune-mediated thrombocytopenia (22, 61).

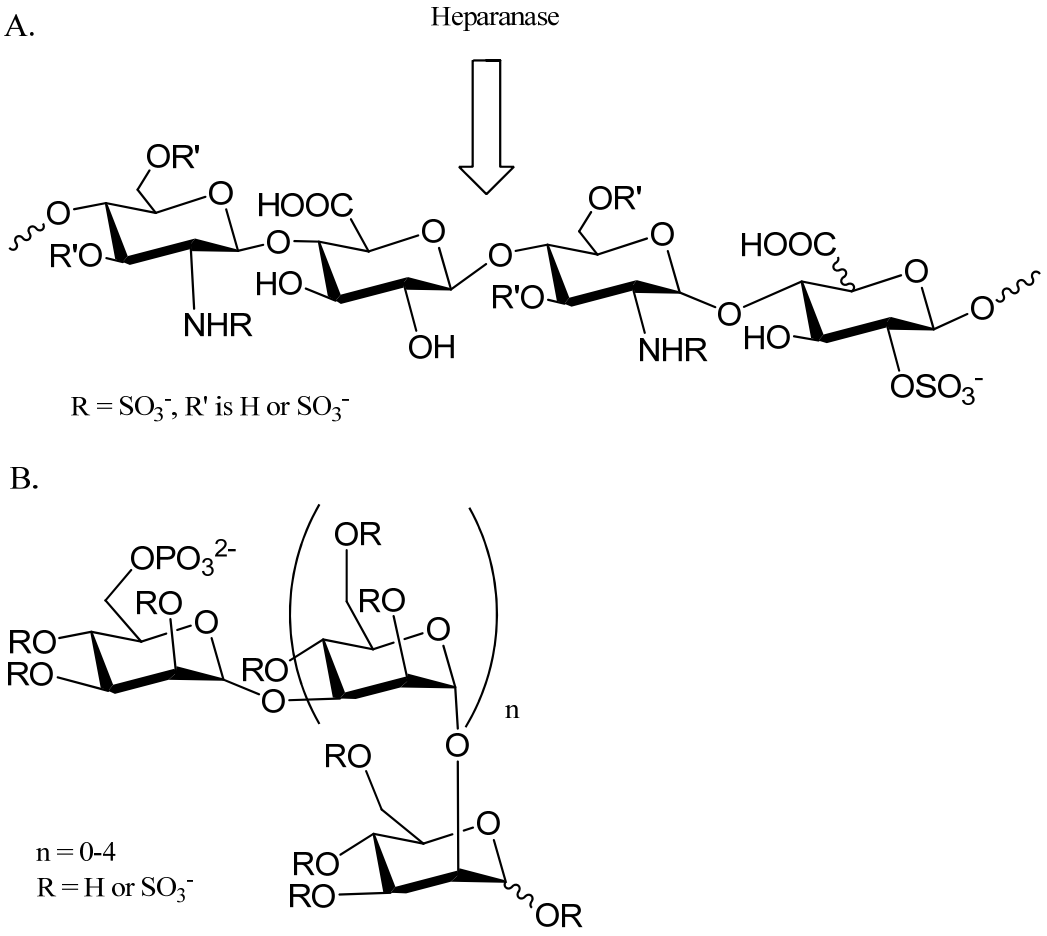

Fig 3. Substrate specificity and inhibitor for heparanase. Panel **A** is the substrate specificity of heparanase. Panel **B** is the Structure of PI-88, the inhibitor of heparanase.

Although the molecular mechanism for the linking cancer and HS is not fully understood, it is suspected that the saccharide structures exhibiting anticancer activity are different from those carrying anticoagulant activity as determined in a mice model (62).

Because the anticoagulant properties of HS/heparin could limit dosing for its anticancer purposes, synthesis of non-anticoagulant HS with antiangiogenic and antimetastatic properties attracts considerable interest in exploiting HS or HS-like molecules for the development of anticancer drugs.

PF4 and thrombocytopenia

PF4, a polypeptide with 70 amino acids, belongs to the chemokine family (4). PF4 is released from platelets and is believed to associate with inflammation and wound healing which is a result of its ability to neutralize the activity of heparin and HS (4). However, when heparin binds to PF4, it can induce heparin-induced thrombocytopenia (HIT), a serious side effect of heparin. HIT occurs in approximately 3% of patients receiving unfractionated heparin and about 0.2% in those patients receiving low molecular weight heparin (63). HIT is an immunologically induced loss of platelets. In HIT, the immune system forms antibodies against heparin when heparin is bound to PF4. The antibodies form a complex with heparin and PF4 in the bloodstream. The tail of the antibody then binds to the FcγIIa receptor, a protein on the surface of the platelet. This results in platelet activation and the formation of platelet microparticles, which initiate the formation of blood clots; the platelet count falls as a result of this clotting (64, 65). It is believed that PF4 recognizes a long sulfated domain in HS and the IdoUA2S residue in HS has been identified to be important for binding to PF4 (4, 66 and 67). The optimal size of oligosaccharide needed to form a complex with PF4 is about a hexadecasaccharide, although the minimal size for PF4 binding is an octasaccharide for heparin (4, 68-70). Furthermore, the interaction of the heparin analogues with PF4 is facilitated by a higher degree of sulfation and a more flexible

conformation on the backbone of heparin (4, 68). Based on this observation, it is viable to design anticoagulant heparin derived oligosaccharides without binding to PF4. For example, Petitou and colleagues have successfully synthesized anticoagulant oligosaccharide without binding to PF4 (71).

Section 3. Structure and activity relationship of HS

AT-binding domain

Only a fraction of HS binds to AT and exhibits anticoagulant activity. About 1-10% of HS binds to AT while about 30% of heparin binds to AT, suggesting that AT recognizes a special sequence of HS (3). Studies have revealed that the anticoagulant drug heparin and HS contain a structurally defined AT-binding pentasaccharide sequence with the structure of –GlcNS (or Ac) 6S-GlcUA-GlcNS3S6S-IdoUA2S-GlcNS6S- (72-74) (Figure 4). The AT-binding site is the essential motif for the anticoagulant activity of heparin and HS. Binding to this pentasaccharide unit will trigger a conformational change of AT and accelerate the inhibition of factor Xa. However, the pentasaccharide unit only inhibits the activity of factor Xa. The structural requirements needed for HS binding to AT were proven via chemically synthesized pentasaccharides with various combinations of sulfo groups and carboxyl groups. The 3-*O*-sulfation of a glucosamine residue (3-*O*-sulfation is circled) is the critical modification to generate the AT binding site. Removal of 3-*O*-sulfo group decreased the binding affinity to AT by nearly 20, 000 fold (3).

A larger oligosaccharide is required to inhibit both anti-Xa and anti-thrombin activity. The oligosaccharide consists of an AT-binding domain, a linker region and a thrombin-

binding domain. Heparin/HS acts as a template to facilitate the AT-mediated inhibition of thrombin. Petitou *et al* proved that the order of the three domains is essential for thrombin inhibition, namely, the AT-binding domain must be positioned at the reducing end of the linker region and the thrombin-binding domain must be located at the nonreducing end of the linker region. The linker region forms a bridge that has no interaction with either of the proteins. Compare to the AT-binding domain, the interaction of thrombin and the thrombin-binding domain is less specific. The minimum size to inhibit both factor Xa and thrombin is found to be a pentadeca-saccharide (71).

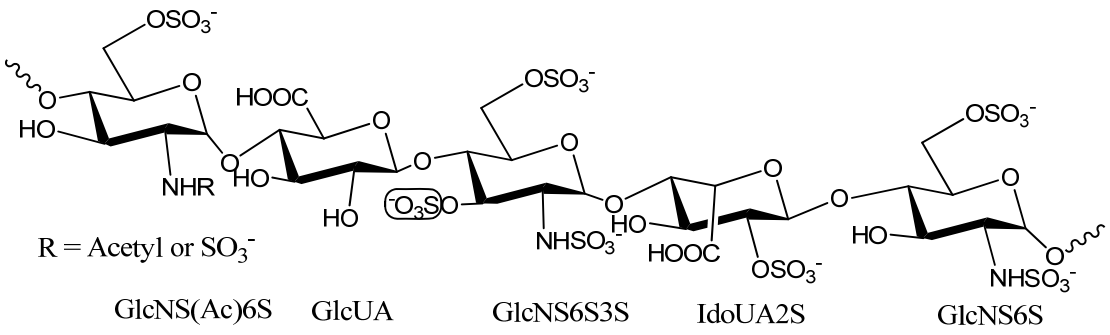

Fig 4. The structure of the AT-binding pentasaccharide. The 3-*O*-sulfation of the glucosamine residue (3-*O*-sulfo group is circled) is the critical modification to generate the AT binding site. GlcNS(Ac)6S, GlcUA, GlcNS3S6S, IdoUA2S and GlcNS6S represent the abbreviation of the individual monosaccharide residues.

HSV-1 gD binding domain

The minimum size of HS that will bind to gD is found to be an octasaccharide (18, 21). An octasaccharide binding to gD was isolated from a 3OST3-modified octasaccharide library with a binding affinity of 18 μM. Based on mass spectrometry, the isolated

octasaccharide was determined to be ΔUA-GlcNS-IdoUA2S-GlcNAc-GlcUA2S (or IdoUA2S)-GlcNS-IdoUA2S-GlcN3S6S (ΔUA is deoxy-α-L-threo-hex-enopyranosyluronic acid) (Figure 5). It is very interesting to find that a rare $GlcNH_2$ unit is involved in the binding of HSV-1 (gD), and that the binding octasaccharide contains an unique GlcN3S6S linked to a IdoUA2S at the non-reducing end (18).

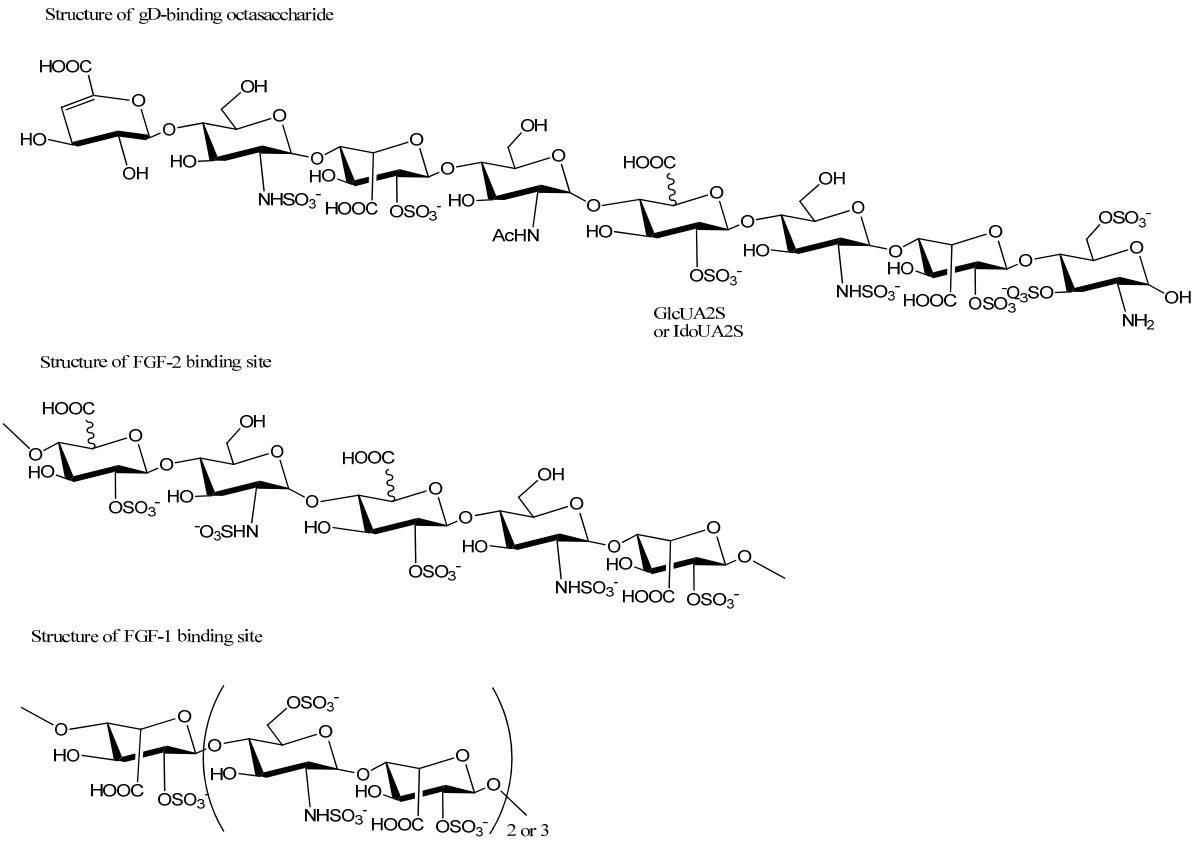

Fig 5. Chemical structures of gD, FGF-2 and FGF-1 binding sites.

FGF binding domain

HS had been shown to enhance the formation of FGF-FGFR complexes and stabilize FGFR oligomers. The most well studied FGFs are FGF-1 and FGF-2. Studies revealed that the minimal heparin structure binding to FGF-2 is a pentasaccharide of –UA-GlcNS-UA-GlcNS-IdoUA2S-, while the HS sequence binding to FGF-1 is 5-7 monosaccharide units and contains a critical trisulfated disaccharide unit with the sequence IdoUA2S-GlcNS6S. It is interesting to find that 6-*O*-sulfation is only necessary for FGF-1 binding (4, 22) (Figure 5). The studies for HS binding to FGFR indicate that FGFR contains a binding site interacting with GlcNS6S. Based on the crystal structure of FGF, FGFR and the heparin decasaccharide and biochemical studies, the active HS fragment must be at least a decasaccharide in order to trigger the dimerization of FGFR and initiate downstream cell signaling (4, 41-44).

Section 4. Biosynthesis of HS

Heparin and HS share the same biosynthetic pathway. Understanding the biosynthetic mechanism of HS provides a tool for altering the synthesis of HS in the cells, and helps to delineate the contribution of HS in a specific biological process. Consequently, the results can be employed to improve the pharmacological drug properties of anticoagulant heparin and aid in the development of HS/heparin-based therapeutic agents with anticancer and antiviral activities. It should be noted that unlike proteins and nucleic acids, the synthesis of polysaccharides does not have a template; the specific saccharide sequences are governed by the expression level of HS biosynthetic enzymes (8, 13). The biosynthesis of HS is accomplished by a complex pathway involving backbone elongation and multiple modification steps (Figure 6). HS biosynthesis takes place in the lumen of the Golgi

apparatus, although the core protein is synthesized in the endoplasmic reticulum (ER). The biosynthesis of HS is initiated as a copolymer of GlcUA and GlcNAc, which is catalyzed by copolymerases (EXT1 and EXT2) (7). The backbone is then modified by a C_5-epimerase (C_5-epi) and different sulfotransferases. The first modification is *N*-deacetylation/*N*-sulfation to form GlcNS by *N*-deacetylase/*N*-sulfotransferase (NDST). NDST is a dual function enzyme that catalyzes the removal of the acetyl group from a GlcNAc residue and the transfer of a sulfo group to form a GlcNS residue. NDST has four different isoforms (75). After the *N*-sulfated backbone is generated, C_5-epi converts the neighboring GlcUA unit on the reducing side to an IdoUA unit. The chain modification proceeds with 2-*O*-sulfation of IdoUA/GlcUA (with a preference to IdoUA), 6-*O*-sulfation of glucosamine, and 3-*O*-sulfation of glucosamine by different *O*-sulfotransferases (OSTs). C_5-epi and 2-*O*-sulfotransferase (2OST) only have one isoform, while 6-*O*-sulfotransferase (6OST) has three (76) and 3-*O*-sulfotransferase (3OST) has seven isoforms (3, 13).

Chain initiation

The biosynthesis of HS is initiated by the formation of a tetrasaccharide which links to the core protein: GlcUAβ1-3Galβ1-3Galβ1-4Xylβ-*O*-Ser. This tetrasaccharide also serves as the linkage for the biosynthesis of CS (14) (Figure 7). The formation of this tetrasaccharide linkage unit is catalyzed by the sequential actions of four glycotransferases: xylotransferase (XT), galactosyltransferase I (GalTI), galactosyltransferase II (GalTII) and glucuronosyltransferase I (GlcUATI). XT is the first enzyme to intiate the synthesis of the linkage tetrasaccharide at a specific serine residue of the core protein (77). Although the mechanism by which XT recognizes the substrate core proteins and selects the Ser residue is

still unclear, a Ser-Gly repeating dipeptide seems to be the minimum structural requirement for the xylosylation to occur, and a Glu or Asp residue of the core protein is often present in the vicinity of the Ser-Gly sequence (78). Once the xylose is transferred to the core protein, two galactosyltransferases, GalTI and GalTII, transfer two galactoses onto xylose to form Galβ1-3Galβ1-4Xylβ1-*O*-Ser (79, 80). The last enzyme GlcUATI transfers a GlcUA molecule to the existing glycan chain to form GlcUAβ1-3Galβ1-3Galβ1-4Xylβ1-*O*-Ser (14).

Chain polymerization

The tetrasaccharide linkage to the core protein is the common precursor for the biosynthesis of both HS and CS polysaccharide chains. The critical step that differentiates polymerization of HS from that of CS is the addition of a GlcNAcα1-unit instead of the GalNAcβ1-unit to the nonreducing end of the tetrasaccharide. The enzyme HS GlcNAc transferase II (GlcNAcTII) adds GlcNAc to the growing HS chain (81). Once the GlcNAc unit is coupled to the linkage tetrasaccharide, polymerization for HS synthesis is committed by adding GlcUA and GlcNAc alternatively. The enzymes encoded by the members of the Exostosin genes, EXT1 and EXT2; carry out the polymerization of the HS backbone (Figure 7). EXT1 and EXT2 function as a hetero-oligomeric complex, exhibiting both GlcNAC transferase and GlcUA transferase activities (82, 83). The complete loss of both EXT genes is embryonic lethal due to the shorter HS chain links to the core protein in EXT knockout mice. Partial loss in either isoform leads to bone exostosis, a genetically heterogeneous human disease characterized by bony outgrowths near the ends of the long bones (22, 84 and 85).

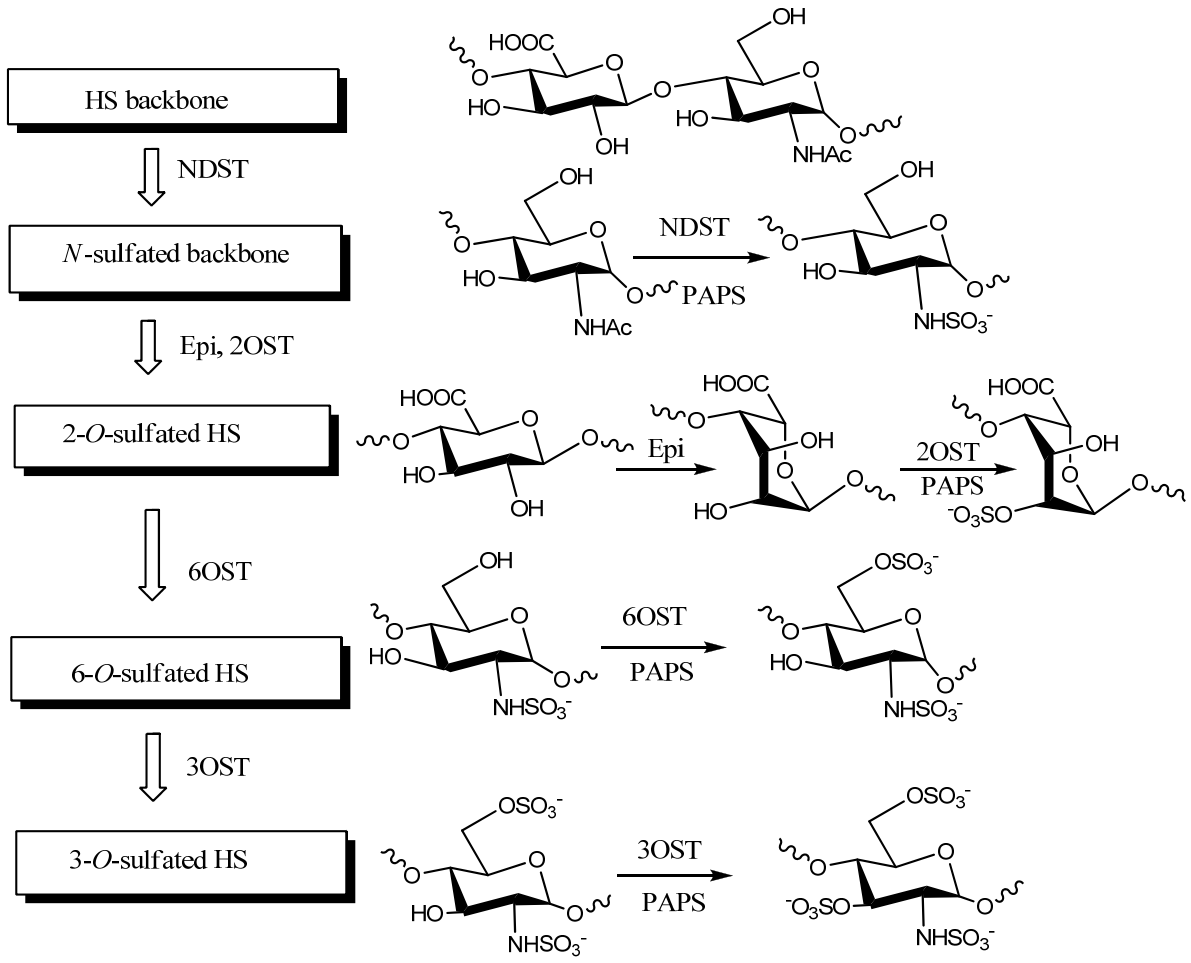

Fig 6. HS biosynthetic pathway. Synthesis is initiated with a copolymer of GlcUA and GlcNAc by HS copolymerases (EXT1 and EXT2). The first modification is to form the *N*-sulfo glucosamine unit (GlcNS) by *N*-deacetylase/*N*-sulfotransferase (NDST). The C_5-epimerase then converts the neighboring GlcUA on the reducing side to an IdoUA unit. Chain modification proceeds with 2-*O*-sulfation at iduronic acid (or to a lesser extent at a GlcUA), 6-*O*-sulfation at glucosamine, and 3-*O*-sulfation at glucosamine by different *O*- sulfotransferases. The reactions involved in polymer elongation are not shown (13). PAPS is the natural sulfo donor.

NDST

The synthesis of GlcNS by NDST is the very first step of a series of modifications of the backbones. NDST has four different isoforms which determine the *N*-sulfation pattern of the HS backbone. It is hypothesized that GlcNS's pattern affects the location of downstream

O-sulfation and epimerization, which consequently dectates the biological function of HS (86-88). Results from cell-based assays demonstrated that the cells that lack of NDST1 or NDST4 synthesize low sulfated HS (89). Targeted gene knockouts of NDSTs also revealed the physiological significance of GlcNS in the biosynthesis of HS. For example, mice deficient in NDST1 displayed dramatically reduced amounts of sulfated HS, and died shortly after birth (90). Studies of the conditional knockout of the NDST1 gene revealed that GlcNS is essential for synthesizing the HS that regulates L-selectin- and chemokine-mediated neutrophil trafficking (91). NDST2 null mice are viable but lack heparin synthesis in mast cells (92). NDST3 null mice are fertile and exhibit only minor hematological and behavioral phenotypes (93). The distinct phenotypes of different NDST knockout mice strongly suggest that unique GlcNS distribution directs the synthesis of HS with specific physiological functions.

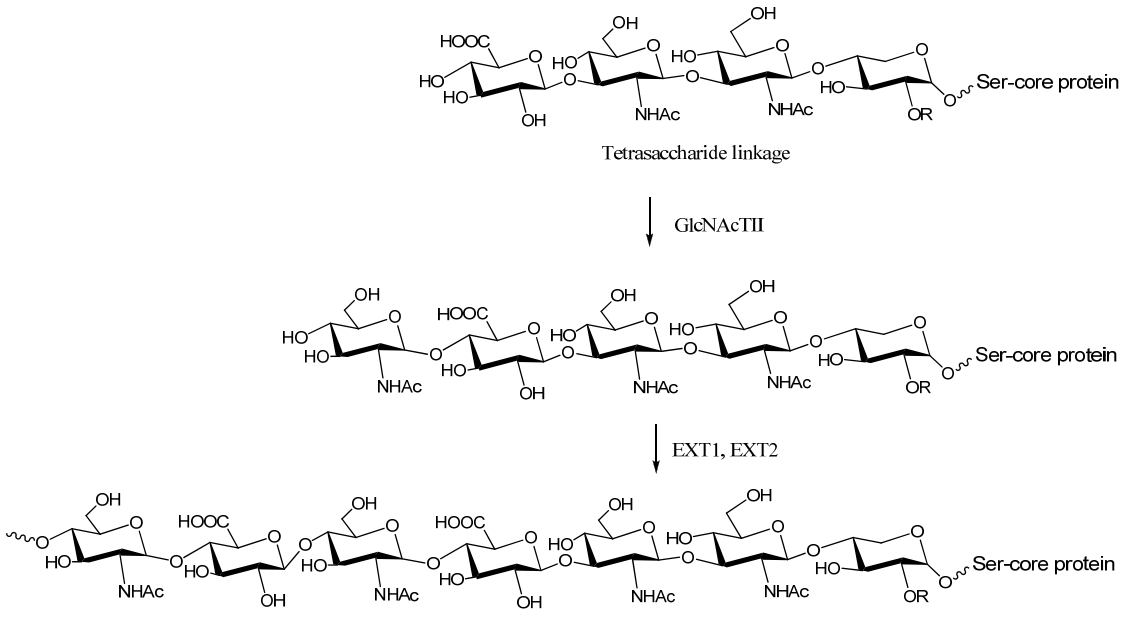

Fig 7. The HS chain initiation and elongation.

C_5-epimerase

The first modification of GlcUA residue is catalyzed by HS C_5-epi, which converts the configuration of the proton at the C_5 position, thus, generating an IdoUA unit (94) (Figure 8). Another possible mechanism is the generation of an enol-intermediate rather than a carbanion intermediate; however, there is no literature report to support this notion. C_5-epi has only one isoform in almost all species examined (14). A GlcNS unit is required at the non-reducing end of the GlcUA for the action of C_5-epi, suggesting the C_5-epimerization rigorously follows *N*-sulfation. IdoUA has been suggested to give HS a more flexible structure. In addition, IdoUA is a much more favorable substrate for HS 2OST (95-97), and the resultant IdoUA2S plays an essential tole for HS biological functions. HS isolated from C_5-epi null mice lacked IdoUA and the predominant sulfated disaccharide is GlcUA-GlcNS6S. The lack of C_5-epi is also lethal to mice due to an immature lung phenotype, abundant skeletal abnormalities, and kidney agenesis (98).

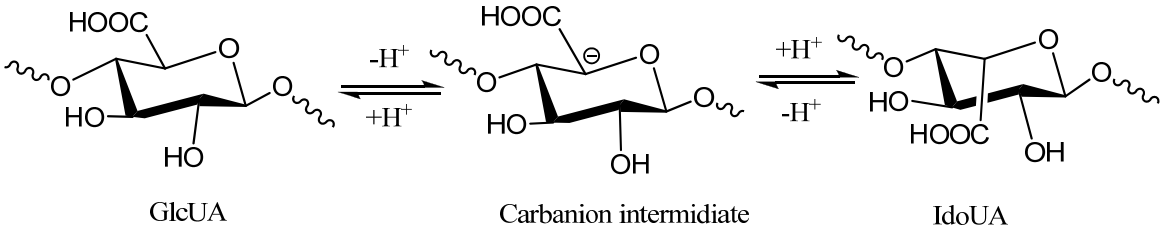

Fig 8. Proposed mechanism of C_5-epimerase.

2OST

2OST transfers a sulfo group to the 2-OH position of IdoUA or GlcUA (with a preference to IdoUA) within HS and 2-*O*-sulfation is the only sulfation that occurs on the uronic acid units. Just as C_5-epi has only one isoform, so does 2OST in most species which forms a complex with C_5-epi *in vivo* (99). The sequence of 2OST is highly conserved across species. Human 2OST shares 97% sequence identity with mouse and 92% identity with chicken (100). It is interesting to note that the phenotypes displayed by 2OST knockout mice are similar to those observed in C_5-epi null mice. However, in contrast to C_5-epi null mice, the loss of 2-*O*-sulfation in mutants is compensated by a 13% increase in 6S and a 9% increase in NS (101, 102). Moreover, unlike C_5-epi-null mice, 2OST knockout mice survive until birth, but die soon after due to kidney agenesis (103). Similar to C_5-epi, GlcNS at the non-reducing end of the acceptor residue significantly enhances the susceptibility of IdoUA or GlcUA to 2OST modification.

6OST

HS 6OST catalyzes the transfer of a sulfo group to the C6 position of glucosamine residue (GlcN) to form 6-*O*-sulfo glucosamine. 6-*O*-sulfation occurs predominantly at the GlcNS residue, generating a GlcNS6S moiety. However, in some cases, it can also occur at the GlcNAc residue, generating a GlcNAc6S moiety; 6-*O*-sulfation is the only type of sulfation that occurs at the GlcNAc residue (104). Three isoforms of 6OST have been identified with approximately 50% similarity (104). The 6-*O*-sulfation by 6OST1 predominantly occurs at the GlcNS residues, while other 6OST isoforms can modifiy

GlcNAc to yield GlcNAc6S. Furthermore, 6OST1 prefers the IdoUA-GlcNS over GlcUA-GlcNS while 6OST2 favors GlcUA-GlcNS more than IdoUA-GlcNS. 6OST3 has almost equal activities towards both disaccharide structures (105) (Figure 9). 6OST1 null mice had growth retardation, aberrant eye and lung morphogenesis, and impaired placenta function and died at or soon after birth (106). More studies are necessary to dissect the individual roles of 6OST isoforms as well as substrate specificity.

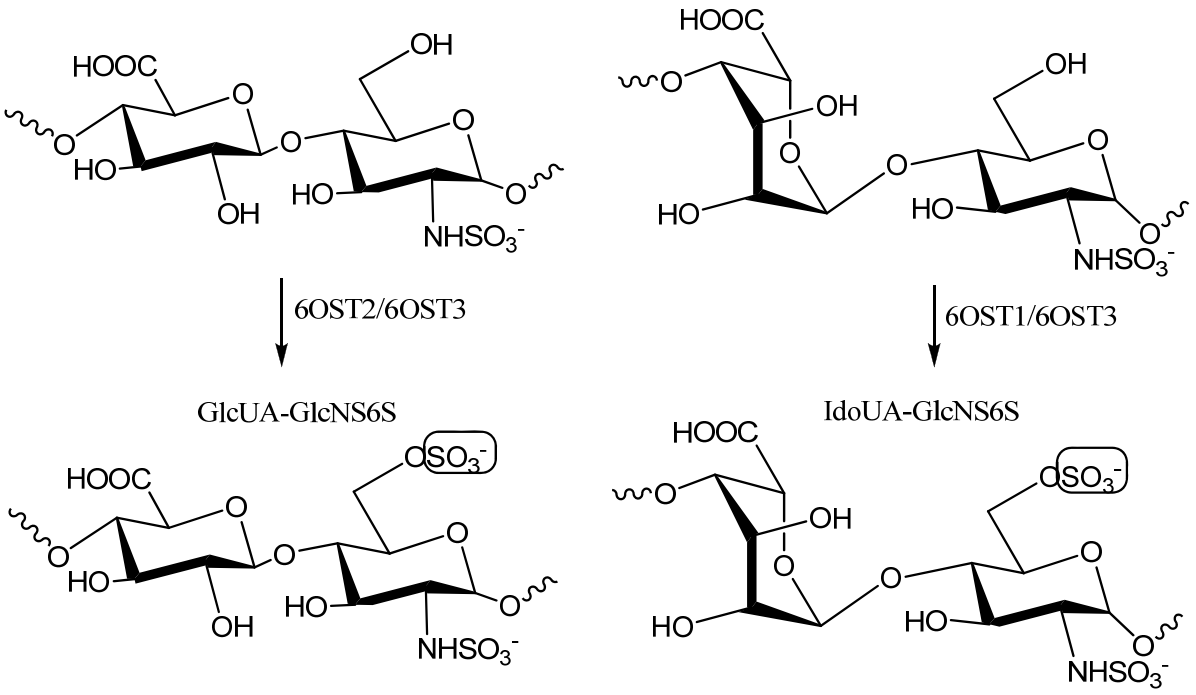

Fig 9. Substrate specificity of 6OSTs. The 6-*O*-sulfation is circled.

3OST

3OST represents the most extended gene family among all HS sulfotransferases. HS 3OST is present in seven isoforms, including 3OST1, 2, 3A, 3B, 4, 5 and 6. Since 3OST3A

and 3OST3B have almost identical amino acid sequence in the sulfotransferase domain, 3OST3 represents both enzymes (3). 3OSTs transfer a sulfo group to the 3-OH position of a GlcN residue. Each isoform of 3OST transfers the sulfo group to the GlcN residue that is linked at the non-reducing end. This modification falls into three types: First, 3OST1 transfers a sulfo group to the glucosamine unit that is adjacent to an unsulfated glucuronic acid. Second, 3OST3 transfers a sulfo group to the glucosamine unit that is adjacent to a 2-*O*-sulfated iduronic acid. Third, 3OST5 has both 3OST1 and 3OST3-like activity. In other word, 3OST5 can transfer a sulfo group to the glucosamine unit that is adjacent to GlcUA, IdoUA and IdoUA2S (3) (Figure 10). As mentioned previously, 3OST1-modified HS binds to AT and regulates the blood coagulation cascade. 3OST3 modified HS is bound by HSV-1 gD, serving as an entry receptor for the virus. HS modified by 3OST5 endows both anticoagulant activity and the ability to promote HSV-1 entry (107-110). Among seven isoforms of 3OST, only 3OST1 has been knocked out in mice; however, 3OST1 null mice do not exhibit any procoagulant phenotype (111). These results can be explained by the fact that other isoforms of 3OST, such as 3OST5, may take place of 3OST1 to synthesize a low level of anticoagulant HS.

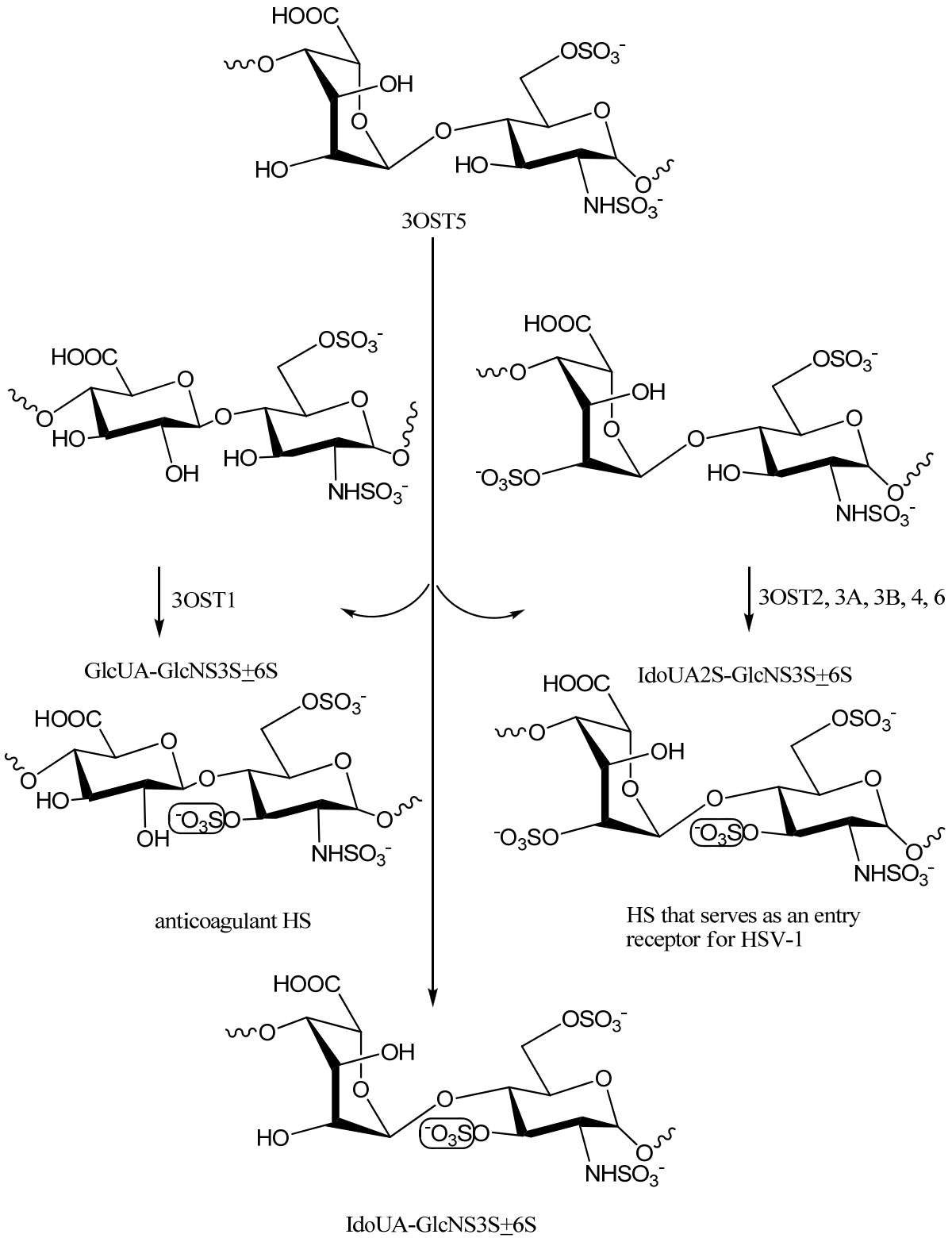

Fig 10. Substrate specificity of 3OSTs. The 3-*O*-sulfation is circled.

Substrate recognition of 2OST and 3OSTs

Understanding the substrate recognition mechanism is essential to advance the enzymatic synthesis and elucidate the biosynthetic mechanism of HS. Recently, our lab, in collaboration with Dr. Lars Pedersen, solved the crystal structure of chicken 2OST (D69–N356) at the resolution of 2.65 Å, in complex with 3′-phosphoadenosine 5′-phosphate (PAP). The crystal structure of 2OST has distinct differences from other existing HS sulfotransferases structures, although their global structure is similar (100). The most distinct structural difference between 2OST and the other HS sulfotransferases is that 2OST appears to function as a trimer. Mutational analysis helped identify amino acid residues that are responsible for substrate specificity. Our lab found that the mutant R189A only transferred sulfates to GlcUA moieties within the polysaccharide while mutants Y94A and H106A preferentially transferred sulfates to IdoUA units. Our results demonstrate the feasibility for modifying the substrate specificity of 2OST to synthesize HS with a specified sulfation pattern carrying unique biological functions (100).

Similar to 2OST, our lab used crystal structures to guide our mechanism of action study for 3OSTs. Our lab, in collaboration with Dr. Lars Pedersen, solved the crystal structure of 3OST1 and 3OST5 with PAP at the resolution of 2.5 Å and 2.3 Å, respectively. A ternary complex of 3OST3/PAP/tetrasaccharide substrate was also solved at the resolution of 1.9 Å (108-110). The overall structures of 3OST1, 3 and 5 are very similar. Based on crystal structures, sulfotransferases were engineered to create more homogenous or novel HS. However, our initial efforts at the mutating the catalytic site failed; these mutants have no catalytic activities, suggesting that these residues are essential for catalytic function. By comparing the substrate binding clefts of 3OSTs, it is noted that two residues (Glu88 and

His271) in 3OST1 appear to form a 'gate' across the end of the substrate binding cleft, which is 6.7 Å in distance. In contrast, in 3OST3 and 3OST5, the distance of the corresponding 'gate' is 14.2 Å. Narrowing the gate by mutating S120 and A306 of 3OST5 to S120 E, A306H enhanced the AT-binding activity of the HS product, transforming 3OST5 toward 3OST-1like enzyme. Similarly, opening the gate by mutating E88 and H271 of 3OST1 to E88G, H271G reduced the AT-binding activity of the HS product, thus demonstrating 3OST5-like activity (110).

Our results have given insight into the mechanism used by 3OST isoforms, especially for 3OST5 and 3OST1, to determine substrate specificity. It appears that the enzyme employs two sites, namely the catalytic site and the gate, to select the appropriate polysaccharide substrate. The catalytic sites are highly homologous among isoforms, and the amino acid residues involved in binding to the substrate are essential for 3-*O*-sulfotransferase activity. The gate residues appear to distinguish the IdoUA2S unit near the catalytic sulfation site. Alterations of the gate residues could allow the isoform to change substrate selectivity (22, 110). Similar to 2OST, our results demonstrate the feasibility of modifying the substrate specificity of sulfotransferases to synthesize HS with a specified sulfation pattern carrying unique biological functions.

Section 5. Biosynthesis of heparosan

Not only mammalians produce HS and HS-like structures. Some bacteria also form surface polysaccharide capsules that are structurally identical or similar to HS polysaccharides although these polysaccharides lack sulfation and iduronic acid unit (112-115). For example, certain pathogenic strains of *E. coli* (112, 113) and *P. multocida* (114,

115) make capsules composed of polymers similar to a unepimerized and unsulfated HS backbone, known as heparosan. Heparosan protects the bacteria from attack by host defenses, giving the bacteria advantages for establishing infections.

Heparosan synthases from *E.coli*

Two enzymes, KfiA and KfiC, are believed to be responsible for the synthesis of heparosan in the *E. coli* K5 strain. KfiA was originally identified by Roberts' group to encode GlcNAc transferase activity, although the purified protein was not obtained (112). Our lab developed an effective approach to express KfiA based on the published sequence (113). The recombinant KfiA was harvested from bacterial culture at the yield of 10 mg/L. The substrate characterization study concluded that KfiA has high specificity for the UDP-GlcNAc substrate. Also, KfiA can efficiently transfer a GlcNAc group to an acceptor of various sizes, including disaccharides. KfiC of *E. coli* K5 has been reported to carry glucuronyl transferase activity. Although we obtained an active form of KfiC by coexpressing with KfiA, the level of expression is insufficient for the use in the synthesis of HS oligosaccharide backbones (13).

Heparosan synthases from *P. multocida*

Additional heparosan biosynthetic enzymes were isolated from *P. multocida*. DeAngelis' group successfully identified and cloned heparosan synthase pmHS1 (114) and pmHS2 (115) from *P. multocida*. Unlike KfiA, pmHS1 and pmHS2 have both GlcNAc and GlcUA transferase activities although the substrate specificities of pmHS1 and pm HS2 are

believed to be distinct. The results from these studies could provide a new approach for the synthesis of heparin/HS backbone (13).

Section 6. Chemical and enzymatic synthesis of HS

Chemical synthesis of AT-binding oligosaccharides

Chemical synthesis is a powerful approach to obtain structurally defined heparin/HS oligosaccharides. The most successful example is the total synthesis of an AT-binding pentasaccharide. This drug is marketed with the trade name Arixtra used for preventing venous thromboembolic incidents during surgery (Figure 11). However, Arixtra only inhibits factor Xa activity and the synthesis of Arixtra requires 60 steps with only a 0.5% yield (72-74). Although the approval of Arixtra by FDA represents the climax in the chemical synthesis of HS oligosaccharides, the high cost of Arixtra limits its application. In the search for antithrombotic saccharides with reduced synthetic complexity and better pharmacological properties, a simplified pentasaccharide analogue, in which the hydroxyl groups are methylated and the *N*-sulfated groups are replaced by *O*-sulfates, was synthesized (Figure 11). This analogue of Arixtra, called Idraparinux, only takes about 25 synthetic routes prepared from glucose. Idraparinux interacts more strongly with AT than Arixtra (K_d of 1 nM compare to 50 nM of Arixtra). Idraparinux also exhibits longer duration of action; $t_{1/2}$ in human is 120 h, compared to 17 h of Arixtra, thus enabling once-weekly administration (116). However, clinical trials for Idraparinux have been halted after a number of participants developed excessive bleeding (117). In order to improve its pharmacological efficacy, a heparin mimetic (SR123781) with 16 saccharide units has been synthesized with

both anti-Xa and anti-thrombin activities (Figure 11). The advantage of this compound is that it is not only capable of inhibiting newly formed thrombin, but it will also block the activity of clot-bound thrombin (116). However, this compound is a simplified hybrid molecule of HS oligosaccharides and highly sulfated glucose units that are not natural occurring heparan sulfate/heparin structures (71, 72). The compound is effective in baboon (118); however, it has not been marketed.

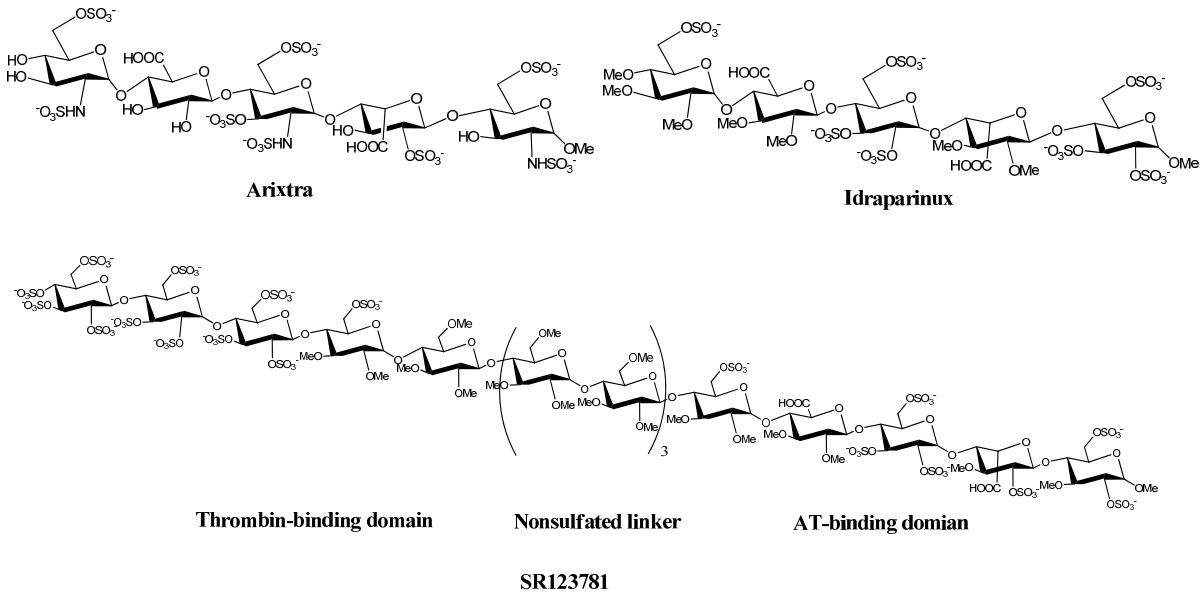

Fig 11. The chemical structures of Arixtra, Idraparinux and SR123781.

Chemical synthesis of peptide/HS oligosaccharide conjugate mCD4-HS12

Recently, researchers have made a synthetic CD4-heparan sulfate conjugate that acts as a novel type of fusion inhibitor for HIV-1 (119) (Figure 12). This inhibitor—mCD4-

HS_{12}—contains a CD4-mimetic peptide linked to a HS dodecasaccharide. The CD4-mimetic peptide binds to the HIV-1 envelope glycoprotein gp120, which drives the exposure of the coreceptor binding domain and renders it to be blocked by the HS part of the inhibitor. Thus, mCD4-HS_{12} targets two conserved regions of gp120 that are crucial for cell entry by HIV-1. The inhibitor has strong antiviral activity toward CCR5-tropic, CXCR4-tropic and dual-tropic HIV-1 strains. The synthesis was divided into two parts: the CD4 mimetic peptide (mCD4g) engineering and chemical synthesis of the HS dodecasaccharide moiety. The mCD4g is a 27 amino acid CD4 mimetic which has three mutations compared to the initial mCD4: F5K mutation, which allows proper HS attachment and two mutations K11S and K18R to avoid the unnecessary HS attachment points. The author also introduced a maleimido group on the side chain of lysine 5, leading to a mCD4-PEO_2-Mal peptide that will conjugate with the HS moiety. The HS docasaccharide was synthesized using a highly convergent method by utilizing a well established chemistry technique. The authors could synthesize up to 20 mg of dodecasaccharide HS12 although only 710 μg mCD4-HS12 was reported (119).

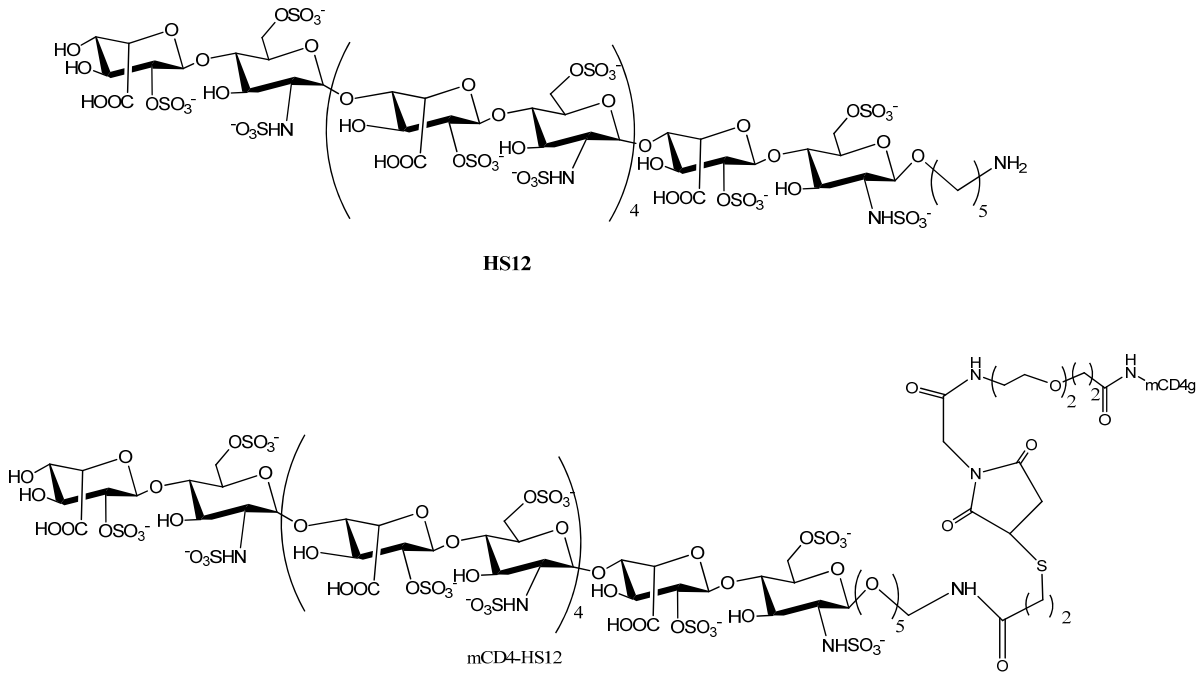

Fig 12. The chemical structures of HS12, CD4-HS12 and mCD4g.

Enzymatic synthesis of biological active polysaccharides

Although many efforts continue to pursue the synthesis of HS oligosaccharides, it has been difficult to generate authentic HS structures larger than a hexasaccharide solely utilizing chemical synthesis. HS biosynthetic enzymes offer a promising alternative approach for the synthesis of large heparin/HS oligosaccharides with the desired biological activities. Several groups have reported their attempts to synthesize HS using biosynthetic enzymes to produce a polysaccharide product with biological activity (13, 120-124). For example, Lindahl and colleagues have reported a chemoenzymatic approach for the synthesis of an anticoagulant

heparin mimic from heparosan (120). The heparosan was initially *N*-deacetylated/*N*-sulfated and then GlcUA units were converted to the IdoUA unit by the C_5-epi. After further chemical persulfation by pyridine sulfate and followed by selective desulfation, a heparin mimic, known as neoparin, was generated. Although neoparin has levels of anti-Xa and anti-thrombin activity similar to those of heparin, unwanted products, such as 3-*O*-sulfo GlcUA/IdoUA, were present in the polysaccharide, suggesting the limitation in the selectivity of chemical sulfation/desulfation in HS synthesis.

Our lab has significantly improved the enzyme-based synthesis of HS in several aspects. First, we enhanced the expression of enzymes and successfully coupled the synthesis with a 3'-phosphoadenosine-5'-phosphosulfate (PAPS) regeneration system, allowing us to prepare HS in milligrams quantities (123). Second, we utilized this approach to identify a new anticoagulant HS, named Recomparin, which has a simplified structure.

PAPS is a sulfo donor for sulfotransferases, which is prohibitively expensive for large scale enzyme-based synthesis. The PAPS regeneration system, initially developed by Wong's lab (125), has been applied in HS/heparin enzymatic synthesis (123). PAP is formed when the sulfo group is transferred to an acceptor. However, PAP inhibits the HS sulfotransferases activity, making milligram-scale synthesis difficult without continuously removing PAP. The PAPS regeneration system converts PAP to PAPS through the action of arylsulfotransferase-IV (AST-IV), which catalyzes the transfer of a sulfo group from *p*-nitrophenyl sulfate (PNPS) to PAP. Thus, HS sulfotransferases use PNPS, instead of PAPS, as the sulfo donor (Figure 13). The PAPS regeneration system offers two advantages for large–scale synthesis. First, it converts PAP to PAPS, eliminating the PAP inhibition effect.

Second, the cost for PNPS is about 1000 times lower than that for PAPS; therefore, its use significantly reduces the cost of sulfotransferase-catalyzed reactions (13).

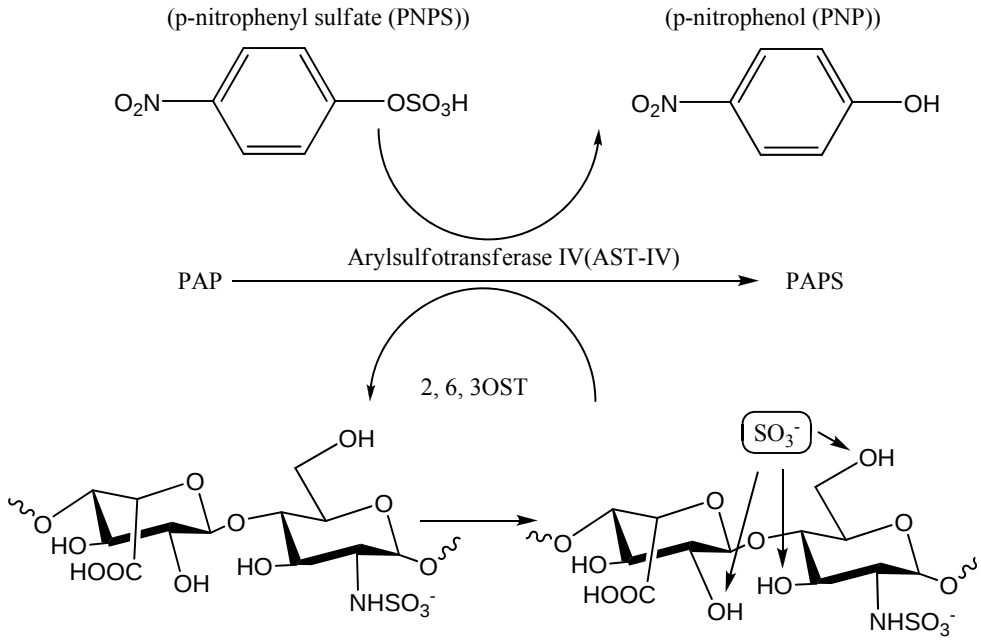

Fig 13. PAPS regeneration system. The PAPS regeneration system converts PAP to PAPS through the action of recombinant arylsulfotransferase-IV, which catalyzes the transfer of sulfo group from *p*-nitrophenyl sulfate (PNPS) to PAP. Thus, HS sulfotransferases use PNPS, instead of PAPS, as the sulfo donor (13).

Our lab, in collaboration with the Linhardt group, has developed an enzymatic approach to the synthesis of bioactive HS polysaccharides from HS backbones, starting from the chemically desulfated *N*-sulfated (CDSNS) heparin (123). Only three enzymatic steps are required to synthesize anticoagulant HS (HS1 in Figure 14) in milligrams. Immobilized enzymes were employed to permit reuse and to improve the stability of HS sulfotransferases. We further tested the activity of HS1 in inhibiting factor Xa and IIa. As expected, HS1 is a potent inhibitor of factor Xa and IIa via AT-mediated process. Its inhibition activity is very similar to heparin, suggesting that our enzyme-based modification system is indeed capable

of converting HS backbones to anticoagulant polysaccharides. We also measured the binding affinity of AT to HS1 by surface plasmon resonance (SPR), which showed that the anti-IIa and anti-Xa activities of HS1 correlated to its binding affinity to AT. We also generated other types of HS polysaccharides which bind to FGF-2 or HSV-1 gD. Taken together, this demonstrates the feasibility of large-scale chemoenzymatic synthesis of heparin/HS with desired biological activities and could be used as a unique tool to explore the biosynthesis of heparin/HS (13).

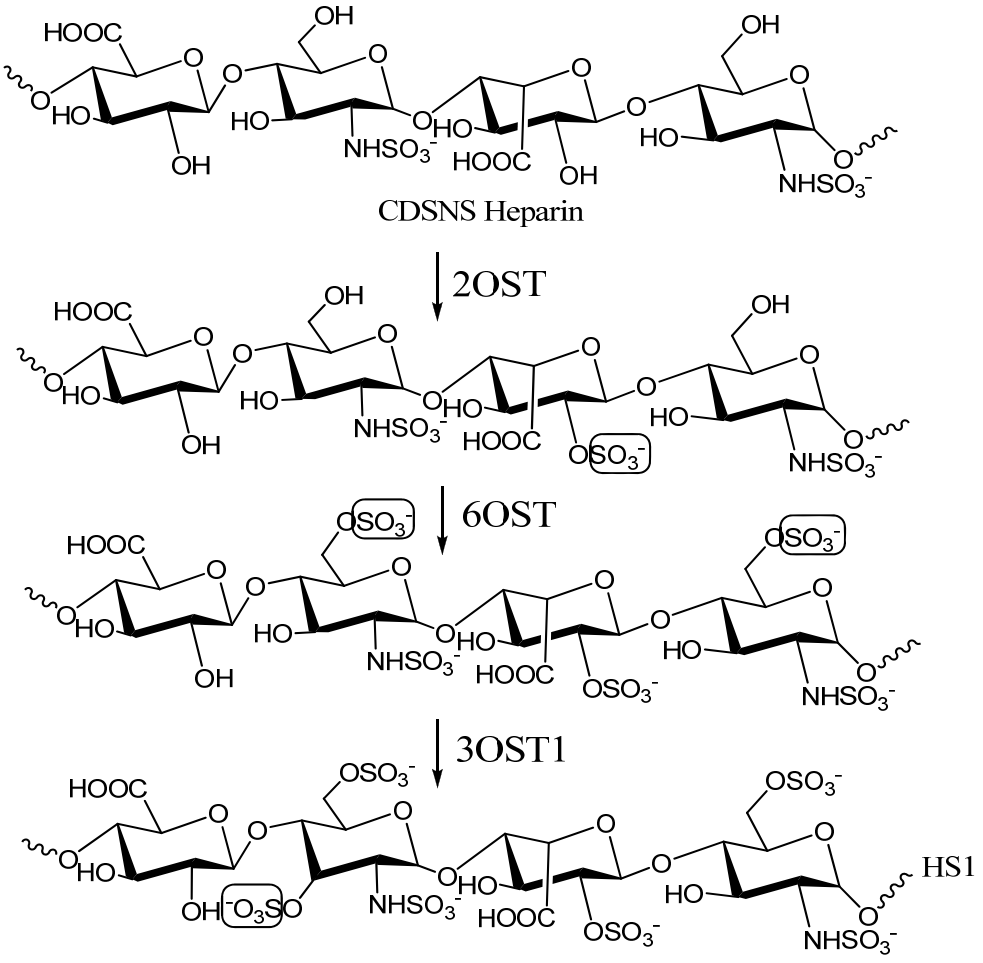

Fig 14. Enzymatic synthesis of anticoagulant CDSNS heparin. The synthesis began with chemical de-sulfated/*N*-sulfated (CDSNS) heparin. CDSNS heparin was modified by 2OST, 6OST and 3OST1 to generate anticoagulant polysaccharide HS1 (13).

Our lab then applied this approach to the synthesis of a small HS library with different sulfation patterns (124). In this study, *N*-sulfo heparosan had been chemoenzymatically prepared from heparosan. A combination of recombinant HS biosynthetic enzymes was used to modify *N*-sulfo heparosan. Our lab discovered one polysaccharide, known as Recomparin (Figure 15). Recomparin showed strong AT-mediated anticoagulant activity. Disaccharide analysis suggested that Recomparin consists of a repeating tetrasaccharide (–GlcUA-GlcNS3S±6S-GlcUA-GlcNS6S-). It was somewhat surprising to discover that Recomparin has strong anticoagulant activity despite the fact that Recomparin contains no IdoUA2S unit. Previous studies showed that the IdoUA2S unit was critical for a pentasaccharide to bind to AT (72). Furthermore, IdoUA adopts a skew boat ($^2S_0$) or chair ($^1C_4$) conformation, while GlcUA is mainly found in the chair conformation ($^4C_1$) (Figure 1) (2). The $^2S_0$ conformation was generally believed to be necessary for binding to AT (126). Our results indicated that the structural flexibility of the IdoUA unit is less important in the polysaccharide-AT interaction. Indeed, further experimental data suggests that the IdoUA unit is essential for binding to AT if the oligosaccharide is smaller than a hexasaccharide, while the IdoUA unit is not essential when the oligosaccharide is larger than an octasaccharide (124). Since IdoUA2S units are responsible for heparin binding to PF4 (20) and FGF (19), our results can help design novel heparin-based anticoagulant drugs with reduced chances of inducing HIT or stimulating cell growth. Indeed, we found that Recomparin, unlike heparin, had no activity in stimulating FGF/FGFR mediated cell proliferation, demonstrating that the anticoagulant activity and the activity in stimulating cell proliferation can be separated at the polysaccharide levels (13).

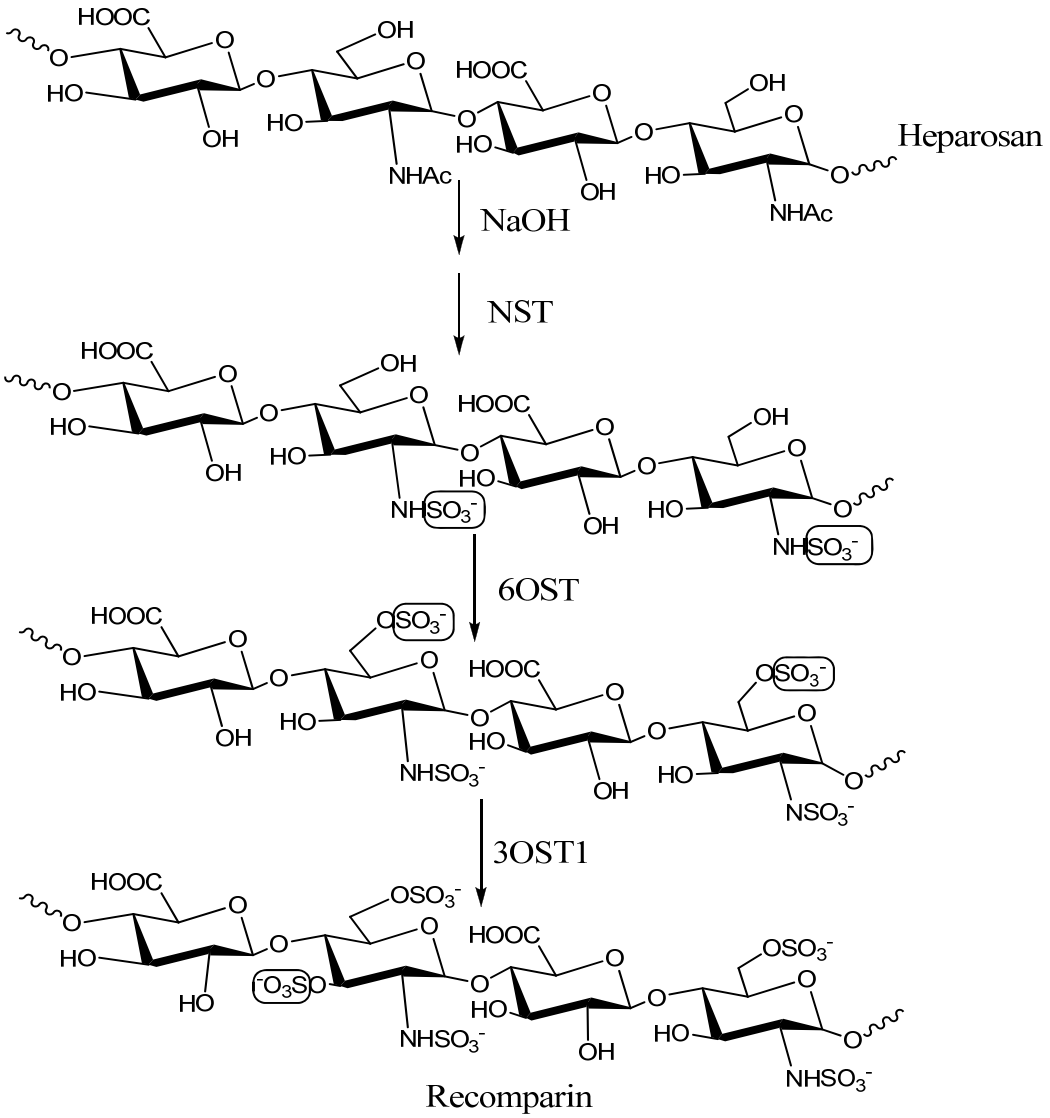

Fig 15. Enzyamtic synthesis of Recomparin. The synthesis began with heparosan. The acetyl group was removed by sodium hydroxide to yield the $GlcNH_2$ unit. The resultant $GlcNH_2$ unit was then *N*-sulfated by NST and it was further modified by 6OST and 3OST1 to generate Recomparin (13).

Enzymatic synthesis of biologically active oligosaccharides

The next goal is to synthesize the oligosaccharide with precise structures. Unlike oligosaccharide, polysaccharide is difficult to get a structurally define compound and it is also difficult to analyze the structure of a polysaccharide. Therefore, without the fully

characterized oligosaccharide products, it is very hard to evaluate the consistency and accuaracy of the enzyme-based methods.

Rosenberg and colleagues achieved notable progress in the enzymatic synthesis of anticoagulant HS/heparin oligosaccharide. For example, they developed an enzymatic route to synthesize a specific HS pentasaccharide that binds to AT (127) (Figure 16). The authors used heparosan as a starting material. Heparosan was treated with NDST2 to prepare a partially *N*-sulfated polysaccharide, which was partially cleaved by heparin lyase I to generate a mixture of oligosaccharides of different sizes. A hexasaccharide fragment was separated by high-performance liquid chromatography (HPLC). This hexasaccharide was further treated with C_5-epi and 2OST1 to generate an IdoUA2S residue at the reducing end. Next, selective 6-*O*-sulfation of two glucosamine units located at middle and non-reducing end was achieved by a 6OST1 and 6OST2a mixture. After removal of the terminal uronic acid residue at non-reducing end by $\Delta^{4,5}$ glycuronidase, 3-*O*-sulfation of the middle glucosamine residue in the resulting pentasaccharide was accomplished by 3OST1, generating the AT-binding pentasaccharide. Either $PAP^{34}S$ or $PAP^{35}S$ was used in the 3OST1 modification step for structural characterization by electrospray ionization mass spectrometry (ESI-MS) or a gel mobility assay, respectively. Gel mobility assays confirmed that the synthetic pentasaccharide effectively binds to AT. This approach accomplished the synthesis of heparin pentasaccharide with fewer steps and a two-fold higher product yield as compared to traditional chemical synthesis. This demonstrated for the first time the feasibility of enzymatic synthetic strategies to synthesize structurally defined HS. However, only microgram amounts of product were generated, precluding further biological function studies (13).

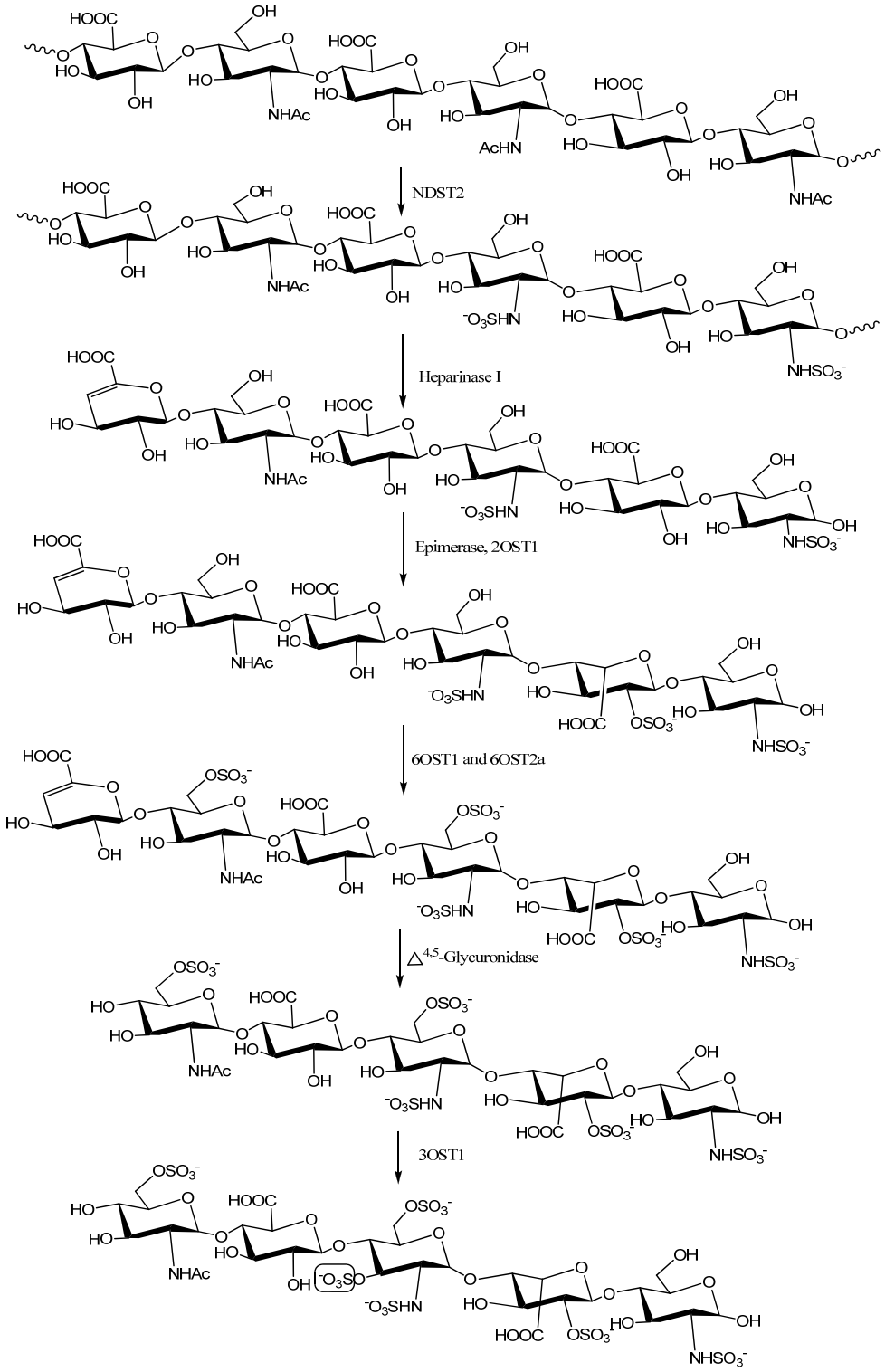

Fig 16. Enzymatic synthesis of AT-binding pentasaccharide. Heparosan was used as starting material. Six enzymatic steps were utilized to synthesize an AT binding pentasaccharide with anticoagulant activity. Either PAP^{34}S or PAP^{35}S was used in 3OST1 modification step (circled) for structural characterization by ESI-MS or gel mobility assay respectively.

Our lab also utilized the enzyme-based approach to prepare a structurally defined octasaccharide with the purpose of developing novel anti-herpes drugs by targeting the viral entry step (13, 128). The synthesis of 3-*O*-sulfated octasaccharide was completed by incubating purified 3OST3 enzyme and an octasaccharide substrate (13) (Figure 17). The octasaccharide substrate was purified from partially depolymerized heparin with heparin lyases. This 3-*O*-sulfated octasaccharide possesses a binding constant (K_d) of 19 μM as determined by affinity co-electrophoresis (29), which is comparable to the gD-binding 3-*O*-sulfated octasaccharide previously isolated from HS (26). Further cell based assays (129, 130) demonstrated that this 3-*O*-sulfated octasaccharide was indeed an inhibitor for HSV-1 infection. The structure of the octasaccharide was characterized by ESI-MS and non-reducing and reducing end sequence analysis. The structure has been determined to be ΔUA2S-GlcNS6S-IdoUA2S-GlcNS6S-IdoUA2S-GlcNS6S3S-IdoUA2S-GlcNS6S. These results demonstrate the application of enzymatic synthesis for a structurally defined HS oligosaccharide to inhibit HSV-1 infection (13).

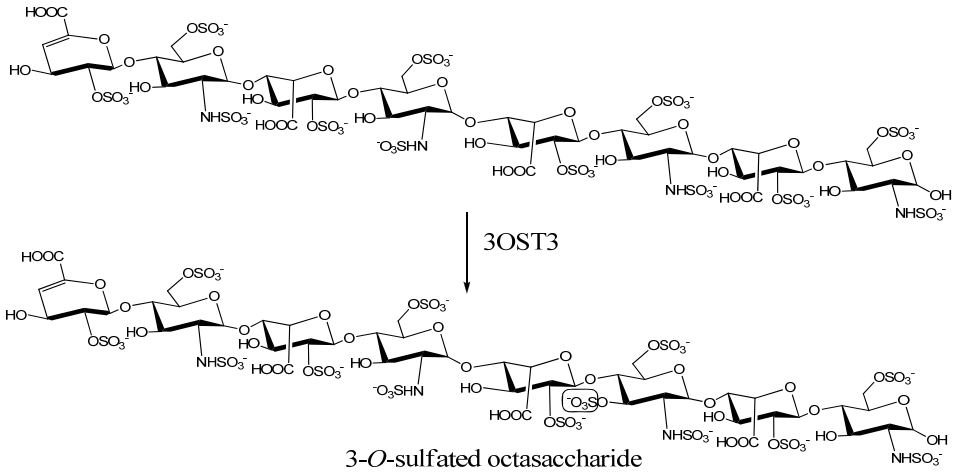

Fig 17. Preparation of 3-*O*-sulfated octasaccharide inhibiting the entry of HSV-1. 3-*O*-sulfation is circled.

Unnatural UDP donors

UDP-*N*-acetylglucosamine (UDP-GlcNAc) and UDP-glucuronic acid (UDP-GlcUA) are widely used in the synthesis of heparin/HS oligosaccharides. The alternative UDP sugar donors can help us in the synthesis of unnatural products with novel biological or chemical properties. Several unnatural UDP-sugars have been synthesized and tested as substrates for GlcNAc or GlcUA transferase. For example, DeAngelis and colleagues reported the enzyme-catalyzed incorporation of unnatural UDP-sugar derivatives by pmHS1 and pmHS2 (131). They found that pmHS1 required highly restricted donor structures, while pmHS2 was able to utilize several unnatural UDP-sugar analogs. For example, pmHS2 can accept UDP sugars with acetamido-containing uronic acid as GlcUA donors and it can tolerate glucosamine derivatives with longer acyl chain as GlcNAc donors. This flexible specificity of pmHS2 could be used to prepare heparin/HS analogs with novel structures. Recently, in order to study the specificity of different GlcUA transferases, Linhardt and colleagues synthesized two UDP-GlcUA analogs: uridine 5′-diphosphoiduronic acid (UDP-IdoUA) and uridine 5′-diphosphohexenuronic acid (UDP-HexUA) (132). In this study, pmHS1 and pmHS2 were utilized as GlcUA transferases. Unfortunately, their results demonstrated that UDP-HexUA failed to serve as a substrate for pmHS1 and pmHS2. When UDP-IdoUA was used as the substrate, sugar residues were transferred with low activity and only GlcUA was incorporated into the products formed. According to the authors, this is either due to the contamination of a small amount of UDP-GlcUA during the chemical synthesis of UDP-IdoUA, or UDP-IdoUA might be isomerized to UDP-GlcUA by the GlcUA transferases via an unknown mechanism. These studies demonstrated the potential application of unnatural UDP-sugars in the chemoenzymatic preparation of synthetic HS/heparin (13).

Section 7. Structural characterization of HS

Due to the chemical structure of HS, the methods to analyze the structure of HS are limited. In the recent years, several techniques have been employed to analyze the HS structures, including disaccharide analysis, mass spectrometry (MS) and nuclear magnetic resonance (NMR).

Disaccharide analysis

Because it is not possible to analyze the structure of full length HS, disaccharide analysis is typically used to profile the structures of HS from various sources. The disaccharide analysis, analogy to the amino acid compositional analysis of protein, provides the relative ratio of disaccharide building blocks. Degradation of HS can be achieved by either enzymatic or chemical methods. The enzymes, heparin lyases, are commonly used to digest heparin or HS and are naturally produced by the soil bacterium *Flavobacterium heparinum* (133). This bacterium is capable of utilizing either heparin or HS as its sole carbon and nitrogen source. Heparin lyases cleave heparin/HS by a β-elimination mechanism (134) (Figure 18A). The action generates an unsaturated double bond between C4 and C5 of the uronate residue (referred as ΔUA). The double bond is a sensitive UV chromaphore, with the maxium absorption at 232 nm, providing a convenient method for detecting the HS fragments produced by enzyme digestion. The identities of the resultant disaccharides can be quantitatively determined by high performance liquid chromatography (HPLC, 135) or capillary electrophoresis (CE, 136). The bacterium produces three lyases, heparinases I, II and III, and each has distinct substrate specificities (137, 138). It is known that heparin lyase I cleaves the glycosidic linkage between IdoUA2S and GlcNS where a

highly sulfated domain resides. Heparin lyase III cleaves 1, 4 linked polysaccharide containing GlcNS/Ac (±6S)-GlcUA/IdoUA (with a preference for GlcUA). Heparin lyase II has more flexibility and cleaves the glycosidic linkage at the site either heparin lyase I or III recognize (Figure 18B). Since heparin lyases cleavage results in an unsaturated uronic acid, the result from disaccharide analysis of heparin lyase degraded HS can not differentiate between GlcUA and IdoUA.

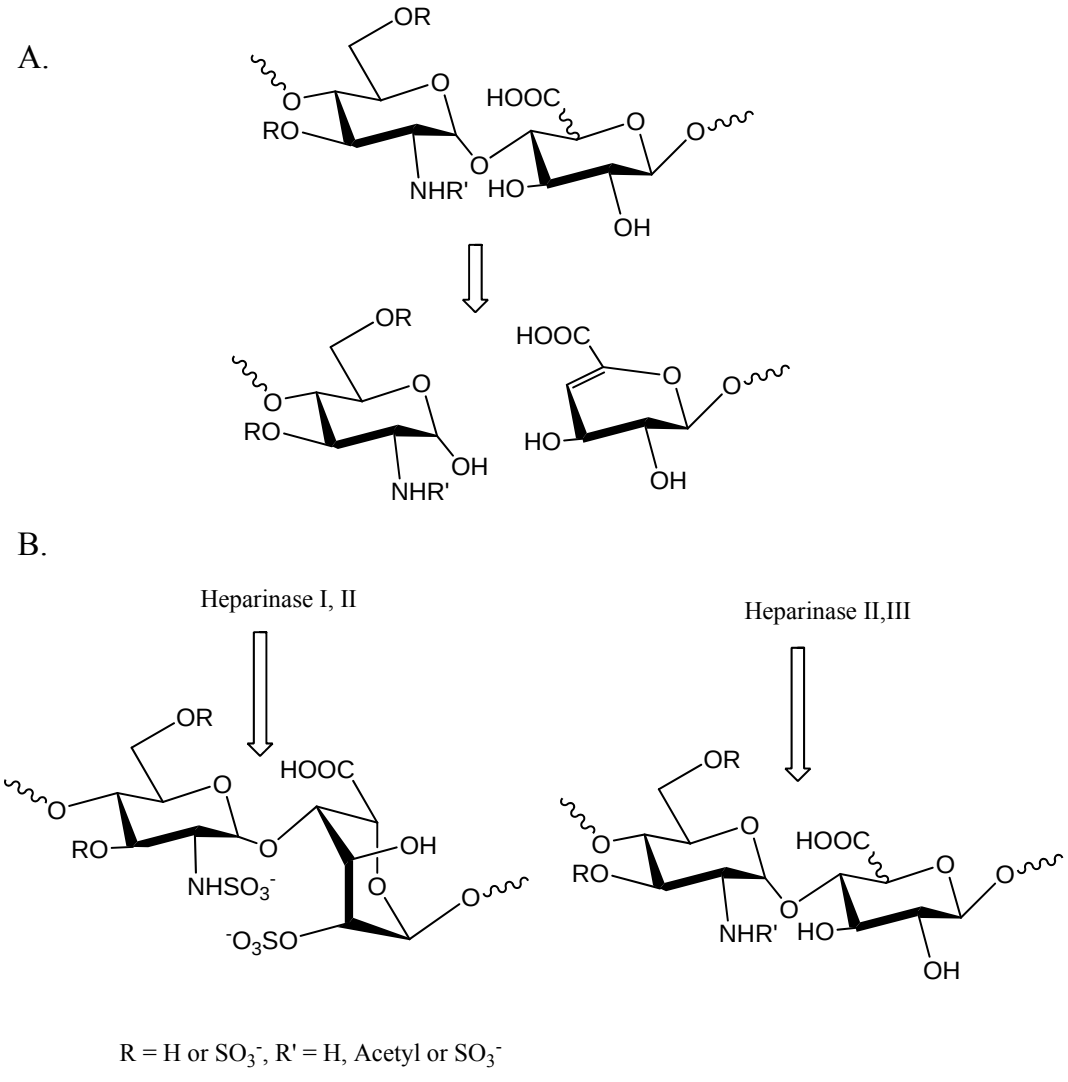

Fig 18. Heparin lyases degradation reaction. Panel **A** is the proposed elimination mechanism. Panel **B** is the substrate specificity of heparin lyase I, II and III.

Nitrous acid degradation is a traditional chemical method to degrade the HS (139), including low pH (pH 1.5) and high pH degradation (pH 4.5). Under both conditions, nitrous acid leads to deaminative cleavage of the chain (Figure 19). Unlike heparin lyase cleavage, the nitrous acid degradation remains the GlcUA/IdoUA unit, regardless of *O*-sulfation carried by either monosaccharide unit; therefore, it allows the differentiation of GlcUA/IdoUA. At high pH, the nitrous acid only reacts with GlcN; while at low pH, the nitrous acid can cleaves HS from GlcNS, therefore, low pH nitrous acid degradation is an effective method to differentiate GlcNS and GlcNAc. Nitrous acid degradation will generate anhydromannose.

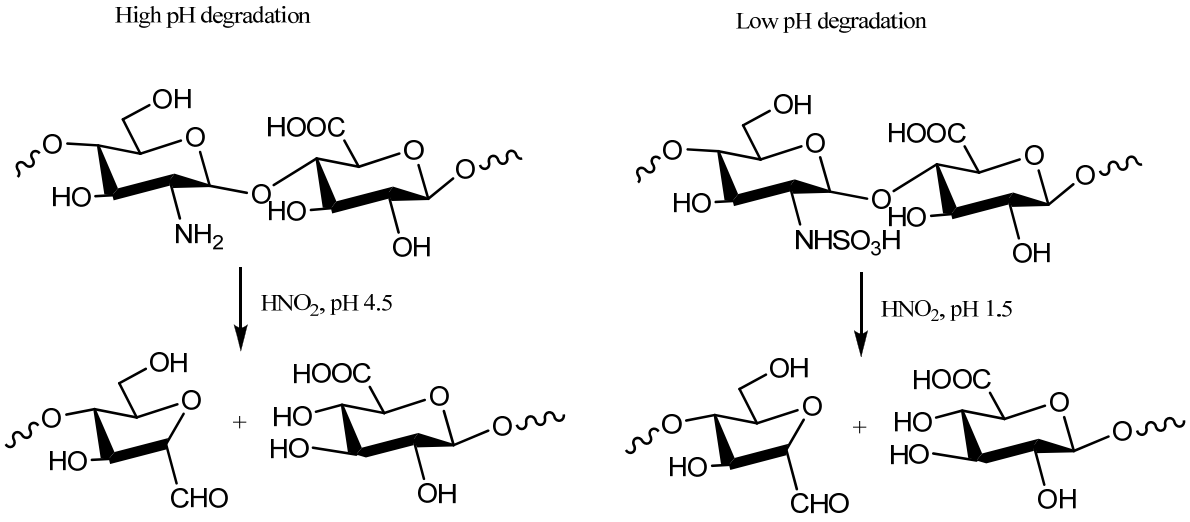

Fig 19. High and low pH degradation of HS.

Mass spectrometry

Mass spectrometry (MS) requires as low as microgram scale of samples, making it a powerful tool to analyze the structure of HS, especially HS oligosaccharides (140-144). Depending on the method for preparing the samples, HS oligosaccharides sometimes have no

UV chromophore. Consequently, it increases the difficulty in identifying and purifying those oligosaccharides by HPLC, which is commonly equipped with an on-line UV detector. Therefore, MS, especially LC-MS, is highly useful to determine the structure of HS oligosaccharides. In HS analysis, electrospray mass spectrometry (ESI) is widely used and typically more sensitive than matrix-assisted laser desorption/ionization (MALDI). Our lab developed a nano ESI-MS method that could detect HS pentasaccharide at a concentration as low as 50 nM (140). MS/MS is rapid and efficient in determining the detailed structures of HS oligomers. For example, Leary and the colleagues developed a heparin oligosaccharide sequencing tool (HOST) to analyze HS/heparin oligosaccharides by enzymatic digestion combined with ESI-MS/MS (142). They were able to sequence HS tetra-and hexa-saccharides by using this tool. The Linhardt group also developed a MS/MS method to distinguish hyaluronic acid and *N*-acetylheparosan (143); furthermore, they could distinguish GlcUA from IdoUA in tetrasaccharide by using electron detachment dissociation (144).

NMR analysis

NMR analysis can be applied to definitively establish the structure and conformation of HS oligosaccharides, especially in solution (145). For example, nuclear overhauser effects (NOEs) have been used to characterize the conformation of IdoUA between $^{1}C_{4}$ and $^{2}S_{0}$ conformers and the NMR data has indicated that the 2-*O*-sulfo group in the IdoA2S residue is not directly involved in binding to AT (146). Moreover, NMR studies of heparin tetrasaccharides in the presence of FGF-1 and FGF-2 indicated that FGF binding stabilizes the $^{1}C_{4}$ conformation of the IdoUA2S residue directly involved in binding. These studies also confirmed a tetrasaccharide is the minimal size binding to FGF-1 and FGF-2 (147, 148).

More recently, the Linhardt group employed NMR spectroscopy to analyze the chemical composition and solution structure of stable isotope-enriched heparin (149), which is chemoenzymatically synthesized from a uniformly labeled [^{13}C, ^{15}N] *N*-acetylheparosan. It was found that isotopic enrichment could provide well-resolved ^{13}C spectra with the high sensitivity required for conformational studies of heparin as well as its [^{13}C, ^{15}N] *N*-acetylheparosan precursor. The structure of the stable isotope-labeled heparin was indistinguishable from heparin derived from animal tissues and provides a novel tool to study the interaction of heparin with proteins (149). The major drawback of NMR analysis is that the methods typically require milligram scale of highly purified HS oligosaccharides, which has been proved to be very difficult to obtain.

Section 8. Statement of problems

Heparin is a commonly used anticoagulant drug with annual sales close to $4 billion worldwide. Drawbacks of the drug include the vulnerable supply of raw materials, severe side effects, and potential risk of contaminants (13, 150). Over the past decade, many groups have achieved considerable progress in understanding heparin/HS synthesis and biosynthesis, especially in the efforts to synthesize structurally defined HS oligosaccharides. Chemical synthesis has been the major route to obtain structurally defined HS/heparin oligosaccharides. The most successful example is the total synthesis of the AT-binding pentasaccharide, Arixtra, used clinically to prevent venous thromboembolic incidents during surgery. Unfortunately, total synthesis is costly and the chemical synthesis of those larger oligosaccharides is extremely difficult if not impossible based on currently available methods. The synthesis of structurally diversified heparin/HS oligosaccharide still remains a daunting

task. Enzymatic synthesis will provide an alternative approach to prepare structurally defined oligosaccharides (13).

Enzymatic approaches have successfully synthesized HS from heparosan, producing polysaccharide and oligosaccharide end products with high specificity for the biological targets (13, 150). Thus, synthetic heparin will eliminate the possibility of contamination and give the drug manufacturer complete control over the safety and purity of the product. Optimizing the synthetic procedure will allow us to produce heparin with maximum pharmacological effects (13, 150).

Enzymatic synthesis of polysaccharide results in a mixture, and thus, it is unlikely to assess the consistency and structural accuracy of the products. One method is to use heparin lyases to digest heparosan. Indeed, Rosenberg's lab has used this method to synthesize an AT-binding pentasaccharide. However, controlling the extent of digestion is difficult and HS oligosaccharides of other sizes and structures are difficult to achieve in large quantities. In contrast, *de novo* synthesis using HS backbone synthases provides a promising alternative approach. Bacterial glycosyl transferases offer the hope for the synthesis of HS oligosaccharide backbone. It is known that some bacteria such as *E. coli* K5 strain and *P. multocida* can produce heparosan. Therefore, one can take advantage of the synthases involved in the biosynthesis of heparosan for HS backbone synthesis (13).

Our central hypothesis is that the structure of HS is controlled by regulating the distribution of GlcNS. Thus, in this dissertation, we report the development of a unique chemoenzymatic approach to synthesize an octasaccharide library with defined positions of GlcNS. Next, a library of oliogosaccharides with defined positions of 6-*O*-sulfation has also

been developed. Finally, multiple HS biosynthetic enzymes are used to synthesize a heparin-like anticoagulant dodecasaccharide with homogeneous structure.

The continuation of this dissertation will improve our understanding of HS biosynthesis. Most importantly, the results will not only allow us to investigate novel synthesis of anticoagulant drugs but also lead to a general method for preparation of structurally more defined HS structures with various other biological functions and help develop novel heparin/HS based therapeutic agents.

Chapter II MATERIALS AND METHODS

Section 1. Preparation of substrate acceptors and UDP-donors

Preparation of heparosan from *E. coli* K5

E. coli K5 strain was used to produce heparosan, a bacterial polysaccharide with a repeating disaccharide *N*-acetylated glucosamine and glucuronic acid residues. Heparosan is structurally similar to unepimerized and unsulfated HS backbone. In this study, heparosan can be used to mimic HS backbone and can be modified by HS biosynthetic enzymes. Heparosan is harvested from *E. coli* cells in large quantities. Six liters of an overnight culture of *E. coli* K5 was prepared and spun to recover the supernatant; the supernatant was adjusted to pH 4.0 by acetic acid and mixed with equal amount of buffer A containing 50 mM NaCl and 20 mM NaoAc at pH 5.0. The sample was then loaded onto 100 mL of diethylaminoethyl (DEAE) column pre-equilibrated with buffer A, the loading was at 10 mL/min by pump for overnight. The DEAE column was washed with 1 liter of buffer A and then eluted with 350 mL buffer B containing 1 M NaCl and 20 mM NaOAc (pH 5.0) until the eluent was no longer brown. The K5 polysaccharide was precipitated from eluent in 75% ethanol at -20 ^{o}C for overnight. After spun down, the precipitate was resuspended into 40 mL water, divided into two tubes and each mixed with 3.4 mL phenol/chloroform to remove

the protein and nucleic acid impurity, the aqueous part was precipitated in 75% ethanol at -20 ^{o}C for overnight again, spun down and the precipitate was dissolved in 25 mL water. The sample was mixed with 45,000 cpm tritium labeled heparosan and was then precipitated with saturated ammonium sulfate; the final concentration of the mixture is about 40% ammonium sulfate. After removal of the supernatant from gel-like precipitate, the supernatant was precipitated again with 50% ammonium sulfate. The gel-like precipitate was resuspended in water and dialyzed overnight against water with MWCO 12,000-14,000. The sample was then loaded onto the DEAE column and purified; the fraction was monitored by the ^{3}H radioactivity in the sample. After DEAE purification, the sample was extracted with phenol/chloroform again and precipitated in 75% ethanol for overnight at -20 ^{o}C. The precipitate was dissolved in water and dried to weigh to obtain pure heparosan. The yield of heparosan is about 100 mg/L of bacteria culture.

Preparation of disaccharide acceptors

Two disaccharide acceptors (GlcUA-AnMan **1** and GlcUA-AnMannose **2**) were prepared from nitrous acid degraded heparosan as previously described (113, 139). Briefly, heparosan (100 mg) was incubated with 10 mL of 2 M NaOH at 68 ^{o}C overnight to prepare the deacetylated heparosan. The deacetylated heparosan was degraded to disaccharide with nitrous acid (1.5 M) at pH 4.5. The resultant disaccharide was reduced by $NaBH_4$ to yield a reducing terminal of 2, 5-anhydromannitol. The resultant disaccharide (GlcUA-AnMan **1**) was dialyzed against water using 1000 MWCO membrane (Spectrum) and served as the acceptor for untagged HS oligosaccharide. In order to synthesize tagged disaccharide donor,

a disaccharide (GlcUA-AnMannose **2**) was also prepared from heparosan followed a very similar procedure as described above omitting the $NaBH_4$ reduction step (Figure 20).

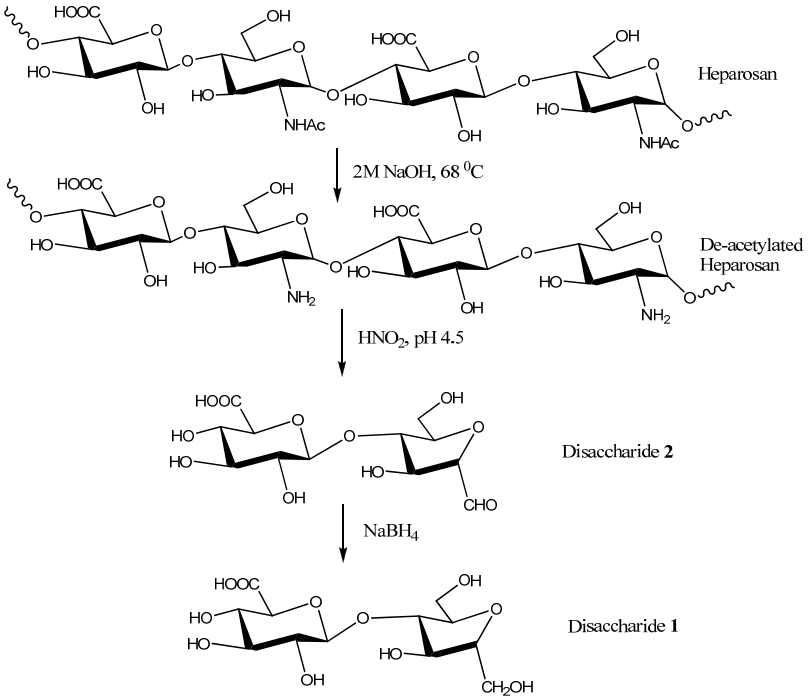

Fig 20. Synthesis of disaccharides **1** and **2**.

Synthesis of [^{3}H]-labeled UDP-*N*-acetylglucosamine

Since radioactively-labeled UDP-sugars are expensive, our lab synthesized [^{3}H]-labeled UDP-*N*-acetylglucosamine (UDP-GlcN[^{3}H]Ac) using a modified method from previous publication starting from [^{3}H]acetate (151). The reaction mixture contained acetyltransferase/*N*-acetylglucosamine-1-phosphate uridyltransferase (GlmU, 0.4 mg/mL), 50 mM Tris-HCl (pH 7.0), 5 mM $MgCl_2$, 200 μM dithiothreitol, 2.5 mM UTP, 20μM CoASH, 200 μM sodium [^{3}H]acetate (0.1 μCi/μL, 500 mCi/mmole purchased from MD Biomedicals) acetyl coenzyme A synthetase (0.1 mg/mL, Sigma-Aldrich), and 0.012 U/μL inorganic

pyrophosphatase (Sigma-Aldrich). Recombinant GlmU was expressed in *E. coli* and purified by a Ni-Agarose column. The reaction was incubated at 30 ^{o}C overnight with mild agitation. The concentration of UDP-GlcN[^{3}H]Ac was determined with RPIP-HPLC as demonstrated by a [^{3}H]-labeled peak coeluted with nonlabeled UDP-GlcNAc standard (Sigma-Aldrich) that has absorbance at 256 nm.

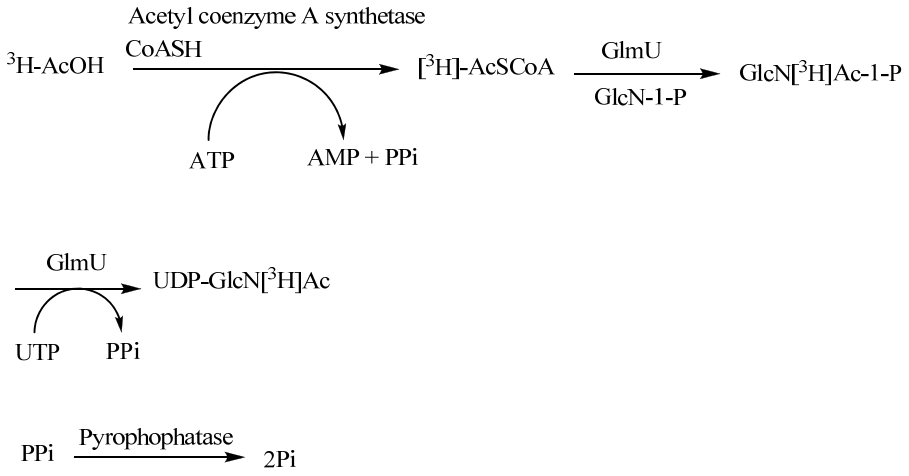

Fig 21. Enzymatic synthesis of UDP-GlcN[^{3}H]Ac.

Preparation of UDP-*N*-trifluoroacetylglucosamine

UDP-*N*-trifluoroacetylglucosamine (UDP-GlcNTFA) (152) is not commercially available, therefore we have developed a chemoenzymatic approach to synthesize this compound using GlmU, in a similar way previously described in the synthesis of UDP-GlcN[^{3}H]Ac. The synthesis involved in preparing a GlcNTFA-1-phosphate (153) and coupling it with UDP (Figure 22). Briefly, 11 mg of $GlcNH_2$-1-phosphate (Sigma-Aldrich) was dissolved in 200 μL of anhydrous methanol and mixed with 60 μL of $(C_2H_5)_3N$ and 130

μL *S*-ethyl trifluorothioacetate (Sigma-Aldrich). The reaction was incubated at room temperature for 24 h. The resultant GlcNTFA-1-phosphate was then converted to UDP-GlcNTFA using GlmU in a buffer containing 46 mM Tris-HCl (pH 7.0), 5 mM $MgCl_2$, 200 μM dithiothreitol, 2.5 mM UTP and 0.012 U/μL inorganic pyrophosphatase (Sigma-Aldrich). The UDP-GlcNTFA was purified by removing proteins using centrifugal filters (10,000 MWCO, Millipore) followed by the dialysis against water using 1000 MWCO membrane for 4 h. The product was confirmed by MS analysis. The concentration was determined by a quantitative analysis with HPLC using a polyamine based column (PAMN column from Waters) and using UDP-GlcNAc as a standard.

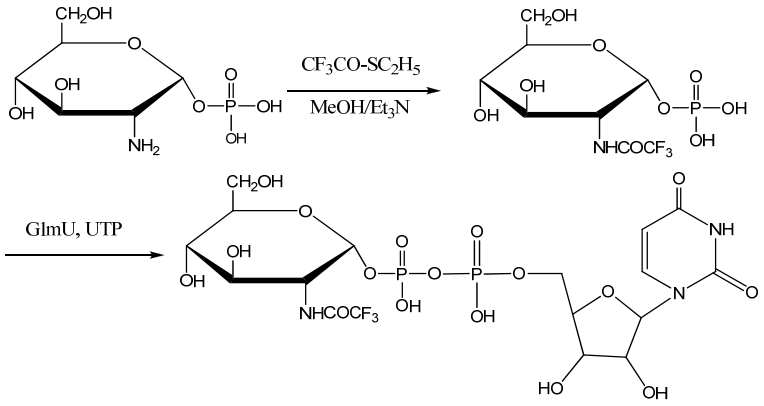

Fig 22. Chemoenzymatic synthesis of UDP-GlcNTFA. Glucosamine-1-α-phosphate is commericially available from sigma. The GlmU enzyme was cloned from *E. coli* K12.

Section 2. Preparation of biosynthetic enzymes

Expression of HS biosynthetic enzymes in *E. coli*

We have made significant improvement on the enzyme-based synthesis of HS by enhancing the expression of enzymes. HS biosynthetic enzymes are traditionally expressed

in mammalian or insect cells. We have expressed these enzymes in bacteria that coexpresses a chaperone protein, which dramatically reduces the difficulty in obtaining the enzymes in large quantities. We used a bacterial cell line that coexpresses chaperone GroEL/GroES to achieve high levels of expression by taking advantage of the fact that the chaperone helps the proteins fold correctly. These recombinant proteins have specific activities and substrate specificity comparable of those expressed in insect cells (Table 1).

Expression of KfiA

The expression of KfiA was carried out in BL21 star (DE3) cells (Invitrogen) carrying pGrp7 plasmid (Takara, Japan) coexpressing bacteria chaperone proteins, GroEL and GroES. Briefly, bacteria cells was grown in LB medium supplemented with 50 μg/mL carbenicillin and 35 μg/mL chloramphenicol at 37 ^{o}C until OD600 reached 0.6, the temperature was then dropped to 22 ^{o}C and 0.1 mM isopropyl-β-D-thiogalactopyranoside (IPTG) and 1 mM sterilized arabinose was added to induce the expression KfiA and chaperone respectively. The culture was shaken overnight at 22 ^{o}C and the bacteria were harvested and lysed by sonication in a buffer containing 25 mM Tris-HCl, pH 7.5, 30 mM immidazole and 500 mM NaCl. The protein was loaded onto a Ni-sepharose 6 Fast Flow column (0.75 x 10 cm, Amersham) pre-equilibrated with buffer A containing 25 mM Tris-HCl, pH 7.5, 30 mM immidazole and 500 mM NaCl. After washed with buffer A, the protein was eluted with 1 mL buffer B containing 25 mM Tris-HCl, pH 7.5, 250 mM immidazole and 500 mM NaCl. The purity of protein was analyzed by precast 10% SDS-PAGE (BioRad). Briefly, samples were diluted with an equal volume of sample buffer containing 2% SDS (BioRad) and 200 mM Tris-HCl, pH 6.8. After the gels were run at

110V for 1 hour, the gels were stained for 30 mins with 0.4 % coomassie blue. Gels were destained using 10% acetic acid (113).

Expression of PmHS2

PmHS2 was expressed as an *N*-terminal fusion to 6 × His using a PET-15b vector (Novagen). The expression of PmHS2 was carried out in BL21 star (DE3) cells (Invitrogen) coexpressing bacteria chaperone proteins, GroEL and GroES. The bacteria were harvested and lyased by sonication in buffer A containing 25 mM Tris-HCl (pH 7.5), 500 mM NaCl and 30 mM imidazole. The protein was loaded onto a Ni-Sepharose 6 Fast Flow column (0.75 x 10 cm, Amersham) pre-equilibrated with buffer A containing 25 mM Tris-HCl, pH 7.5, 30 mM immidazole and 500 mM NaCl. After washed with buffer A, the protein was eluted with buffer B containing 25 mM Tris-HCl, pH 7.5, 250 mM immidazole and 500 mM NaCl.

Expression of NST

NST was expressed according to previous report (88). NST was expressed in *E. coli.* For NST, a glutathione S-transferase fusion was prepared and purified by a glutathione Sepharose column (GE Healthcare). The protein, although carrying a glutathione S-transferase, exhibited high level of *N*-sulfotansferase activity, thus, no cleavage of the GST-tag is necessary.

Table 1. List of HS biosynthetic enzymes expressed in *E. coli*

Enzyme	Bacterial expression cells	fusion protein	Yield (mg/L)
NDST2	Rosetta-gami-B with GroEL	MBP-fusion protein	2
NDase1[a]	Rosetta-gami-B with GroEL	Thioredoxin-fusion protein	5
NDase2[a]	Rosetta-gami-B with GroEL	MBP-fusion protein	10
NDase3[a]	Rosetta-gami-B with GroEL	Thioredoxin-fusion protein	5
NST[b]	BL21	GST-fusion protein	20
Epi	Rosetta-gami-B with GroEL	MBP-fusion protein	15
2OST	Rosetta-gami-B	MBP-fusion protein	12
6OST1	Rosetta-gami-B with GroEL	MBP-fusion protein	14
6OST2	Rosetta-gami-B with GroEL	$(His)_6$-fusion protein	4
6OST3	Rosetta-gami-B with GroEL	$(His)_6$-fusion protein	6
3OST1	BL21(DE3)RIL	$(His)_6$-fusion protein	8
3OST3	BL21(DE3)RIL	$(His)_6$-fusion protein	3
3OST5	Rosetta-gami-B with GroEL	$(His)_6$-fusion protein	8
KfiA	BL21 Star with GroEL	$(His)_6$-fusion protein	10
pmHS2	BL21 Star	$(His)_6$-fusion protein	20

a. NDase1, 2 and 3 represents the *N*-deacetylase domain of NDST1, NDST2, and NDST3, respectively.
b. NST represents the *N*-sulfotransferase domain of NDST1.

Expression of C_5-epi

The full length cDNA of C_5-epimerase was a gift from Dr. Rosenberg from MIT (124). The catalytic domain of human C_5-epi (E53-N609) was firstly cloned into pMAL-c2X vector (New England Biolabs) using the BamH1 and HindIII restriction enzyme sites to generate a maltose-binding protein (MBP)-epimerase fusion protein. C_5-epi was expressed in origami-B cells (Novagen) carrying pGro7 plasmid (Takara, Japan) which expresses chaperone protein GroL and GroES. The bacteria were grown in LB medium supplemented with 12.5 μg/mL tetracycline, 15 μg/mL kanamycin, 50 μg/mL carbenicillin, 2 mg/mL glucose and 35 μg/mL chloramphenicol at 37 ^{o}C until OD600 reached 0.6, the temperature was then dropped to 22 ^{o}C and 0.1 mM IPTG and 1 mM sterile arabinose was added to induce the expression of C_5-epi and chaperone respectively. The protein was purified by an amylase-agarose column following the protocol provided by the manufacturer (New England Biolabs).

Expression of 2OST

The full length cDNA of 2OST was a gift from Dr. Rosenberg from MIT (124). The catalytic domains of 2OST of Chinese hamster ovary (CHO, Arg51-Asn356) was cloned into pMAL-c2X vector (New England Biolabs) using the BamH1 and HindIII restriction enzyme sites to generate a maltose-binding protein (MBP)-epimerase fusion protein. Expression of 2OST was achieved in Rosetta-gami B (DE3) cells (Novagen) using a standard procedure. Briefly, the bacteria were grown in LB medium with 2 mg/mL glucose, 12.5 μg/mL tetracycline, 15 μg/mL kanamycin, 50 μg/mL carbenicillin and 35 μg/mL chloramphenicol at 37 ^{o}C until OD600 reached 0.6, the temperature was then dropped to 22 ^{o}C and 0.1 mM

IPTG and 1 mM sterile arabinose was added to induce the expression of 2OST and chaperone respectively (124). The protein was purified by an amylase-agarose column following the protocol provided by the manufacturer (New England Biolabs).

Expression of 6OST1 and 6OST3

6OST1 and 6OST3 were expressed in *E. coli*. The catalytic domains of 6OST1 of mouse (His53-Trp401) was cloned into pMAL-c2X vector (New England Biolabs) using the BamH1 and HindIII restriction enzyme sites to generate a maltose-binding protin (MBP)-epimerase fusion protein (124). The full length cDNA of 6OST1 was a gift from Dr. Kimata (Aichi University, Japan). Expression of 6OST1 was achieved in Rosetta-gami B (DE3) cells (Novagen) using a standard procedure. Briefly, the bacterica were grown in LB medium with 2 mg/mL glucose, 12.5 μg/mL tetracycline, 15 μg/mL kanamycin, 50 μg/mL carbenicillin and 35 μg/mL chloramphenicol at 37 ^{o}C until OD600 reached 0.6, the temperature was then dropped to 22 ^{o}C and 0.1 mM IPTG and 1 mM sterile arabinose was added to induce the expression of 6OST1 and chaperone, respectively. The protein was purified following the protocol provided by the manufacturer (New England Biolabs).

Expression of 6OST3 was somewhat different from 6OST1 (125). The catalytic domain of 6OST3 of mouse (Pro121-Pro450) was cloned into pMAL-c2X vector (New England Biolabs) from a mouse brain Quick clone cDNA library (BD Biosciences). Expression of 6OST3 was achieved in origami-B cells (Novagen) carrying pGro7 plasmid (Takara, Japan) which expresses chaperone protein GroL and GroES. The cells were grown in LB medium with 2 mg/mL glucose, 12.5 μg/mL tetracycline, 15 μg/mL kanamycin, 50 μg/mL carbenicillin and 35 μg/mL at 37 ^{o}C until OD600 reached 0.4-0.7, the temperature

was then dropped to 22 ^{o}C and 0.1 mM IPTG and 1 mM sterile arabinose was added to induce the expression of 6OST3 and chaperone respectively. The protein was purified by an amylase-agarose column following the protocol provided by the manufacturer (New England Biolabs).

Expression of 3OST1

The expression of 3OST1 was also carried out in *E. coli.* The catalytic domain of mouse 3OST1 (Gly48-His311) (154) was amplified from m3OST1-pcDNA3 with 5' overhang containing an NdeI restriction enzyme site and 3' overhang containing an EcoRI restriction enzyme site. This construct was inserted into the pET28a vector (Novagen) using the NdeI and EcoRI restriction enzyme sites to produce a His6-tagged protein. The resultant plasmid (b3OST1-pET28) was sequenced in the DNA sequencing core facility (University of North Carolina) to confirm the reading frame and the lack of mutations within the coding region. The plasmid was then transformed into BL21 (DE3) RIL cells (stratagene) to express 3OST1. Briefly, bacteria cells containing the b3OST1-pET28 were grown in LB media with 50 μg/mL kanamycin at 37 ^{o}C until the OD600 reached 0.6-0.8; the temperature was then dropped to to 22 ^{o}C and 0.2 mM IPTG was added to induce the expression and the cells were allowed to shake overnight. The bacteria were harvested and lyased by sonication in buffer A containing 25 mM Tris-HCl, pH 7.5, 10 mM immidazole and 500 mM NaCl. The protein was loaded onto a Ni-Sepharose 6 Fast Flow column (0.75 x 10 cm, Amersham) pre-equilibrated with buffer A containing 25 mM Tris-HCl, pH 7.5, 30 mM immidazole and 500 mM NaCl. After washed with buffer A, the protein was eluted with buffer B containing 25 mM Tris-HCl, pH 7.5, 250 mM immidazole and 500 mM NaCl.

Expression of GlmU

Recombinant GlmU was expressed in *E. coli* and purified by a Ni-Agarose 6 FastFlow column. Briefly, cells was grown in LB medium with 50 μg/mL carbenicillin and 35 μg/mL at 37 ^{o}C until OD600 reached 0.6, the temperature was then dropped to 22 ^{o}C and 0.1 mM IPTG and 1 mM sterile arabinose was added to induce the expression GlmU and chaperone respectively. The culture was shaked overnight at 22 ^{o}C and the bacteria were harvested and lyased by sonication in a buffer containing 25 mM Tris-HCl, pH 7.5, 30 mM immidazole and 500 mM NaCl. The protein was loaded onto a Ni-sepharose 6 Fast Flow column (0.75 x 10 cm, Amersham) pre-equilibrated with buffer A containing 25 mM Tris-HCl, pH 7.5, 30 mM immidazole and 500 mM NaCl. After washed with buffer A, the protein was eluted with 1 mL buffer B containing 25 mM Tris-HCl, pH 7.5, 250 mM immidazole and 500 mM NaCl.

Section 3. Preparation of *N*-sulfo tagged octasaccharide library

Preparation of tagged disaccharide

The disaccharide (**2**) starting material was prepared from nitrous acid degraded heparosan as previously described to prepare octasaccharide library **3-6**.

To synthesize fluorous-tagged disaccharide GlcUA-AnMan-Rf (**7**), the disaccharide (**2**) was incubated with 2 equivalent 4-(1H, 1H, 2H, 2H-perfluoropentyl) benzylamine hydrochloride (Fluorous Technologies) and $NaBH_3CN$ (10 equiv.) in 75% MeOH, pH 4.5, overnight at room temperature (155). The fluorous tag allowed isolation of the product with a FluoroFlash affinity chromatography and has absorbance at 260 nm that facilitated HPLC

analysis during the preparation. The resulting tagged disaccharide was purified by FluoroFlash column. The sample was loaded to a PD-10 column (GE healthcare) containing fluorous silica gel (40 μm, fluorous Technologies). The column was pre-equibrated with water. After the samples were loaded, the column was initially washed with 100% water to remove protein and UDP-sugars, then the tagged oligosaccharides were eluted with 100% methanol. The tagged disaccharide was further purified by paper chromatography using Whatman 3 MM chromatography paper (Fisher) and developed with 100% acetonitrile. The tagged disaccharide was spotted at the bottom of the paper and the paper chromatography was carried out into a solvent tank. The paper chromatography was completed when the acetonitrile reach to the top of the paper. The original spot was cut out and tagged disaccharide was eluted with methanol. After paper chromatography, the tagged disaccharide was finally purified by a C_{18} column (0.46 × 25 cm, Thermo scientific) under reverse phase HPLC (RP-HPLC) conditions. The column was eluted with a linear gradient from 90% solution A (0.1% TFA in water) to 50% solution A for 40 min at a flow rate of 0.5 mL/min, then followed by an additional wash for 20 min with 100% solution B (0.1% TFA in acetonitrile) at a flow rate of 0.5 mL/min. The tagged glucose was prepared in 7:3 DMSO/ acetic acid at 65 ^{o}C overnight and was purifed by the same procedure.

Preparation of fluorous tagged octasaccharide backbones

To prepare the fluorous-tagged octasaccharide backbones, the synthesis was started with the fluorous-tagged disaccharide (**7**). The size of oligosaccharide backbone was controlled by the number of KfiA and PmHS2 modifications. In each monosaccharide incorporation step, we supplied the reaction mixture with either KfiA or PmHS2 and

appropriate UDP-monosaccharide donor. As a result, only one sugar residue was transferred into the backbone. At the end of each round of modification, fresh PmHS2 or KfiA enzymes was added to transfer a second monosaccharide in the next cycle. FluoroFlash column was used to purify the products from unreacted UDP-monosaccharides and enzymes.

Selective de-*N*-trifluoroacetylation of GlcNTFA units

Various amounts of tagged oligosaccharides (50 to 100 μg) were dried and re-suspended in a solution (500 μL) containing CH_3OH, H_2O and $(C_2H_5)_3N$ (v/v/v = 2:2:1). The reaction was incubated at 37 ^oC overnight. The samples were dried and reconstituted in H_2O. The de-*N*-trifluoroacetylated tagged oligosaccharides were then purified by a C_{18} column (0.46 × 25 cm, Thermo scientific) under reverse phase HPLC (RP-HPLC) conditions to remove the protein contamination. The column was eluted with a linear gradient from 90% solution A (0.1% TFA in water) to 50% solution A for 40 min at a flow rate of 0.5 mL/min, then followed by an additional wash for 20 min with 100% solution B (0.1% TFA in acetonitrile) at a flow rate of 0.5 mL/min. Selective de-*N*-trifluoroacetylation of untagged oligosaccharide was similar, the reaction was incubated at room temperature overnight. Unlike the tagged oligosaccharide, the further HPLC purification for untagged oligosaccharide is not necessary.

Preparation of *N*-sulfo tagged octasaccharides **3-6**

After purification by a C_{18} column under RP-HPLC conditions and dried, the octasaccharides were then *N*-sulfated by NST. Various amounts of tagged octasaccharide

(20 to 30 μg) were incubated with NST (80 μg), and PAPS (2 equiv.) in 300 μL buffer containing 50 mM MES (pH 7.0) and 1% Triton X-100. The reactions were incubated at 37 ^{o}C. After overnight, another 80 μg fresh NST enzyme was added and was incubated for additional 8 h. The tagged *N*-sulfo-octasaccharides were purified by RP-HPLC as described above.

Section 4. Preparation of untagged oligosaccharides

Preparation of HS untagged oligosaccharide backbones

Both untagged and fluorous-tagged oligosaccharide backbones were prepared using very similar conditions although the fluorous-tagged oligosaccharides were purified by FluoroFlash column (Fluorous Technologies), while untagged oligosaccharides were purified by BioGel P-10 (BioRad).

Disaccharide (GlcUA-AnMan, **1**) (4.5 μmoles) was incubated with UDP-GlcNTFA 3.9 μmoles and KfiA (0.1 mg) in a 1 mL buffer containing 25 mM Tris-HCl (pH 7.2), 10 mM $MgCl_2$. The reaction was incubated at room temperature overnight. An aliquot of reaction mixture was analyzed by PAMN-HPLC to ensure >95% of UDP-GlcNTFA was converted to UDP. Upon the complete consumption of UDP-GlcNTFA, PmHS2 (0.5 mg) and UDP-GlcUA (4 μmoles) were added into the reaction mixture for additional 4-5 h at room temperature. Another aliquot of PmHS2 (0.5 mg) and UDP-GlcUA (4 μmoles) was added to drive the transfer of GlcUA unit to completion. It is important to note that PmHS2 has both activities in transferring GlcNAc (or GlcNTFA in less efficiency) and GlcUA. Without removal of UDP-GlcNTFA, PmHS2 led to polymerization or uncontrollable

oligomerization of the saccharide, resulting in low yield of the tetrasaccharide product. The reaction mixture was resolved on a BioGel P-10 (0.75 × 200 cm), which was equilibrated with 20 mM Tris (pH 7.5) and 1 M NaCl at a flow rate of 4 mL/h. The elution position of the tetrasaccharide was determined by a ^{3}H-labeled tetrasaccharide. The product was dialyzed against water using 1000 MWCO membrane. The reaction cycle was repeated four and five times to prepare the decasaccharide **8**, undecasaccharide **9**, and dodecasaccharide **10**.

Preparation of *N*-sulfo decasaccharide **11**, undecasaccharide **12** and dodecasaccharide **13**

N-sulfation of oligosaccharide was carried out by incubating the de-*N*-trifluoroacetylated oligosaccharide substrates with NST and PAPS. The reaction mixture typically contained 6 μg de-*N*-trifluoracetylated decasaccharide, undecasaccharide and dodecasaccharide, 80 μM PAPS, 50 mM MES, pH 7.0, 1.0% Triton X- 100 (v/v) and 4 μg of NST in a total volume of 300 μL. The reaction mixture was incubated at 37 ^{o}C overnight.

The oligosaccharides were purified by a DEAE column. The reaction mixture (300 μL) was mixed with 1 mL of 0.01% Triton X-100 buffer at pH 5.0 containing 150 mM NaCl, 50 mM NaOAc, 3 M Urea, 1 mM EDTA, then followed by four washes with the same buffer, each time 1 mL, and was eluted with 1 M NaCl in 0.001% Triton X-100 buffer. The purified oligosaccharides were dialyzed using MWCO 3500 membrane and dried. Final product was further purified by a DEAE-HPLC column (0.46 × 7.5 cm, Tosohaas).

Preparation of *N*-sulfo-6-*O*-sulfo decasaccharide **14** and dodecasaccharide **15**

The 6-*O*-sulfo oligosaccharides were prepared by incubating 6OST1 and 6OST3 with *N*-sulfo oligosaccharide substrates. The reaction mixture contained 6 μg *N*-sulfated decasaccharide (**11**) and dodecasaccharide (**13**), 80 μM PAPS, 50 mM MES, pH 7.0, 0.5% Triton X-100 (v/v), 4 μg of 6OST1 and 4 μg of 6OST3 proteins in a total volume of 300 μL. The reaction mixture was incubated at 37 ^{o}C overnight. Prepraration of tagged *N*-sulfo-6-*O*-sulfo oligosaccharides is followed the same procedure. The tagged oligosaccharides were purified by RP-HPLC as described above.

Preparation of *N*-sulfo-3, 6-*O*-sulfo decasaccharide **16** and dodecasaccharide **17**

The 3-*O*-sulfo oligosaccharides were prepared by incubating oligosaccharide substrates with 3OST1 and 3OST5 enzymes. The reaction mixture contained 6 μg decasaccharide **14** or dodecasaccharide **15**, 80 μM PAPS, 50 mM MES, pH 7.0, 10 mM $MnCl_2$, 5 mM $MgCl_2$, and 0.5% Triton X- 100 (v/v) and 4 μg of 3OST1 and 4 μg of 3OST5 proteins in a total volume of 300 μL. The reaction mixture was incubated at 37 ^{o}C for 8 h. The products were purified by DEAE-HPLC as described above.

Section 5. Structural analysis

Nitrous acid degradation of untagged oligosaccharides

The untagged *N*-sulfated/*N*, *O*-sulfated oligosaccharide was degraded by low pH nitrous acid degradation. Briefly, about 100,000 cpm oligosaccharide was dried and dissolved in 20 μL ddH_2O. 20 μL 0.5M H_2SO_4 was mixed with 20 μL 0.5M $Ba(NO_2)_2$ and

spun down. The supernatant was added to the sample and incubated on ice for 30 min with occasional vortex. The reaction was quenched by a mixture of 20 μL 1 M Na_2CO_3 and 1 M $NaHCO_3$ (v/v 1:1). The resultant disaccharide was mixed with 0.5 μL of 5% phenol red and purified by BioGel P-10 (BioRad) column. The resultant disaccharide was dialyzed against double-distilled water using 1000 MWCO membrane (Spectrum) for 5 hours and ready for HPLC analysis

HPLC analysis

Several HPLC conditions were used depending on the nature of the analytes. To conduct the analysis of disaccharides resulted from nitrous acid or heparin lyases-degraded oligosaccharides, ion-pairing reverse phase (RPIP)-HPLC was employed. Here, a C_{18} column (0.46 × 25cm, Vydac) was eluted with a stepwise gradient of acetonitrile in the solution of 38 mM $NH_4H_2PO_4$, 2 mM H_3PO_4, 1 mM tetrabutyl ammonim phosphate monobasic (Sigma) for disaccharide analysis of oligosaccharides **14**, **15**, **16**. Alternatively, the C_{18} column was eluted with the solution containing 10 mM $NH_4H_2PO_4$, 0.5 mM H_3PO_4, 1 mM tetrabutyl ammonim phosphate monobasic for disaccharide analysis of dodecasaccharide **17**, first 7% (v/v) for 30 min, then 15% (v/v) for 15 min, and 19.5% (v/v) for 75 min. DEAE-HPLC (Tosohaas) was utilized to purify and analyze oligosaccharides with sulfo groups. The DEAE- HPLC column was eluted with a linear gradient of NaCl in 20 mM pH 7.0 Tris-HCl buffer from 0 to 0.5 M for 60 min for *N*-sulfated oligosaccharides (**11-13**). Alternatively, the column was eluted with gradient NaCl from 0 to 1 M for 60 min for 6-*O*-sulfated and 3-*O*-sulfated oligosaccharides (**14-17**), then, followed by an additional wash with 1 M NaCl in 20 mM pH 7.0 Tris-HCl buffer at a flow rate of 0.4 mL/min.

Microdialysis of oligosaccharides

In order to improve the sensitive of the analysis by MS, the synthesized oligosaccharides were subjected to microdialysis to remove the salt. The dialysis was carried out using hollow fiber dialysis tubing (MWCO 13,000 Da, Spectrum) against 20 mM ammonium acetate.

Liquid chromatography linked mass spectrometry analysis

Liquid chromatography linked mass spectrometry (LC-MS) analyses were performed at the ADME Mass Spectrometry Center on an Agilent 1100 HPLC-MSD-Trap. Backbone oligosaccharides were injected onto an Aquasil C_{18} column (3 μm 50 × 2.1 mm, Thermo). A gradient of acetonitrile with a flow of 0.4 mL/min was directed into the ion trap mass spectrometer. The gradient consisted of an initial 5 min hold at 90% aqueous (0.1% formic acid in water), a change to 90% organic (0.1% formic acid in acetonitrile) over 2 min, a 2 min hold at 90% organic, a change to 90% aqueous over 2 min, and a 4 min re-equilibration at 90% aqueous. Experiments were performed in positive ionization mode for untagged backbone oligosaccharide. Alternatively, the analyses were performed in negative ionization mode for tagged backbone oligosaccharides. Under both conditions, the electrospray source set to 3000V and 350 ^{o}C, and the compound stability set to 30%. Nitrogen was used for both nebulizer (8L/min) and drying gas (45 psi). Helium was used for collision-induced dissociation. The MS and MS/MS data were acquired and processed using Bruker Trap Software 4.1. All product ions in MS/MS data were labeled according to the Domon-Costello nomenclature (156).

Mass spectrometry analysis

Oligosaccharides with sulfo groups were dissolved in 70% acetonitrile and 10 μM imidazole. A syringe pump (Harvard Apparatus) was used to introduce the sample via direct infusion (10μL/min) into an Agilent 1100 MSD-Trap at the ADME Mass Spectrometry Center. Experiments were performed in negative ionization mode with the electrospray source set to 3000V and 200 °C, and the compound stability set to 30%. Nitrogen was used for both nebulizer (5 L/min) and drying gas (15 psi). Helium was used for collision-induced dissociation. The MS and MS/MS data were acquired and processed using Bruker Trap Software 4.1. All product ions in MS/MS data were labeled according to the Domon-Costello nomenclature.

Section 6. Activity analysis

Antithrombin binding assay

Antithrombin (AT) binding assay was done as previously report (123). Briefly, [^{35}S] labeled oligosaccharide sample (approximately 4000 cpm) was mixed with 100 μL of a buffer containing 10 mM Tris (pH 7.5), 150 mM NaCl, 1mM Me^{2+} (Mn^{2+}, Mg^{2+}, and Ca^{2+}), 10 μM dextran sulfate, 0.1 mg/mL antithrombin, 0.02% NaN_3 and 0.004% Triton X-100. The solution was incubated at room temperature for 30 min and 200 μL slurry of aged ConA-Sepharose gel was added. After shaking at room temperature for 3-4 hours, the solution was spun down and the supernatant was removed. The bead was then washed three times with a buffer containing 10 mM Tris (pH 7.5), 150 mM NaCl, and 0.004% Triton X-100. The entire bead was taken to measure the radioactivity.

Determination of the binding affinity of oligosaccharides to AT

The dissociation constant (K_d) of each sample and AT was determined using affinity co-electrophoresis (157). Approximately 4000-5000 cpm of antithrombin-binding ^{35}S-labeled oligosaccharide was loaded per lane with zones of AT at concentrations 0 to 12.5 μM. The gel was performed at 400 mA for 2 h, dried and analyzed on a PhosphoImager (Amersham Biosciences, Storm 860). The retardation coefficient was calculated at $R = (M_0-M)/M$, where M_0 is the mobility of the polysaccharide through the zone without AT, and M is the mobility of the oligosaccharide through each separation zone. The retardation coefficient was then plotted against the retardation coefficient divided by its respective concentration of AT. The slope of the line represents $-1/K_d$.

Chapter III SYNTHESIS OF *N*-SULFO OCTASACCHARIDE LIBRARY

Section 1. Introduction

The biosynthesis of HS is not a template-controlled process thus the level of sulfation and the positioning of IdoUA residues are thought to depend on the substrate specificities of *O*-sulfotransferase and C_5-epi. The placement of the GlcNS residue is believed to be critical in modulating susceptibility to the subsequent *O*-sulfation and epimerization (22). Therefore, synthesis of oligosaccharides having defined *N*-sulfation positions is an important step in developing a route for the controlled enzymatic synthesis of HS oligosaccharides and polysaccharides. However, it is unclear how to introduce a GlcNS residue into a specific position using NDST due to limited knowledge of its substrate specificity. Here, we tried to develop a general approach to synthesize octasaccharides with GlcNS residues at specific locations. We used KfiA and pmHS2 to build the oligosaccharide backbone. Since KfiA does not utilize UDP-$GlcNH_2$ as a donor substrate, an unsubstituted glucosamine residue cannot be directly introduced into an octasaccharide backbone. We have used an unnatural monosaccharide donor, UDP-trifluoroacetylglucosamine (UDP-GlcNTFA), to empower the placement of a GlcNS residue at any desired position in the oligosaccharide backbone. By selecting either UDP-GlcNAc or UDP-GlcNTFA, we are able to position the $GlcNH_2$ residue in an oligosaccharide. The $GlcNH_2$ residue is then readily converted to GlcNS by NST.

The synthesis started from a disaccharide. Because the synthesis of HS oligosaccharides requires numerous steps, a method for easy separation with high recovery yield of product is critical for the multi-step *de novo* synthesis. Traditional purification methods for carbohydrates by size-exclusion column or reverse phase ion pairing (RPIP)-HPLC are time consuming, and the yield is only around 50% at each purification step. Developing an affinity-tag based purification method is highly significant for carbohydrate synthesis. Therefore, it is endeavored to develop an affinity-tag based approach.

The purification of reaction mixture is time-consuming process in the synthesis, especially in the throughput synthesis for large number of compounds. Affinity tagging is a general strategy for the purification of reaction mixture. One of these strategies is fluorous affinity tag. Fluorous tag based synthesis employs perfluoroalkyl group (Rf) as affinity tags. This technology allows solution phase synthesis. The advantages of fluorous tag include fast reaction, chemically stable, easy separation and flexibility in reaction scale (158, 159). In fluorous tagged based synthesis, fluorous tags are only applied for separation while have no interaction with the function groups (158, 159). One fluorous tagged based separation is fluorous solid-phase extraction (160, FSPE). In FSPE, the separation is based on strong and highly selective fluorine-fluorine interactions between the flurous tag and fluorous silica gel. The samples without fluorous tag will be eluted by fluorophobic wash, which is generally low percentage of methol while fluorous compound will be stick on the fluorous silica gel and is eluted by fluorophilic wash, which is generally 100% methol. A fluorous affinity tag technique has been reported for the chemical synthesis of combinatorial libraries and total synthesis of complex natural products, such as pyridovericin, and mappicine (161-164). For example, Curran and his colleagues have reported a fluorous mixture synthesis. In this study,

a series of compounds was tagged with a series of fluorous tags with different length. These compounds were mixed and conducted to the synthesis of a mixture of enantiomers of analogs of mappicine. After mixture synthesis, these analogs were easily separated by fluorous HPLC based on the fluorine content (161).

Fluorous tag approach has also been applied in the synthesis and microarray analysis of carbohydrate (165, 166). For example, Pohl and her colleagues have synthesized fluorous tagged carbohydrates which are purified by fluorous tag. Furthermore, the tagged carbohydrates can be directly spotted onto fluorous slides to make carbohydrate microarrays for screening (166).

Fluorous tag techniques have an additional advantage for structure analysis by mass spectrometry (165, 167). The flurous tags are stable, making MS spectra less complicated. Furthermore, fluorous tagged molecules are easily ionized and have molecular ions that are readily identified (165). Therefore, in this Chapter, the use of fluorous tagged oligosaccharide substrates has been demonstrated to carry out these studies.

Section 2. Optimization of fluorous tagged saccharides

Preparation of tagged glucose

To prove the feasibility of tagging oligosaccharides, glucose was used as a model compound in searching for the optimal preparation procedure. 3 mg glucose mixed with 100,000 cpm ^{3}H-glucose was used to prepare 5.7 mg of tagged glucose (**18**) as described in Chapter II. The reaction was monitored by the incorporated tritium with a yield of 73%. Nonradioactive tagged glucose was also prepared for MS analysis. The MS analysis revealed

a molecular weight of 467.2, very close to the calculated molecular weight 467.4 (Figure 23). This study demonstrated that the tagged oligosaccharide could be prepared in milligram scale with ready purification.

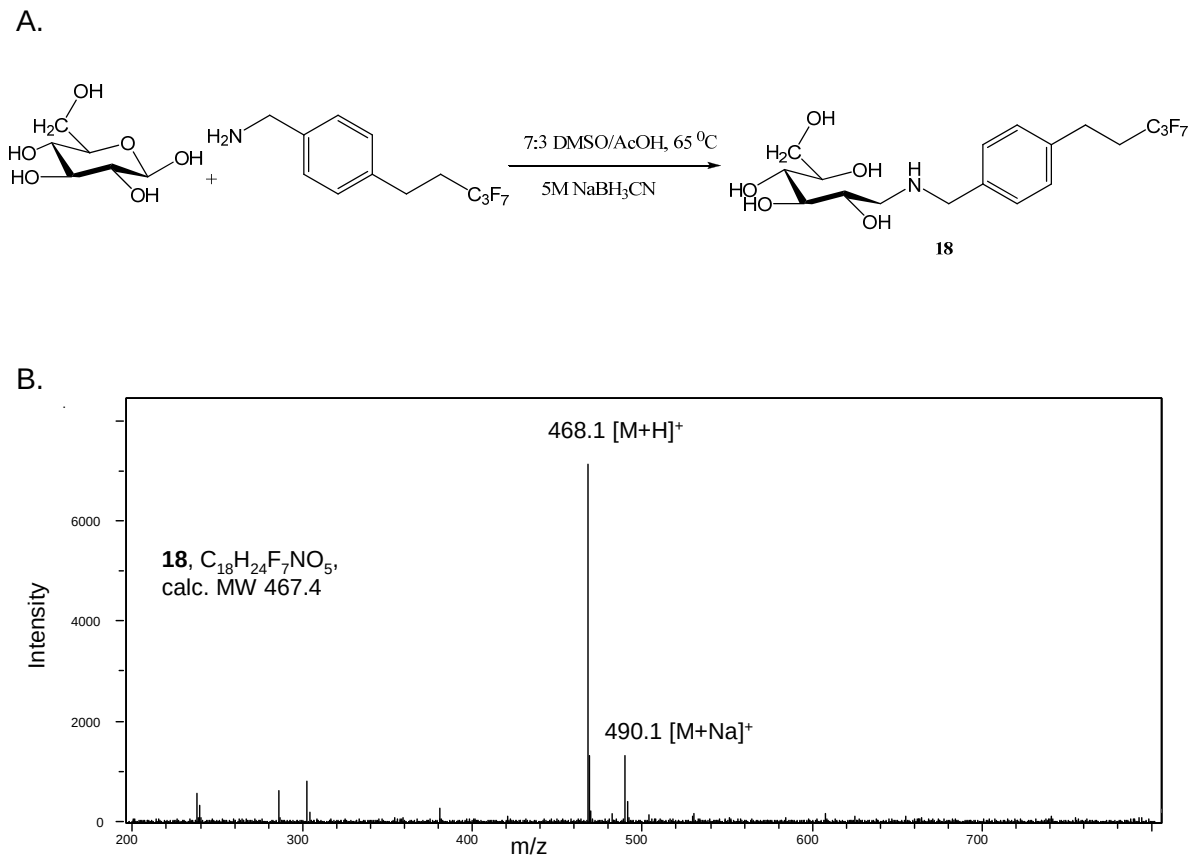

Fig 23. Synthesis and characterization of tagged glucose **18**. Panel **A** shows the preparation of tagged glucose **18**. Panel **B** shows the MS spectrum of tagged glucose **18**. The MS analysis is conducted by ESI-MS in positive mode. MS analysis revealed a molecular weight of 467.1 Da, close to the calculated value of 467.4 Da.

Removal of fluorous tag by catalytic hydrogenolysis

The fluorous tag should be removed from the HS oligosaccharide product when the synthesis is completed. To prove feasibility, tritium labeled tagged glucose was chosen as a model compound. The tag was cleaved with nearly 100% yield when the tagged glucose was

treated with 5% formic acid in 50% MeOH, using Pd/C as catalyst (Figure 24). The results suggest that it is possible to remove the fluorous tag after sulfated oligosaccharidess are synthesized.

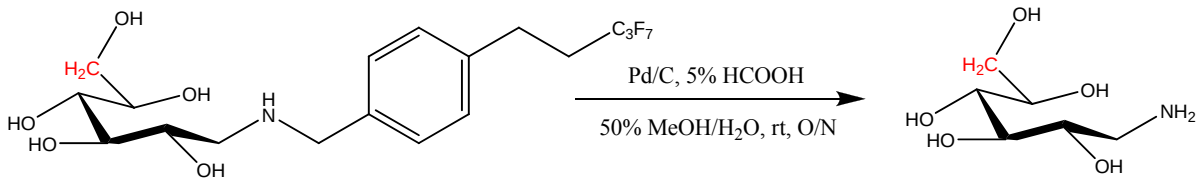

^{3}H labeled tagged glucose **18**

19, ~ 100%

Fig 24. Catalytic hydrogenolysis to remove the fluorous tag. ^{3}H-label is shown in red. The reaction is monitor by the incorporated tritium.

Optimization of fluorous tag

It is known that the fluorous compound dose not dissolve well in water, while the enzymatic reaction has to be in aqueous solution. One approach to improve the water solubility of the tagged oligosaccharide is to use a short tag without compromising the binding affinity to the FluoroFlash column. To examine the binding affinity, the tritium-labeled gluose was coupled with fluorous tag of different length: C_3F_7, C_4F_{10}, C_6F_{13} and C_8F_{17} (Fluorous Technologies). The tagged glucose was loaded on the fluorous column and eluted with a MeOH gradient. The binding and eluting efficiency from a fluorous column was monitored according to the ^{3}H count, provided that ^{3}H labeled glucose was employed in this experiment. It was found that C_3F_7-tagged glucose bound to the column until 60% MeOH, while C_4F_{10}-tagged glucose and C_6F_{13}-tagged glucose bind to the fluorous column until 70% MeOH. All tagged glucoses regardless the number of CF2 number, bound to the

fluorous column. The tagged glucose maintained the binding to the column when the column was washed with 100% water. The tagged glucose was eluted by 100% MeOH. Our data suggest that the tagged glucose can bind to fluorous column and be eluted efficiently by choosing the appropriate solutions. The results are summarized on Table 2. Because the C_3F_7 tagged glucose has the best water solubility among the tested compounds and has adequate affinity to the fluorous column, the C_3F_7 tag (Rf) was chosen to proceed with the subsequent work.

Table 2. Binding affinity of fluorous tag

MeOH%	C_3F_7	C_4F_{10}	C_6F_{13}	C_8F_{17}
0%	not eluted	not eluted	not eluted	not eluted
50%	not eluted	not eluted	not eluted	not eluted
60%	eluted	not eluted	not eluted	not eluted
70%	eluted	eluted	eluted	not eluted
80%	eluted	eluted	eluted	not eluted
100%	eluted	eluted	eluted	eluted

Section 3. Susceptibilities of acceptors and donors to glycotransferases

Preparation of tagged disaccharide

Tagged disaccharide **7** was prepared as described in Chapter II. The molecular weight of the resulting product was confirmed by ESI mass spectrometry as shown in Figure 25 B. It is very important to note that it is essential to obtain pure tagged disaccharide for subsequent synthesis since unreacted tags inhibited the activity of glycotransferase. Tagged disaccharide could be prepared on a milligram scale, sufficient enough for further biological studies.

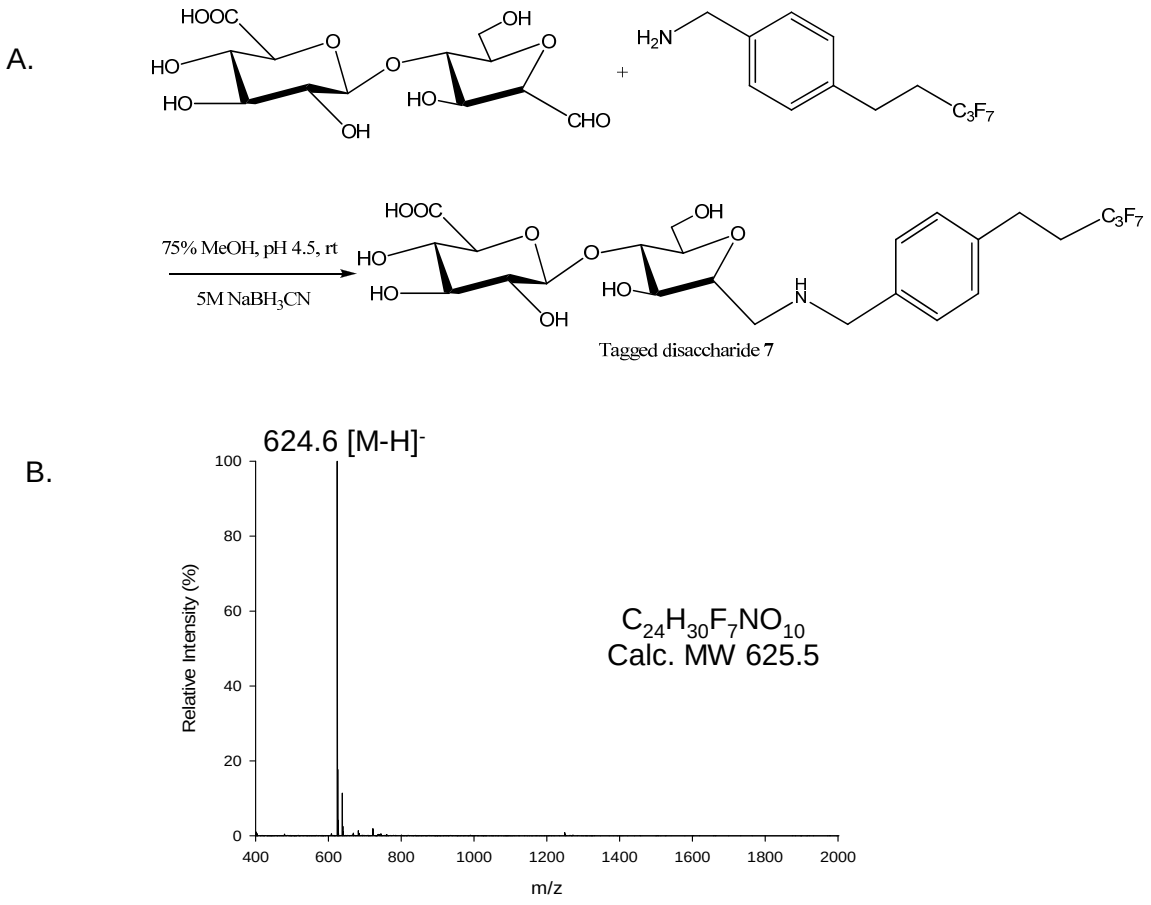

Fig 25. Synthesis and characterization of tagged disaccharide **7**. Panel **A** shows the preparation of tagged disaccharide **7**. Panel **B** shows the MS spectrum of disaccharide **7**. The MS analysis is conducted by ESI-MS in negative mode. MS analysis revealed a molecular weight of 625.6 Da, very close to the calculated value of 625.5 Da.

Susceptibilities of tagged disaccharide to KfiA and pmHS2

To demonstrate that tagged disaccharides serve as the substrates for heparosan biosynthetic enzymes KfiA and pmHS2, the tagged disaccharides were first subjected to the modification of KfiA by using a tritium-labeled UDP- GlcN[^{3}H]Ac. It was found that KfiA could efficiently transfer GlcNAc group to the tagged disaccharide **7**. The resulting tagged trisaccharide **20** was purified by a FluoroFlash column with at least 75% efficiency. The reaction was monitored by the incorporated GlcN[^{3}H]Ac. The yield is calculated based on

the recovery of [^{3}H] counts. Similarly, tagged trisaccharide **20** was subjected to the modification of pmHS2, by using non-radioactive labeled UDP-GlcUA. We found that pmHS2 could transfer a GlcUA group to the tagged trisaccharide with high effiency, and the resulting [^{3}H] labeled tagged tetrasaccharide **21** were purified by a fluorous column. After two additional cycles, we prepared tritium-labeled pentasacchride **22** and hexasaccharide **23**, and the molecular size of this hexasaccharide **23** was determined by the migration position on a Bio-Gel P10 (Bio-Rad) column. Furthermore, only a single symmetric ^{3}H-peak was observed after P-10 column analysis, suggesting that the hexasacchride is pure (Figure 26B). Meanwhile, nonradioactive hexasaccharide **23** was resynthesized using same synthetic route. MS analysis revealed a molecular weight of 1384.2 Da in close agreement to the calculated value of 1384.1 Da. MS/MS analysis confirmed the position of the GlcNAc residues from the two characteristic daughter ions, Y_3 (*m/z*, 827.3) and B_3 (*m/z*, 554.1), products of the cleavage of an internal glycosidic linkage. The product ions in MS/MS data were labeled according to the classic Domon-Costello nomenclature (Figure 27). The data conclude that we could generate a pure tagged hexasaccharide with high efficiency and purity.

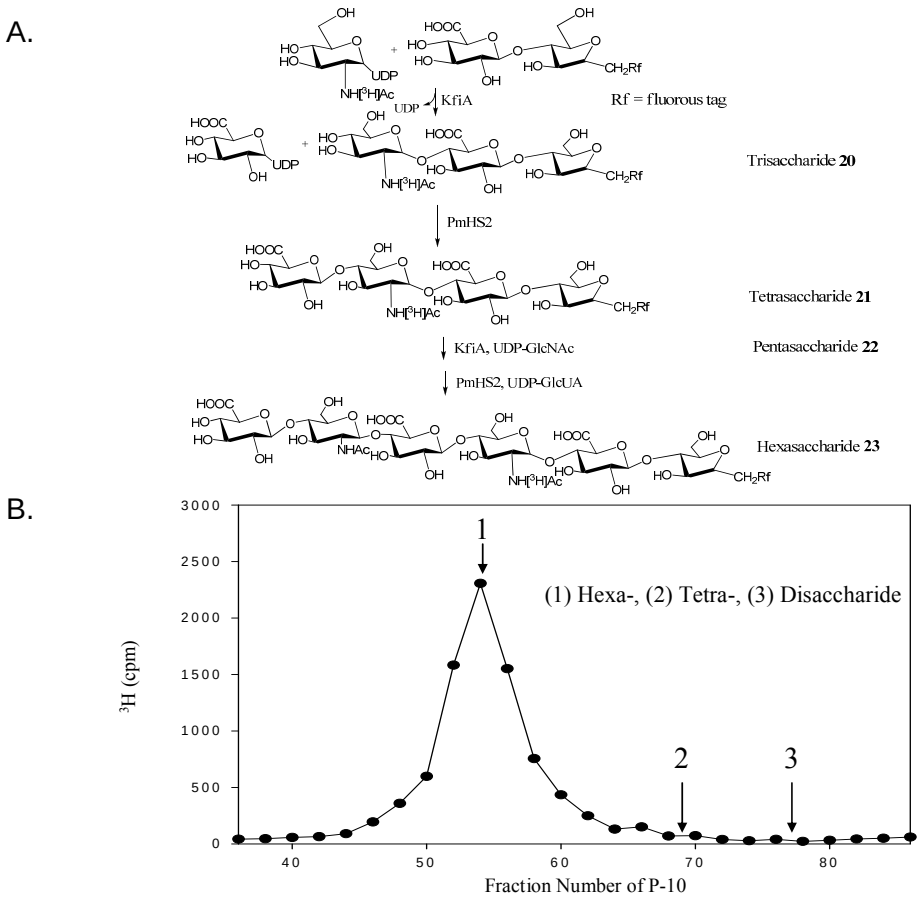

Fig 26. Tagged oligosaccharides are substrates of KfiA and pmHS2. Panel **A** shows tagged non-sulfated HS hexasaccharide could be generated from tagged disaccharide by treated with by KfiA and pmHS2 for four cycles. Panel **B** shows gel filtration column separation of resultant tagged hexasaccharide **23**. Arrows indicate the elution positions of oligosaccharide standards: (1) hexa-, (2) tetra-, and (3) di-saccharides.

A.

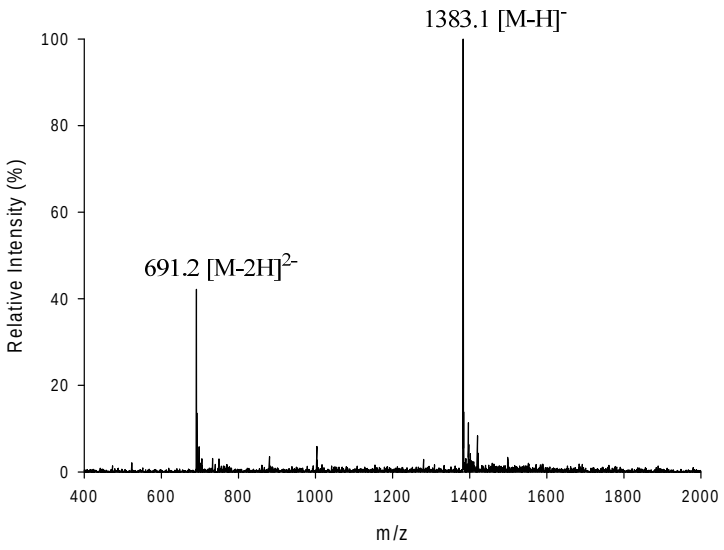

B.

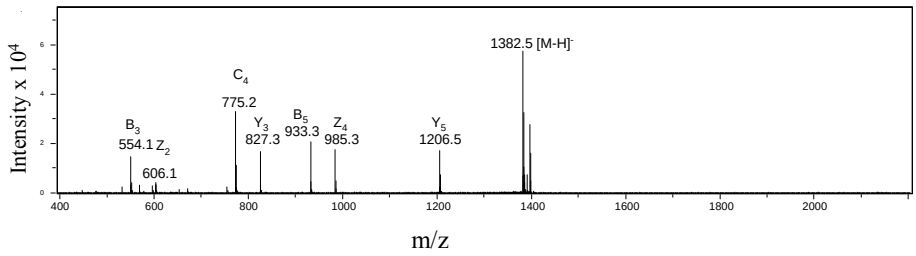

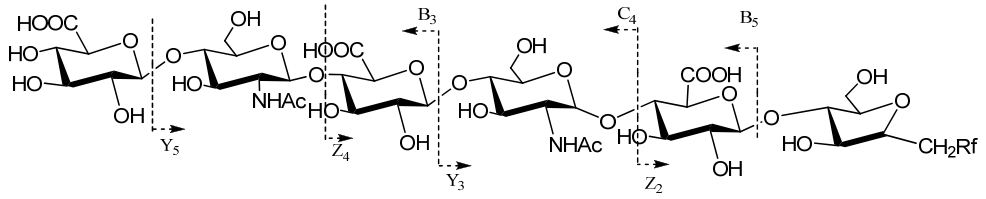

Hexsaccharide **23** $C_{52}H_{72}F_7N_3O_{32}$ Calc. MW 1384.1

Fig 27. Structural characterization of hexasaccharide **23**. Panel **A** shows the MS spectrum of nonradioactive hexasaccharide **23**. The MS analysis is conducted by ESI-MS in negative mode. Panel **B** shows MS/MS of hexasaccharide **23**. The fragmentation pattern is depicted on the bottom. The product ions in MS/MS data were labeled according to the Domon-Costello nomenclature.

Susceptibilities of UDP-GlcNTFA as the donor to KfiA

To demonstrate the reactivity of the unnatural monosaccharide donor UDP-GlcNTFA to glycosyltransferase modification, tagged tetrasaccharide **21** was prepared using the same route as described above and subjected to the modification of KfiA by using UDP-GlcNTFA. Indeed, KfiA efficiently transfered the GlcNTFA group to the tagged tetrasaccharide **21**, the resulting tagged pentasaccharide **24** were purified by a fluorous column. MS analysis of pentasacchride **24** revealed the molecular weight to be 1262.0 Da identical to the calculated molecular weight of 1262.0 Da. MS/MS analysis confirmed the position of the GlcNTFA residues from the two characteristic daughter ions, Y_3 (*m/z*, 827.4) and C_3 (*m/z*, 653.3), products of the cleavage of internal glycosidic linkages (Figure 28). This demonstrated that UDP-GlcNTFA could serve as a good substrate for KfiA. Tagged disaccharide was also subjected to the modification of KfiA in the presence of UDP-GlcNTFA. Although the disaccharide can accept GlcNTFA, the effiency is only 30% compare to UDP-GlcNAc.

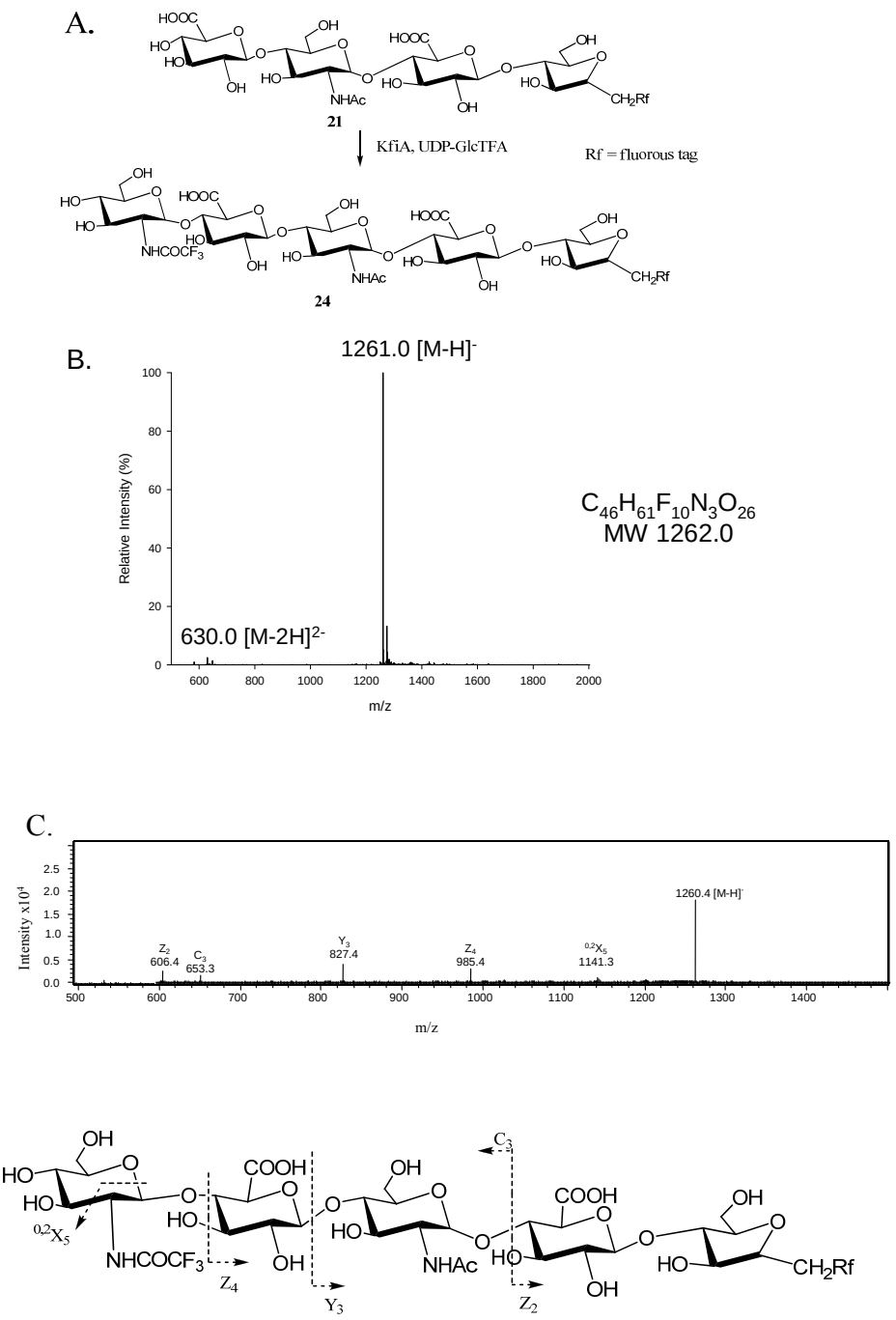

Fig 28. Structural characterization of pentasaccharide **24**. Panel **A** shows the synthesis of pentasaccharide **24**. Panel **B** shows the MS spectrum of **24**. The MS analysis is conducted by ESI-MS in negative mode. Panel **C** shows the MS/MS analysis of **24.** The fragmentation pattern is depicted on the bottom. The product ions in MS/MS data were labeled according to the Domon-Costello nomenclature. Rf is the fluorous tag.

Section 4. Preparation of *N*-sulfo hexasaccharide

Selective de-*N*-trifluoroacetylation of tagged hexasaccharide

To demonstrate the GlcNTFA group could be selective de-*N*-trifluoroacetylated. Tagged pentasaccharide **24** was first extended to hexasaccharide **25** using PmHS2 and UDP-GlcUA as substrate (Figure 29A). This demonstrated that GlcNTFA could also serve as a good acceptor for PmHS2. It's known the GlcNTFA unit is highly susceptible to a mild base deacetylation (152). The hexasaccharide **25** was treated with CH_3OH, H_2O and $(C_2H_5)_3N$ (v/v/v = 2:2:1) to remove the $–COCF_3$ group to yield $GlcNH_2$ unit with nearly 100% efficiency as described in Chapter II. The samples were then dried and reconstituted in H_2O to recover de-*N*-trifluoroacetylated hexasaccharide **26**. MS analysis revealed a molecular weight of 1437.7 Da and 1342.2 Da for hexasaccharide **25**, and **26** respectively, very close to the calculated molecular weight 1438.1 Da and 1342.1 Da, respectively (Figure 29). This study clearly demonstrated that the GlcNTFA group could be selectively de-*N*-trifluoroacetylated while GlcNAc group remains intacted.

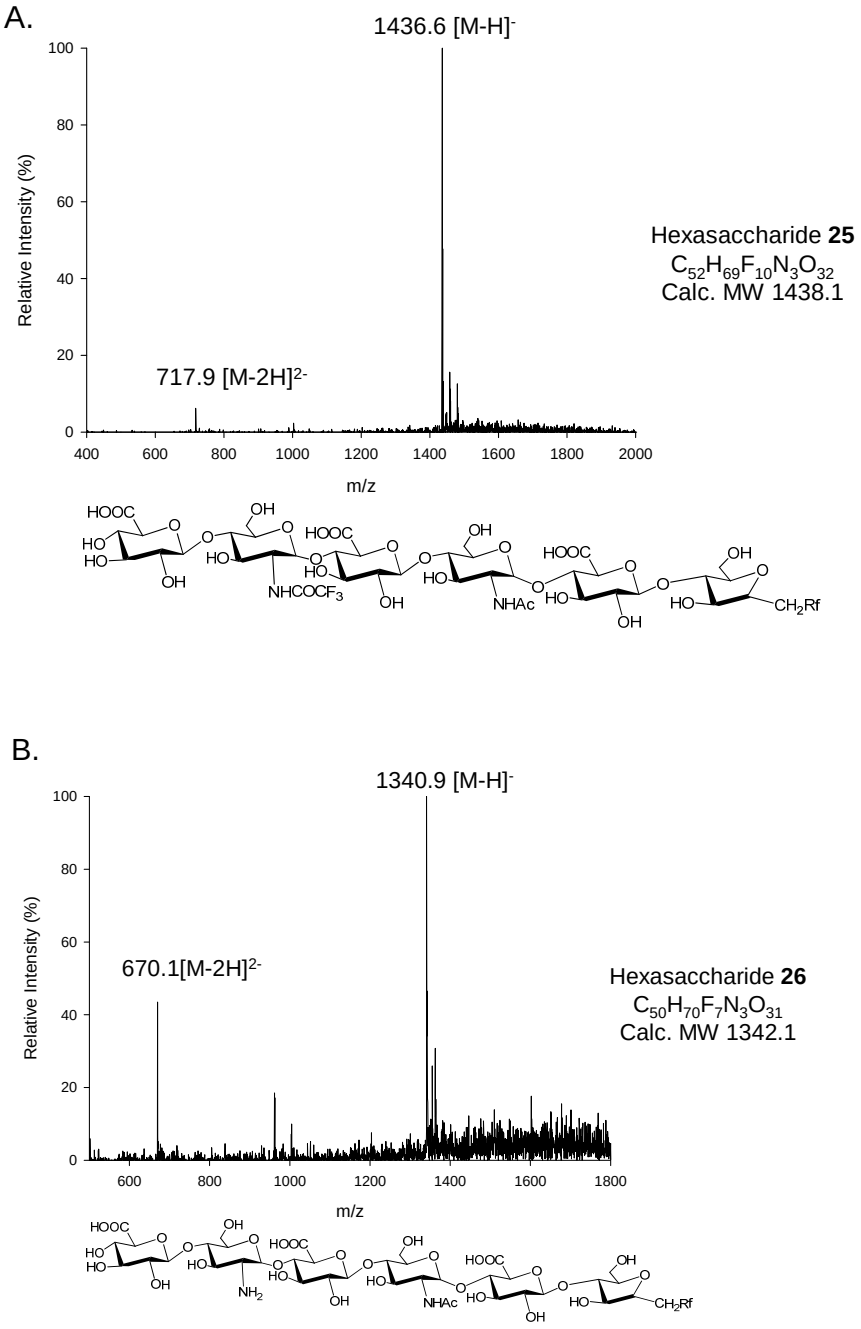

Fig 29. Structural characterization of hexasaccharide **25** and **26**. Panel **A** shows the MS spectrum of hexasaccharide **25**. The MS analysis is conducted by ESI-MS in negative mode. Panel **B** shows the MS spectrum of de-*N*-trifluoroacetylated hexasaccharide **26**. The MS analysis is conducted by ESI-MS in negative mode. Rf is the fluorous tag.

Preparation of *N*-sulfo tagged hexasaccharide

To preprare *N*-sulfated hexasaccahride **27**, the de-*N*-trifluoroacetylated hexasaccharide **26** was modified by NST and purified as described in Chapter II. Hexasaccharide **27** was resolved as a symmetric peak by HPLC using a C_{18} column (Figure 30A). MS analysis revealed a molecular weight of 1422.2 Da in close agreement to the calculated mass of 1422.1 Da. The structure of *N*-sulfo hexasaccharide **27** was characterized by MS/MS. The product ions in MS/MS data were labeled according to the classic Domon-Costello nomenclature. MS/MS analysis confirmed the position of the GlcNS residues from the two characteristic daughter ions, Y_3 (*m/z*, 827.4) and B_3 (*m/z*, 592.4), products of the cleavage of internal glycosidic linkage (Figure 30C). This study demonstrated that the de-*N*-trifluoroacetylated oligosaccharide could be modified by NST. About 300 μg hexasaccharide **27** with about 40 % yield starting from tagged disaccharide **7** were generated, sufficient enough for further studies.

Optimization of mass spectrometry

Oligosaccharides carrying sulfo groups are notorious for ionization, resulting extremely low sensitivity. In order to search for optimal condition for sulfated oligosaccharides, two oligosaccharide standards, including Arixtra (GSK) and heparin disaccharide ΔUA-GlcNS6S **28** (Sigma-Aldrich), were applied to optimize the MS condition. It was found that lower temperature and higher voltage is able to increase ionization ability while desulfation remains low. Further, samples dissolved in 70% ACN and 10μM imidazole enhanced the sensitivity. Therefore, the optimal condition for sulfated samples were found to be in negative ionization mode with the electrospray source set to 3000 V and

200 °C. Arixtra could be detected at the concentration as low as 10 μM while the disaccharide **28** could be detected at the concentration as low as 0.5 μM. Such difference could be due to the fact that Arixtra carried more sulfo groups and intrinsically difficult to be ionized. The optimization was critical for subsequent study for characterizing *N*-sulfo and *O*-sulfo oligosaccharides.

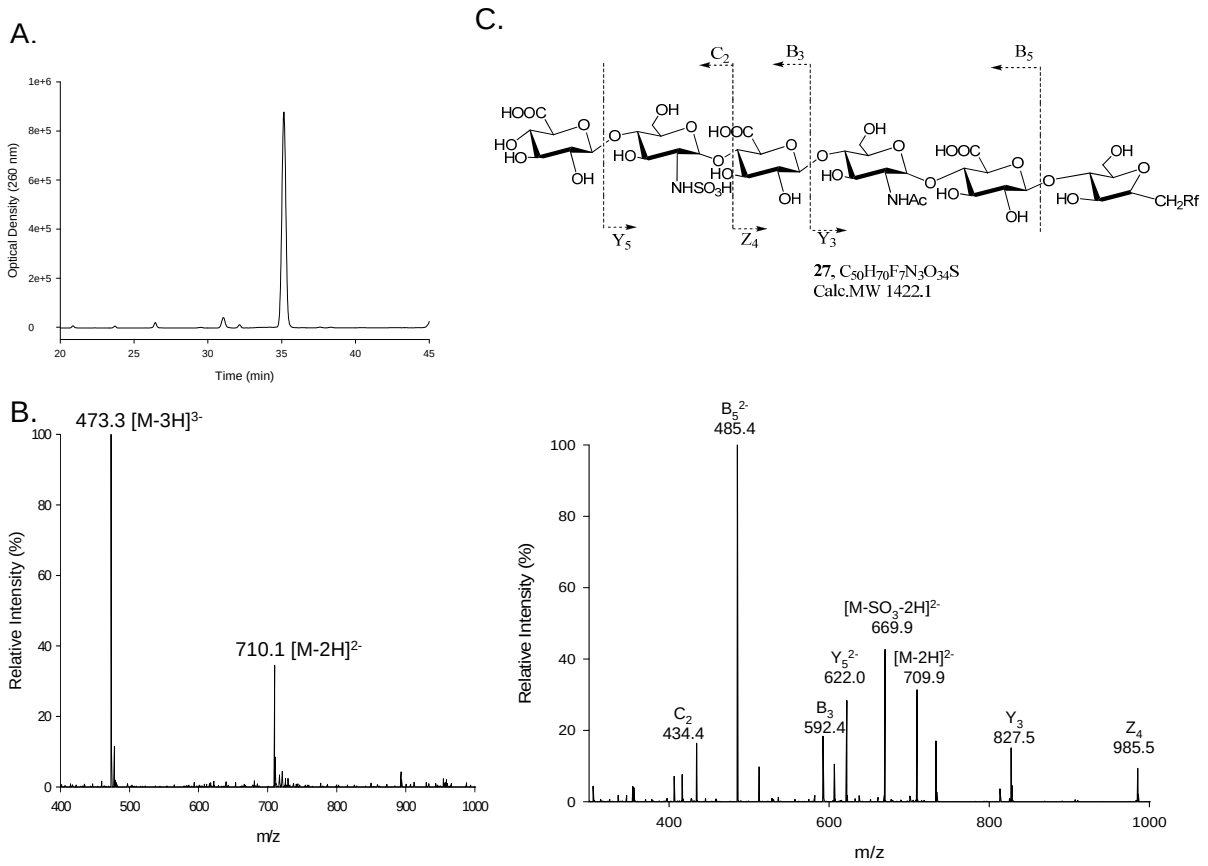

Fig 30. Structural characterization of *N*-sulfated hexasaccharide **27**. Panel **A** shows the HPLC chromatogram of hexasaccharide **27** using a C_{18} column under reverse phase condition. Panel **B** shows the MS spectrum of **27**. The MS analysis is conducted by ESI-MS in negative mode. Panel **C** shows MS/MS of **27** (precursor ion selection at m/z 473.3). The fragmentation pattern is depicted on the bottom. The product ions in MS/MS data were labeled according to the Domon-Costello nomenclature. Rf is the fluorous tag.

Section 5. Preparation of *N*-sulfo octasaccharide library

Preparation of HS octasaccharide library

Encouraged by the results from hexasaccharide, an octasaccharide library differing in the numbers and positions of *N*-sulfo and *N*-acetyl substituted glucosamine residues was prepared. The synthesis was started with the same fluorous-tagged disaccharide GlcUA-AnMan-Rf (**7**). The size of oligosaccharide backbone was controlled by the number of KfiA and PmHS2 modifications. FluoroFlash column was used to purify the products from unreacted UDP-monosaccharides and enzymes. The position of *N*-sulfo and *N*-acetyl substituted glucosamine residues was controlled by selecting UDP-GlcNTFA or UDP-GlcNAc as donor. After the backbones were built up, the oligosacchrides were selective de-*N*-trifluoroacetylated and purified by RP-HPLC. The de-*N*-trifluoroacetylated octasaccharides were then *N*-sulfated by NST (Figure 31). The pure *N*-sulfated octasaccharides could be prepared in only eight steps starting from the tagged disaccharide **7**. 100 μg scale of octasaccharide **5** could be generated. The octasaccharide library was further characterized by MS and MS/MS.

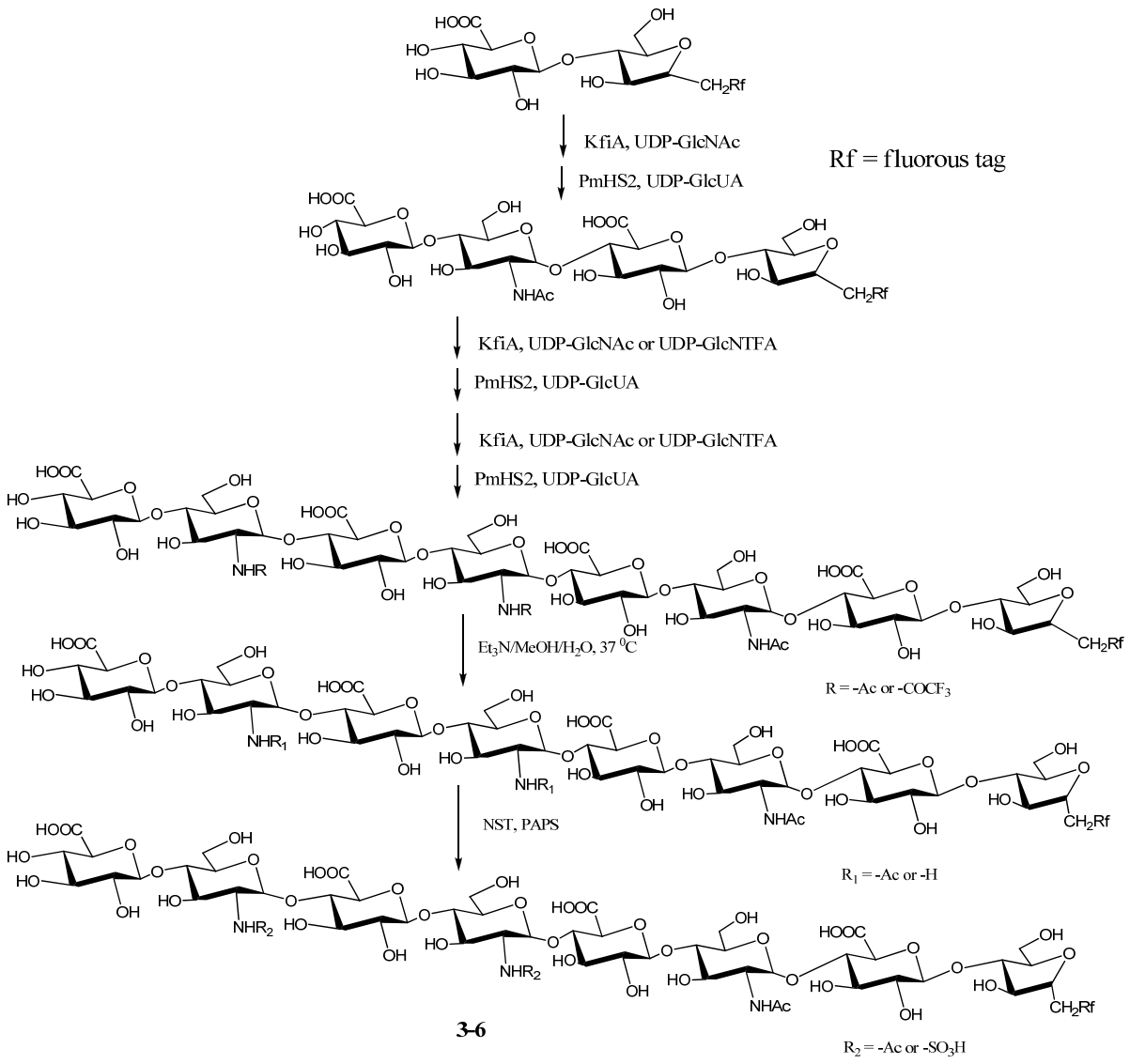

Fig 31. Scheme for the synthesis of octasaccharide library **3-6**. The synthesis was begun with GlcUA-AnMan-Rf. The product was then elongated to the octasaccharides. Either $GlcNCOCF_3$ or GlcNAc residue will be incorporated into the octasaccharide by KfiA according to target compound. The $-COCF_3$ group was selectively removed to yield the $GlcNH_2$ unit and was then *N*-sulfated by NST.

Characterization of *N*-sulfo octasaccharide library

Octasaccharide **3** & **4** (single GlcNS at different positions) and octasaccharide **5** (two GlcNS residues) and **6** (no GlcNS), were purified by RP-HPLC and characterized by MS and MS/MS. For example, octasaccharide **3** and **4** has same molecular weight as revealed by MS, however, they showed significant different MS/MS pattern. MS/MS analysis confirmed the position of the GlcNS residues in **3** from the two characteristic daughter ions, Y_5^{2-} (*m/z*, 621.9) and B_3 (*m/z*, 554.4), products of the cleavage of an internal glycosidic linkage (Figure 32) while MS/MS analysis confirmed the position of the GlcNS residues in **4** from the two characteristic daughter ions, Y_5 (*m/z*, 1206.6) and B_3 (*m/z*, 592.2), products of the cleavage of an internal glycosidic linkage (Figure 33). Furthermore, octasaccharide **5** was resolved as a symmetric peak by HPLC using a C_{18} column (Figure 34A). ESI-MS analysis revealed its molecular weight to be 1839.6 Da in close agreement to the calculated mass of 1839.5 Da (Figure 34B). MS/MS analysis confirmed the position of the GlcNS residues in **5** (Figure 34C) from the two characteristic daughter ions, Y_5 (*m/z*, 1244.5) and B_3 (*m/z*, 592.3), products of the cleavage of an internal glycosidic linkage. Octasaccharide **6** has no GlcNS with repeating disaccharide structure; therefore, the MS/MS study was not performed (Figure 35). The results from these studies demonstrated that we were able to synthesize oligosaccharides having defined *N*-sulfation positions.

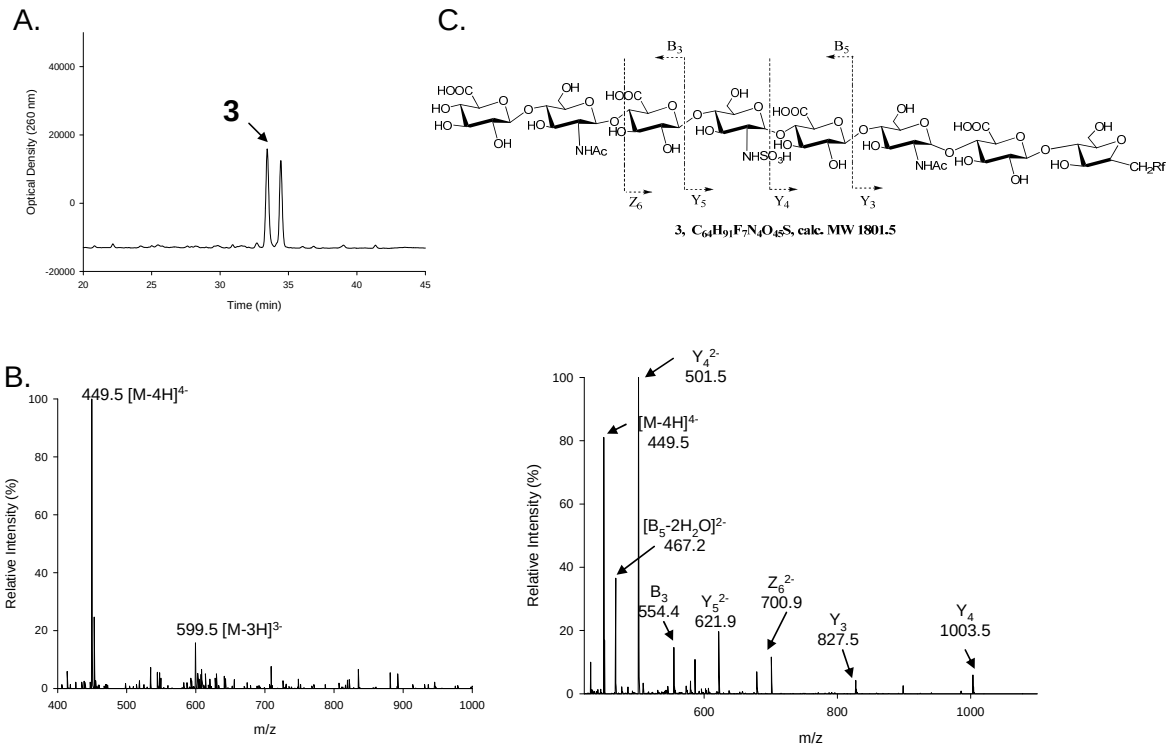

Fig 32. Structural characterization of octasaccharide **3**. Panel **A** shows the HPLC chromatogram of octasaccharide **3** using a C_{18} column under reverse phase condition. Panel **B** shows the mass spectrometry spectrum of octasaccharide **3**. The MS analysis is conducted by ESI-MS in negative mode. MS analysis revealed a molecular weight of 1801.8 Da in close agreement to the calculated mass of 1801.5 Da. Panel **C** shows MS/MS of octasaccharide **3**. MS/MS analysis (precursor ion selection at m/z 449.5) confirmed the position of the GlcNS residues in **3** from the two characteristic daughter ions, Y_5^{2-} (*m/z*, 621.9) and B_3 (*m/z*, 554.4), products of the cleavage of an internal glycosidic linkage. The fragmentation pattern is depicted in the top. The product ions in MS/MS data were labeled according to the Domon-Costello nomenclature. Rf is the fluorous tag.

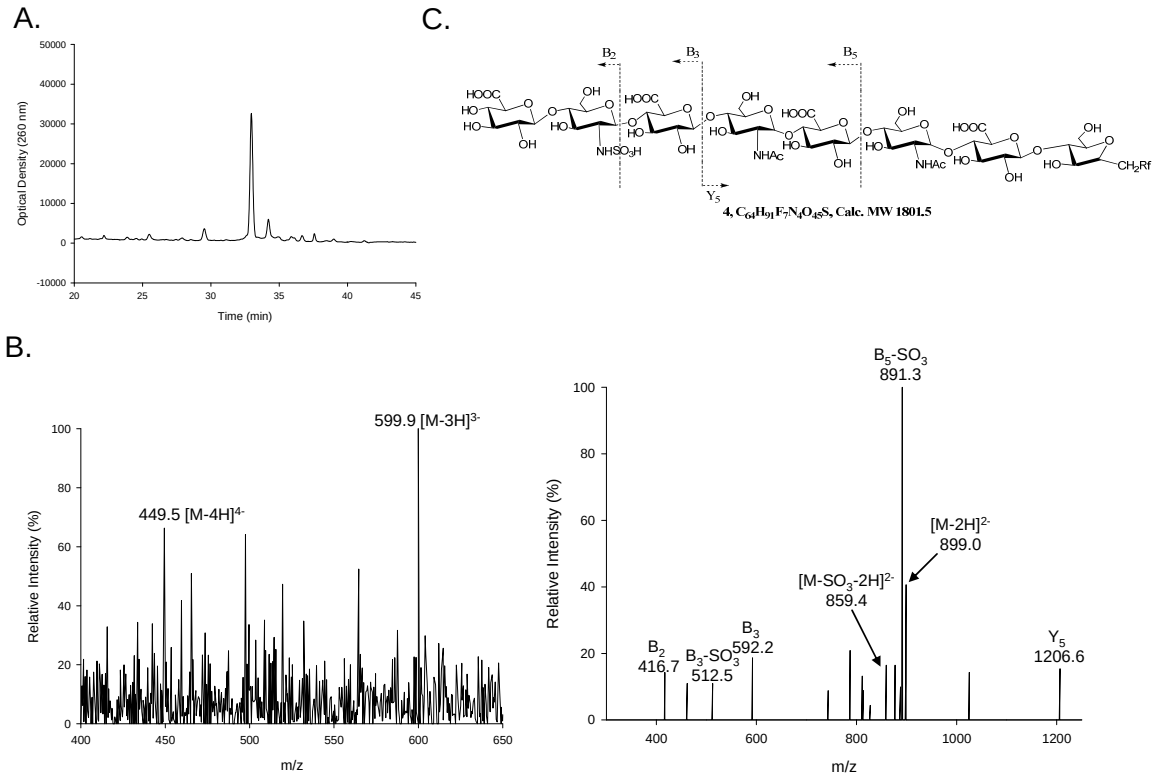

Fig 33. Structural characterization of octasaccharide **4**. Panel **A** shows the HPLC chromatogram of octasaccharide **4** using a C_{18} column under reverse phase condition. Panel **B** shows the mass spectrometry spectrum of octasaccharide **4**. The MS analysis is conducted by ESI-MS in negative mode. MS analysis revealed a molecular weight of 1802.1 Da in close agreement to the calculated mass of 1801.5 Da. Panel **C** shows MS/MS of octasaccharide **4**. MS/MS analysis (precursor ion selection at m/z 449.5) confirmed the position of the GlcNS residues in **4** from the two characteristic daughter ions, Y_5 (*m/z*, 1206.6) and B_3 (*m/z*, 592.2), products of the cleavage of an internal glycosidic linkage. The fragmentation pattern is depicted in the top. The product ions in MS/MS data were labeled according to the Domon-Costello nomenclature. Rf is the fluorous tag.

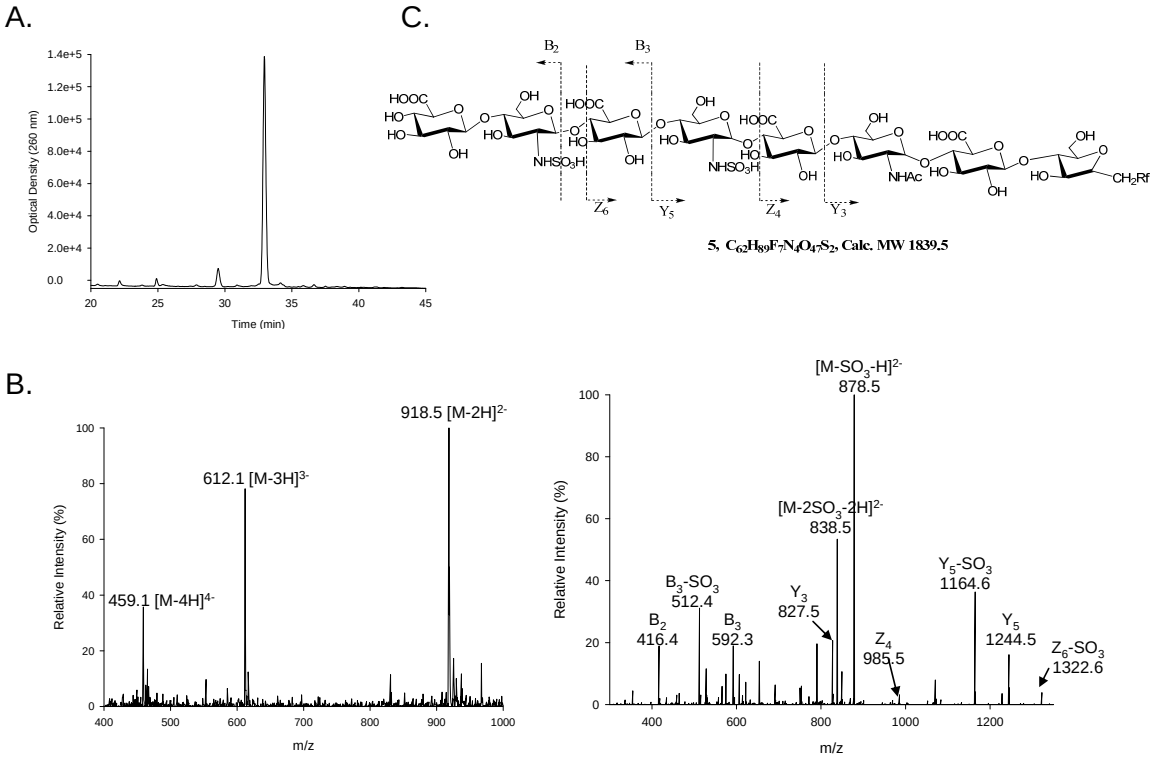

Fig 34. Structural characterization of octasaccharide **5**. Panel **A** shows the HPLC chromatogram of octasaccharide **5** using a C_{18} column under reverse phase condition. Panel **B** shows the MS spectrum of octasaccharide **5**. The MS analysis is conducted by ESI-MS in negative mode. MS analysis revealed its molecular weight to be 1839.6 Da in close agreement to the calculated mass of 1839.5 Da. Panel **C** shows MS/MS of octasaccharide **5** (precursor ion selection at m/z 459.1). MS/MS analysis confirmed the position of the GlcNS residues in **5** from the two characteristic daughter ions, Y_5 (*m/z*, 1244.5) and B_3 (*m/z*, 592.3), products of the cleavage of an internal glycosidic linkage. The fragmentation pattern is depicted in the top. The product ions in MS/MS data were labeled according to the Domon-Costello nomenclature. Rf is the fluorous tag.

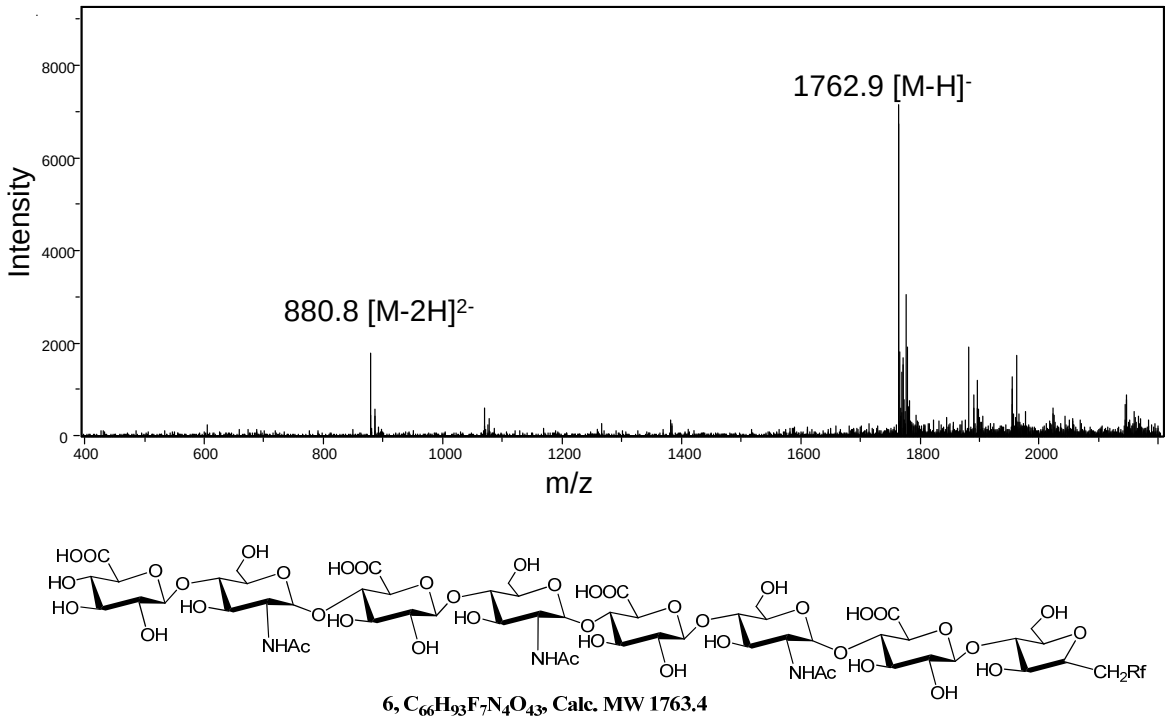

Fig 35. Structural characterization of octasaccharide **6**. The MS analysis is conducted by ESI-MS in negative mode. MS analysis revealed a molecular weight of 1763.8 for octasaccharide **6** in close agreement to the calculated mass of 1763.4 Da. Rf is the fluorous tag.

Section 6. Conclusion

The current study demonstrates the feasibility of a total synthesis of structurally defined HS oligosaccharides using a chemoenzymatic approach. This method is capable of synthesizing oligosaccharides with different *N*-sulfation patterns and structures by transferring UDP-sugars onto an easily prepared disaccharide acceptor. A key advance involves the utilization of an unnatural UDP-donor that allows the controlled placement of

GlcNS and GlcNAc residues throughout the oligosaccharide backbone. The GlcNS/GlcNAc patterning likely controls the subsequent positioning of *O*-sulfo groups.

One challenge in using oligosaccharides for the substrate specificity study is to purify the products from the reaction mixture. The application of a fluorous tag at the reducing end of the substrate allows us to obtain salt-free oligosaccharides in much fewer steps with very high efficiency. For example, we can prepare about 100 μg pure *N*-sulfated octasaccharide **5** in only eight steps starting from the tagged disaccharide **7** with about 30% yield. The purified oligosaccharides are also amendable for the analysis by ESI-MS and MS/MS as demonstrated in this project.

Chapter IV SYNTHESIS OF 6-*O*-SULFO OLIGOSACCHARIDES

Section 1. Introduction

In Chapter III, an octasaccharide library with different *N*-sulfation patterns was synsthesized. However, whether this method is capable of further converting to oligosaccharides with *O*-sulfo group is unclear. In this chapter, the *N*-sulfo oligosaccharides are modified with 6OSTs to prepare different oligosaccharides with defined 6-*O*-sulfation patterns.

Section 2. *N*-sulfo-6-*O*-sulfo oligosaccharides

Preparation of *N*-sulfo-6-*O*-sulfo hexasaccharides

The synthesis of *N*-sulfo-6-*O*-sulfo hexasacchride was carried out by modifying *N*-sulfo hexasaccharide **27** with 6OSTs using ^{35}S-labeled PAPS as a sulfo donor, permitting to introduce ^{35}S-label for purification and characterization. The 6-*O*-sulfo hexasaccharide **29, 30** were prepared by controlling the amount of PAPS. Hexasaccharide **29** carrying only one 6-*O*-sulfo group was successfully prepared under the condition that insufficient amount of PAPS was added. In contrast, if excess amount of PAPS was added, two 6-*O*-sulfo groups were introduced to form hexsaccahride **30** (Figure 36). The tagged 6-*O*-sulfo hexasaccharides

were initially purified by a C_{18} column under reverse phase HPLC (RP-HPLC) conditions. Hexasaccharide was then analysis by a DEAE-HPLC column. Both **29** and **30** was resolved as a symmetric peak by DEAE-HPLC. However, **29** and **30** exhibit different retention times, suggesting two hexasacchrides have different amount of 6-*O*-sulfo groups. Since **30** was eluted later than **29,** 6-*O*-sulfo hexasaccharide **29** likely has only one 6-*O*-sulfo group while 6-*O*-sulfo hexasaccharide **30** has two 6-*O*-sulfo groups (Figure 37).

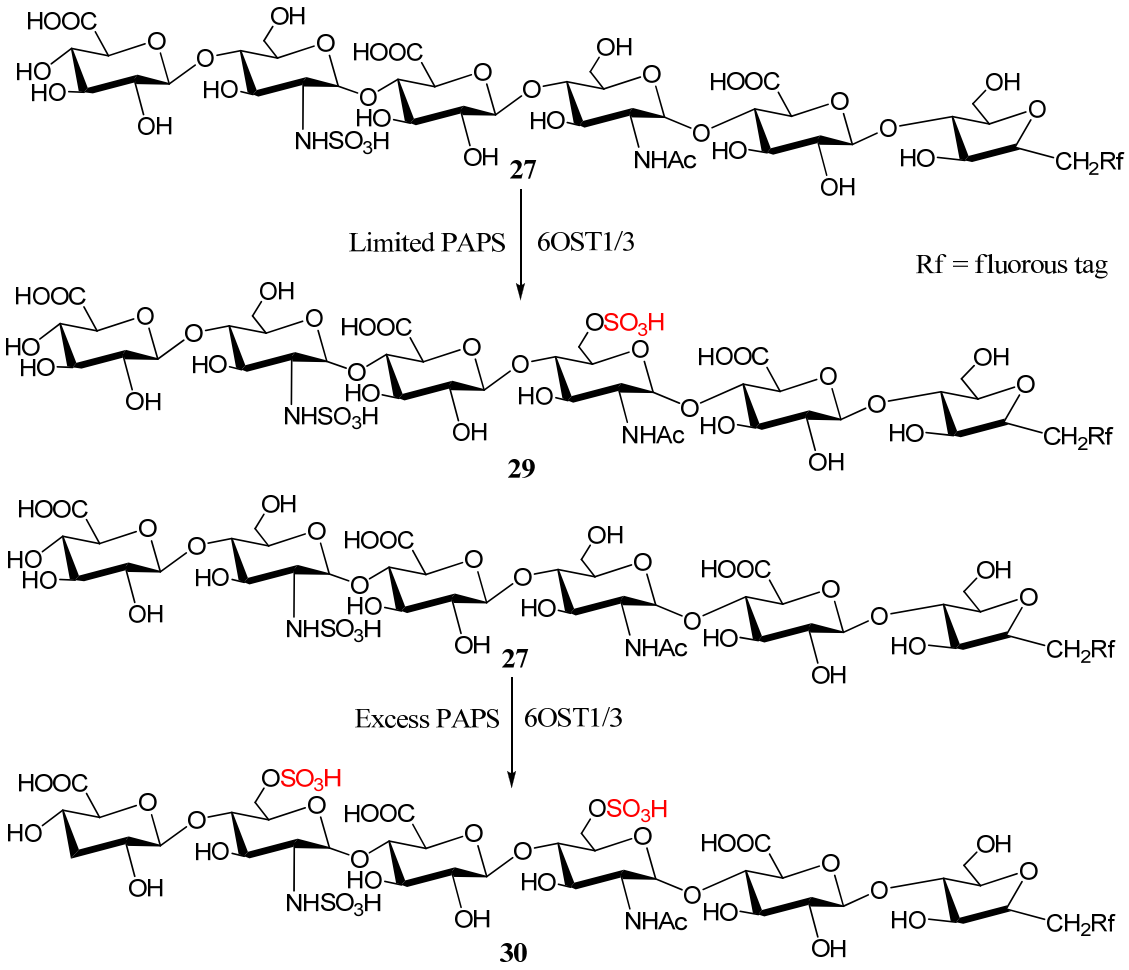

Fig 36. Preparation of *N*-sulfo-6-*O*-sulfo hexasaccharide **29** and **30**. In preparation of **29**, insufficient amount PAPS was applied while excess amount of PAPS was applied in preparation of **30**. The 6-*O*-[^{35}S]sulfo group was colored in red to indicate the site of radioactive sulfate. Rf is the fluorous tag.

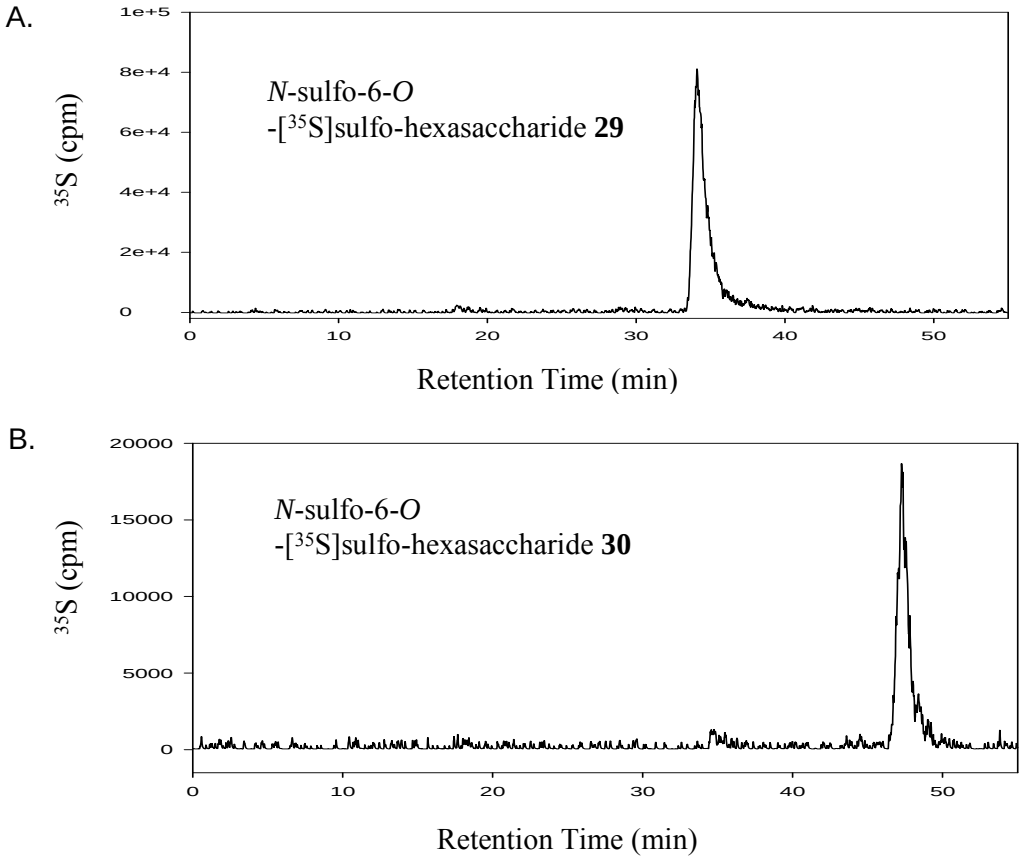

Fig 37. HPLC analysis of 6-*O*-sulfo hexasaccharide **29** and **30**. Panel **A** shows the HPLC chromatogram of 6-*O*-[^{35}S]sulfo-labeled hexasaccharide **29** using a DEAE-HPLC column. Panel **B** shows the HPLC chromatogram of 6-*O*-[^{35}S]sulfo-labeled hexasaccharide **30** using a DEAE-HPLC column. The HPLC chromatogram shows **29** and **30** have different retention time, hexasaccharide **29** eluted at 35 min while hexasaccharide **30** eluted at 48 min. These results suggested **29** and **30** have different amount of 6-*O*-sulfo groups.

Characterization of *N*-sulfo-6-*O*-sulfo hexasaccharides

Hexasaccharide **29** was analyzed by disaccharide analysis to elucidate the structure. The reaction mixture contained approximately 50,000 cpm **29**, 50 mM NaH_2PO_4, pH 7.0, 30 μL Hep I, 10 μL Hep II and 10 μL Hep III proteins in a total volume of 250 μL. The reaction was incubated at 37 °C for 2 days, another dose of Hep I, II and III was added after initial 24 hours incubation. The disaccharide sample was then analyzed by using a C_{18} column under

RPIP-HPLC conditions, which was resolved as a single symmetric peak by HPLC at 18 minutes, indicating a ΔUA-GlcNAc6S group, but not ΔUA-GlcNS6S (Figure 38). Therefore, the structure of **29** was GlcUA-GlcNS-GlcUA-GlcNAc6S-GlcUA-AnMan-Rf.

Since hexasaccharide **30** has two 6-*O*-sulfo groups, the structure of **30** should be GlcUA-GlcNS6S-GlcUA-GlcNAc6S-GlcUA-Anman-Rf. The hexasaccharide **30** was resynthesized by the same procedure as described previously using 80 μM ublabeled PAPS as sulfo donor. The sample was analyzed by MS and MS/MS. MS analysis revealed the molecular weight to be 1582.7 Da in close agreement to the calculated mass of 1582.3 Da, confirming the structure of the hexasaccharide **30**. The structure of *N*-sulfo-6-*O*-sulfo hexsaccahride was further proved by MS/MS. MS/MS analysis confirmed the position of the GlcNS6S residues from the two characteristic daughter ions, Y_3 (*m/z*, 907.4) and [B_3-SO_3] (*m/z*, 592.3), products of the cleavage of internal glycosidic linkage (Figure 39). These studies demonstrated the tagged hexasaccharide with defined 6-*O*-sulfation patterns could be synthesized by taking advantage of 6OSTs substrate specificity.

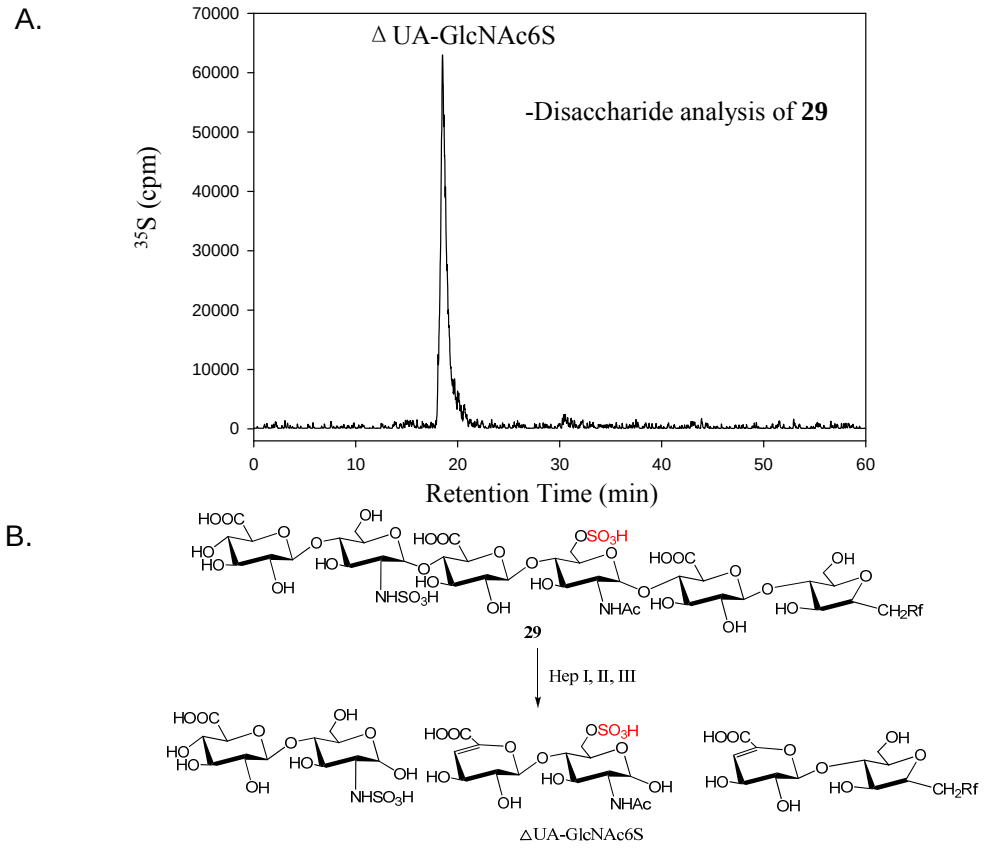

Fig 38. Determination of the structure for 6-*O*-sulfo hexasaccharide **29**. Panel **A** shows the HPLC chromatogram of the disaccharide analysis of **29** using a C_{18} column under RPIP-HPLC conditions. Only a single ^{35}S-labeled disaccharide (ΔUA-GlcNAc6S) was observed, suggesting that **29** is GlcUA-GlcNS-GlcUA-GlcNAc6S-GlcUA-Anman-Rf. Panel **B** shows the reaction involved in the disaccharide analysis of **29**. The 6-*O*-[^{35}S]sulfo group was colored in red to indicate the site of radioactive sulfate. The identitiy of ^{35}S-labeled disaccharide was confirmed by coeluting with authetic disaccharide standard. Rf is the fluorous tag.

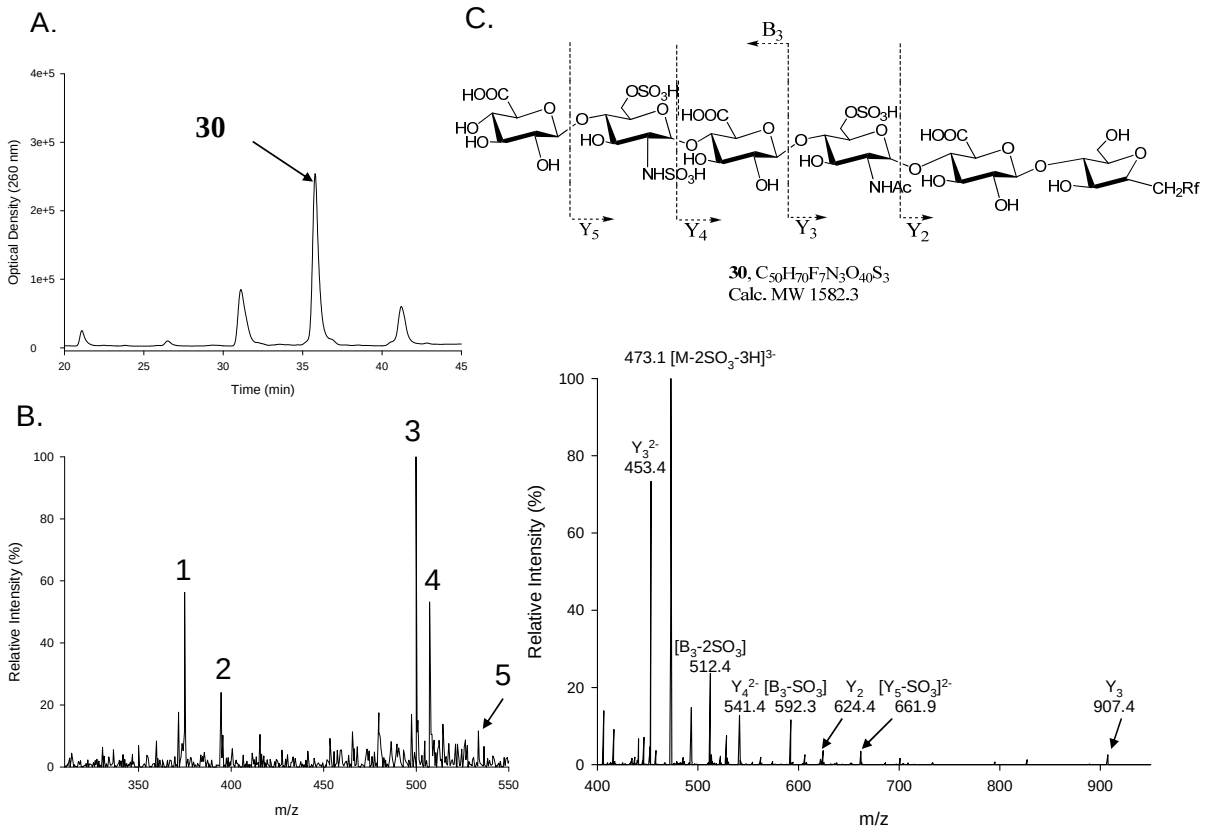

Fig 39. Structural characterization of hexasaccharide **30**. Panel **A** shows the HPLC chromatogram of octasaccharide **3** using a C_{18} column under reverse phase condition. Panel **B** shows the MS spectrum of hexasaccharide **30**. The MS analysis is conducted by ESI-MS in negative mode. Molecular ions are labeled as 1 through 5, where 1 is 374.9 $[M\text{-}SO_3\text{-}4H]^{4-}$; 2 is 394.6 $[M\text{-}4H]^{4-}$; 3 is 499.9 $[M\text{-}SO_3\text{-}3H]^{3-}$; 4 is 507.2 $[M+Na\text{-}SO_3\text{-}4H]^{3-}$; 5 is 533.7 $[M+Na\text{-}4H]^{3-}$. Panel **C** shows MS/MS of hexasaccharide **30**. The fragmentation pattern is depicted on the bottom. The product ions in MS/MS data were labeled according to the Domon-Costello nomenclature. Rf is the fluorous tag.

Preparation of *N*-sulfo-6-*O*-sulfo octasaccharide

The 6-*O*-sulfo octasaccharide **31** was prepared by incubating 6OST1 and 6OST3 with *N*-sulfo octasaccharide substrate **5**. MS analysis revealed a molecular weight of 2080.7 Da in close agreement to the calculated mass of 2079.7 Da. The detailed structure of octasaccharide **31** was analyzed by MS/MS. MS/MS analysis confirmed the position of the

GlcNS6S residues from the two characteristic daughter ions, $[Y_6–SO_3]^{4-}$ (*m/z*, 374.7) and B_4^{2-} (*m/z*, 497.4), products of the cleavage of internal glycosidic linkage (Figure 40). These studies demonstrated different size of tagged oligosaccharide could be fully *O*-sulfated by 6OSTs.

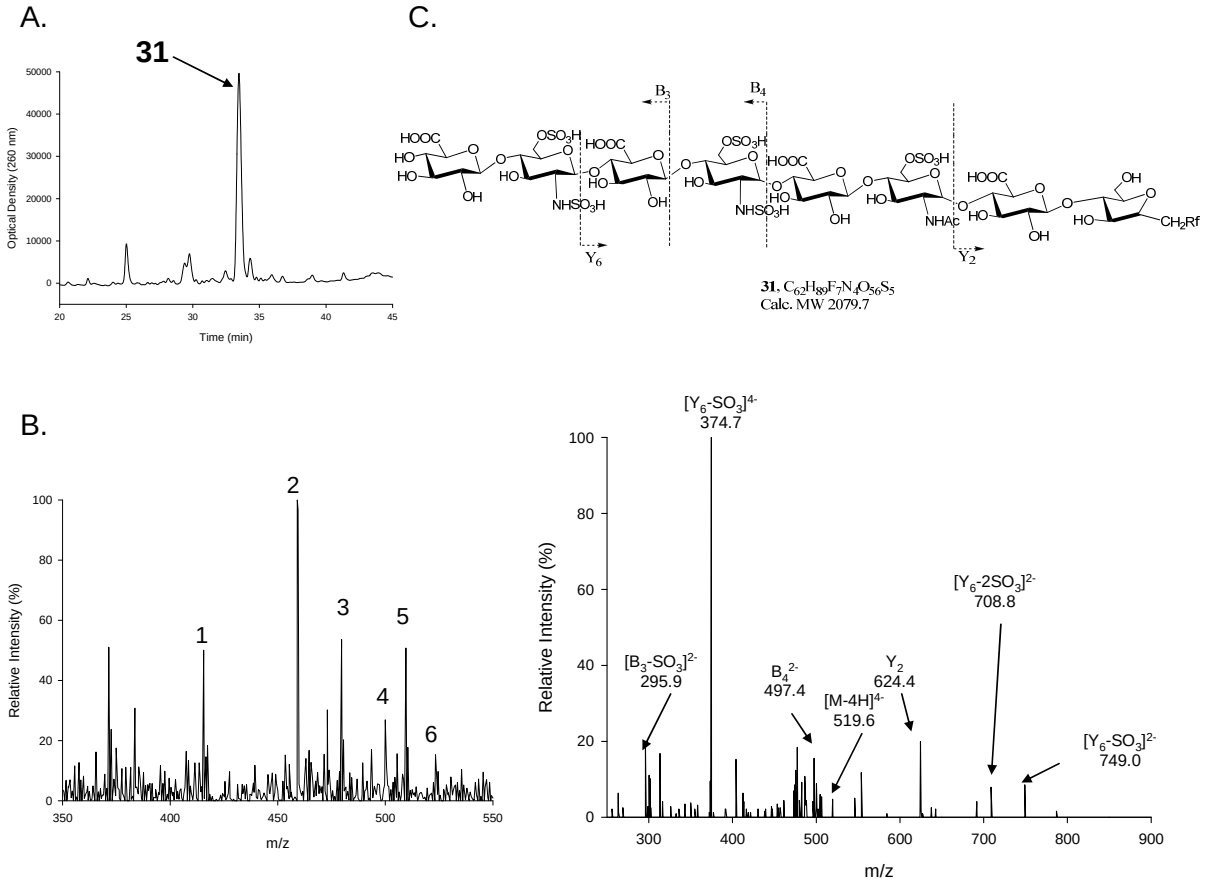

Fig 40. Structural characterization of octasaccharide **31**. Panel **A** shows the HPLC chromatogram of octasaccharide **3** using a C_{18} column under reverse phase condition. Panel **B** shows the MS spectrum of octasaccharide **31**. The MS analysis is conducted by ESI-MS in negative mode. Molecular ions are labeled as 1 through 6, where 1 is 415.6 $[M-5H]^{5-}$; 2 is 459.1 $[M-3SO_3-4H]^{4-}$; 3 is 479.7 $[M-2SO_3-4H]^{4-}$; 4 is 500.0 $[M-SO_3-4H]^{4-}$; 5 is 509.6 $[M+2Na-SO_3-6H]^{4-}$; 6 is 523.4 $[M+Na-5H]^{4-}$. Panel **C** shows MS/MS of octasaccharide **31**. The fragmentation pattern is depicted on the bottom. The product ions in MS/MS data were labeled according to the Domon-Costello nomenclature. Rf is the fluorous tag.

Fluorous tag does not bind with AT

The fluorous tagged oligosaccharide library could be used for microarray for probing the structural selectivity of HS for interacting wth proteins, especially with AT. However, it is possible that nonspecific interaction between protein and fluorous tag exist. Therefore, *N*-sulfo-6-*O*-[^{35}S]sulfo hexasaccharide **30** was applied for AT-binding assay. Since hexasaccharide **30** has no 3-O-sulfation, it should not bind to AT. A nonasaccharide **32** from Dr. Yongmei Xu with known AT-binding activity was used as a positive control (Figure 41) while [^{35}S] labeled PAPS worked as a negative control. The results were summarized in Table 3. The result indicates there is no binding affinity of *N*-sulfo-6-*O*-[^{35}S]sulfo hexasaccharide **30** to the AT, suggesting the fluorous tag is not able to increase the binding of tagged oligosaccharide to AT through nonspecific interactions. However, it's not clear whether the tag will prohibit the AT-binding.

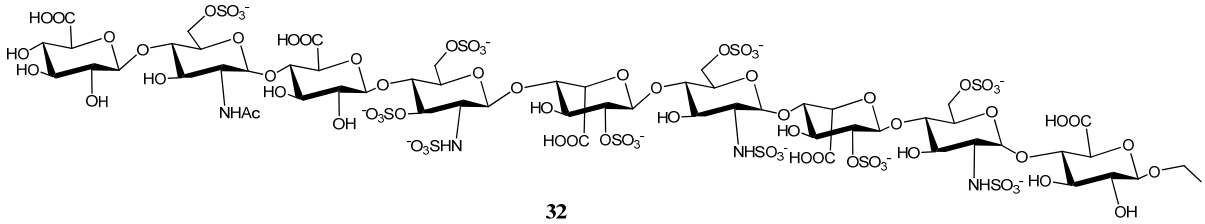

32

Fig 41. Structure of nonasaccharide **32**. Nonasaccharide **32** is received from Dr. Yongmei Xu with known AT-binding activity.

Table 3. AT binding assay for **30**, **32** and [^{35}S] PAPS.

	Amount of samples (cpm)	Binding affinity (%)
Nonasaccharide **32**	4820	35%
hexasaccharide **30**	3820	< 1%
[^{35}S] PAPS	7690	< 1%

Section 3. Conclusion

In this study, two different hexasaccharides **29** and **30** have been successfully prepared. The HPLC indicating that hexasacchride **29** only has one 6-*O*-sulfo group, however, it could be GlcNAc6S or GlcNS6S or mixture of both. To our surprise, disaccharide analysis of **29** only gave ΔUA-GlcNAc6S, indicating **29** is GlcUA-GlcNS-GlcUA-GlcNAc6S-GlcUA-Anman-Rf. This could be due to the reason that the GlcNAc residue is in the middle of hexasaccharide, favoring the substrate recognition. Therefore, 6OSTs prefer to modify GlcNAc residue first if the amount of PAPS is not sufficient. If excess amount of PAPS applied, the tagged hexasaccharide could be fully *O*-sulfated by 6OSTs to generate hexasaccharide **30**. These studies demonstrated that we could prepare oligosaccharide with different 6-*O*-sulfation patterns. The synthesis of octasaccharide **31** demonstrated tagged *N*-sulfo oligosaccharide of different size could be fully *O*-sulfated by 6OSTs.

The success of this project can help to develop a reliable protocol to position the remaining modifications, such 2-*O*- and 3-*O*-sulfation as well as IdoUA. For example, we can investigate the substrate specificities of these enzymes in greater details using a series of structurally defined *N*-sulfo oligosaccharides. The studies from 6OST modified oligosaccharide demonstrate the potential of this approach.

While this method is fully capable of synthesizing large libraries of diverse HS oligosaccharide structures, it is currently limited by the time and effort required for the full structural characterization of the resulting oligosaccharide products. More studies will be performed to generate structurally defined oligosaccharides with various biological functions.

Chapter V SYNTHESIS OF AT-BINDING OLIGOSACCHARIDES

Section 1. Introduction

In this chapter, in collaboration with Dr. Yongmei Xu, a reliable protocol has been developed to position the remaining modifications, such as 3-*O*- and 6-*O*-sulfation. Here, the introduction of *O*-sulfo groups was completed using *O*-sulfotransferases. Deca, undeca and dodecasaccharides with *N*-sulfo groups was synthesized, as the actions of *O*-sulfotransferases require the presence of GlcNS residues. The synthesis began with the disaccharide acceptor **1**. The disaccharide will be extended to a large oligosaccharide with *N*-sulfation. As mentioned previously, $GlcNCOCF_3$ residue will be incorporated into the oligosaccharides by KfiA. The $-COCF_3$ group will selectively be removed by mild-base and is then *N*-sulfated by NST. Furthermore, we will modify the *N*-sulfated oligosaccharides by 6OSTs and 3OSTs to design a structurally defined dodecasaccharide with AT-binding activity (Figure 42).

It's known that the AT-binding correlates to HS anticoagulant activity. Our lab previously demonstrated that an AT-binding HS does not require the presence of IdoUA or IdoUA2S residues, which simplified the synthesis of AT-binding HS (123). However, the minimum length and the precise structure of this novel AT-binding domain were not known. The purified oligosaccharides have been examined for their AT binding activity.

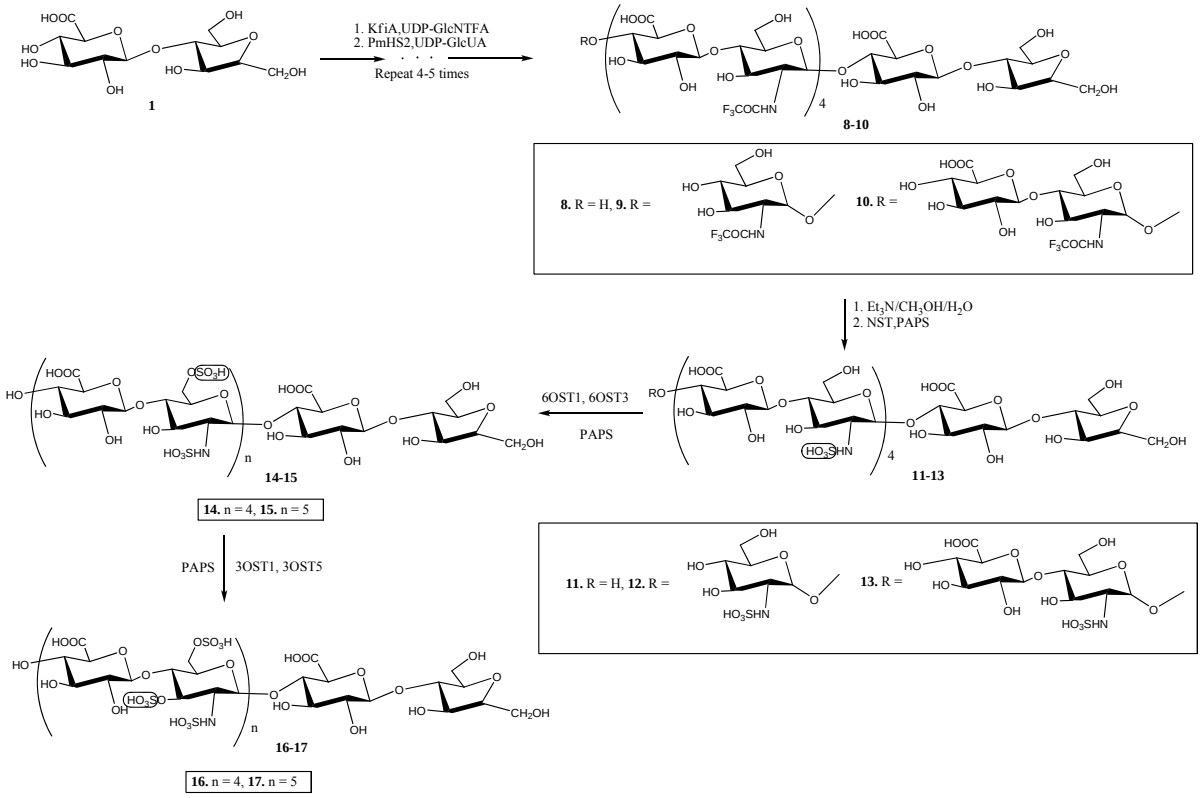

Fig 42. Scheme for the synthesis of oligosaccharides. The synthesis is begun with a disaccharide **1** (GlcUA-AnMan). The product was then elongated to the decasaccharide (**8**), undecasaccharide (**9**), dodecasaccharide (**10**) as described. $GlcNCOCF_3$ residue will be incorporated into the oligosaccharides by KfiA. The $-COCF_3$ group has selectively been removed by mild-base to yield the $GlcNH_2$ unit. The resultant $GlcNH_2$ unit was then *N*-sulfated by NST to prepare decasaccharide (**11**), undecasaccharide (**12**), dodecasaccharide (**13**). The synthesized *N*-sulfo decasaccharide (**11**) and dodecasaccharide (**13**) were modified by 6OST1 and 6OST3 to prepare *N*-sulfo 6-*O*-sulfo decasaccharide (**14**) and dodecasaccharide (**15**), respectively and further modified by 3OST1 and 3OST5 to prepare 3-*O*-sulfo decasaccharide (**16**) and dodecasaccharide (**17**), respectively.

Section 2. Preparation of AT-Binding oligosaccharides

Preparation of backbone oligosaccharides

Disaccharide acceptor **1** was extended to backbone decasaccharide **8**, undecasaccharide **9** and dodecasaccharide **10** respectively using the UDP-GlcNTFA and UDP-GlcUA donors. The structures of the backbone oligosaccharides were confirmed by

LC-MS (Table 4). In eight enzymatic steps at the milligram-scale, a disaccharide was converted to a decasaccharide. Further extension to undeca- and dodecasaccharide was also highly effective. While some unexpected partial detrifluoroacetylation occurred for those backbones, it did not affect the subsequent synthesis to prepare *N*-sulfated oligosaccharides.

Table 4. List of the synthesized oligosaccharide backbones

Oligosaccharides	Amount (mg)	Molecular formula	Molecular weight (Da) [a]	
			Calculated	Determined
Decasaccharide **8**	4.5	$C_{64}F_6H_{94}N_4O_{53}$	1881.4	1882.2
Undecasaccharide **9**[b]	2.1	$C_{72}F_9H_{104}N_5O_{58}$	2138.6	2138.0
Dodecasaccharide **10**[b]	0.9	$C_{78}F_9H_{112}N_5O_{64}$	2314.7	2314.8

a. Oligosaccharides **8**-**9** lost two trifluoroacetyl groups during the purification. The calculated molecular mass was based on the lost of two trifluoroacetyl groups.
b. Only half of the decasaccharide **8** was converted to the undecasaccharide **9**. Similarly, only half of the undecasaccharide **9** was converted to the dodecasaccharide **10**.

Preparation of *N*-sulfo oligosaccharides

Conversion of the GlcNTFA in decasaccharide **8**, undecasaccharide **9** and dodecasaccharide **10** to $GlcNH_2$ were through de-trifluoroacetylation as previously described, the samples were further treated with NST using [^{35}S]PAPS afforded *N*-[^{35}S]sulfated products. The oligosaccharides showed predominantly a single ^{35}S-peak on high resolution DEAE-HPLC chromatography, suggesting the products were homogeneous (Figure 43A, C and E). The *N*-sulfo oligosaccharides (**11** to **13**) were resynthesized using NST and unlabeled PAPS and purified by DEAE-HPLC. The results of ESI-MS analysis of the unlabeled oligosaccharides (Figure 43B, D and F) confirmed that all three compounds are fully *N*-sulfated with the structures shown in Figure 42.

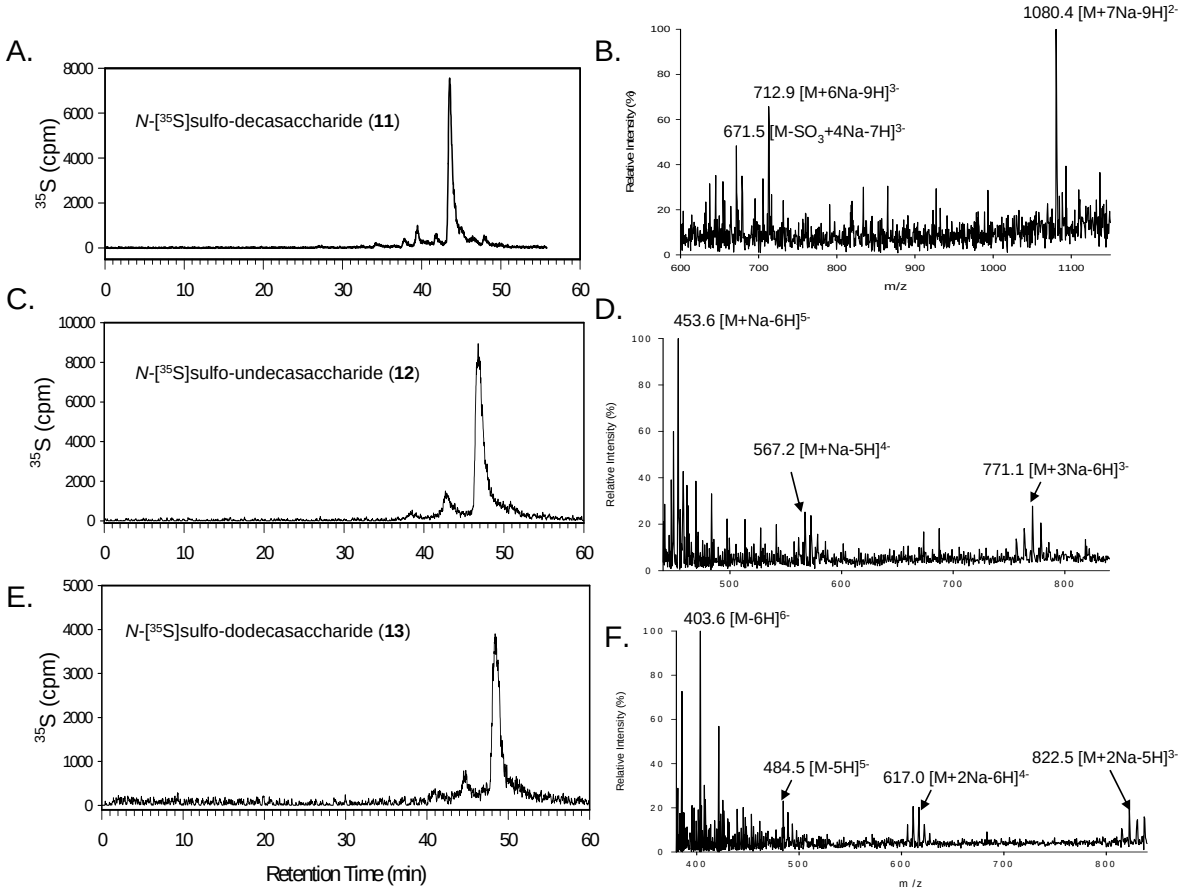

Fig 43. Structural characterization of *N*-sulfo oligosaccharides **11-13**. Panel **A, C, E** shows the HPLC chromatogram of decasaccharide **11**, undecasaccharide **12** and dodecasaccharide **13** respectively using a DEAE-column. Panel **B, D, F** shows the MS spectrum of decasaccharide **11**, undecasaccharide **12** and dodecasaccharide **13** respectively. The MS analysis is conducted by ESI-MS in negative mode. MS analysis revealed that decasaccharide **11**, undecasaccharide **12** and dodecasaccharide **13** had molecular weights of 2009.3 Da, 2250.7 Da and 2427.4 Da, respectively, consistent with a calculated mass of 2009.7 Da, 2250.9 Da and 2427.0 Da.

Preparation of *N*-sulfo-6-*O*-sulfo deca and dodecasaccharide

Next, we introduced 6-*O*-sulfo groups using a mixture of 6OST1 and 6OST3 affording the *N*-sulfo-6-*O*-sulfo decasaccharide **14** and *N*-sulfo-6-*O*-sulfo-dodecasaccharide **15** (Figure 44). DEAE-HPLC analysis of the ^{35}S-labeled oligosaccharide displayed a symmetric ^{35}S-peak, suggesting that the 6-*O*-sulfated product was homogeneous (Figure 44A and C). Both nonradioactively labeled decasaccharide **14** and dodecasaccharide **15** were resynthesized using unlabeled PAPS, purified by DEAE-HPLC and subjected to MS analysis. Data of ESI-MS analysis revealed that decasaccharide **14** and dodecasaccharide **15** (Figure 44B and D) had molecular weights of 2329.9 Da and 2828.1 Da, respectively, consistent with a calculated mass of 2329.9 Da and 2827.3 Da for a decasaccharide with eight sulfo groups and a dodecasaccharide with ten sulfo groups.

The disaccharide analysis of decasaccharide **14** and dodecasaccharide **15** carrying site-specific [^{35}S]sulfo groups also confirmed their structures. Here, the [^{35}S]sulfo groups were selectively introduced at the *N*-[^{35}S]sulfation sites of the oligosaccharides **14** and **15**. The oligosaccharides were then degraded to the disaccharides using heparin lyases followed by the analysis using RPIP-HPLC. We observed two types of disaccharides, namely GlcUA-[*N*-^{35}S]GlcNS6S and ΔUA-[*N*-^{35}S]GlcNS6S. Furthermore, the molar ratio of ΔUA-GlcNS6S and GlcUA-GlcNS6S was 2.9 and 3.5 for decasaccharide **14** and dodecasaccharide **15**, respectively. It should be noted that the theoretical value of the ratio of two disaccharides is 3 for the decasaccharide **14** and 4 for the dodecasaccharide **15** respectively (Table 5).

Table 5. Summary of disaccharide analysis of decasaccharide **14** and dodecasaccharide **15**

Oligosaccharides	Method for degradations	Composition [2]	Measured molar ratio
N-[^{35}S]sulfo-6-*O*-sulfo decasaccharide **14**[1]	Heparin lyase I, II and III	GlcUA-GlcNS6S and ΔUA-GlcNS6S	1 : 2.9 (1:3)[3]
N-[^{35}S]sulfo-6-*O*-sulfo dodecasaccharide **15**[1]	Heparin lyase I, II and III	GlcUA-GlcNS6S and ΔUA-GlcNS6S	1 : 3.5 (1: 4)[3]

1. The decasaccharide **14** was prepared by incubating the *N*-[^{35}S]sulfo decasaccharide **11** with 6OST1 and 6OST3. To this end, all the radioactive [^{35}S]sulfate was at the *N*-sulfo group. Likewise, the dodecasaccharide **15** was prepared by incubating the *N*-[^{35}S]sulfo dodecasaccharide **13** with 6OST1 and 6OST3.
2. Disaccharide analysis was carried out using reverse phase ion-pairing HPLC (RPIP-HPLC).
3. The numbers presented in parenthesis indicate the calculated values based on the proposed structures.

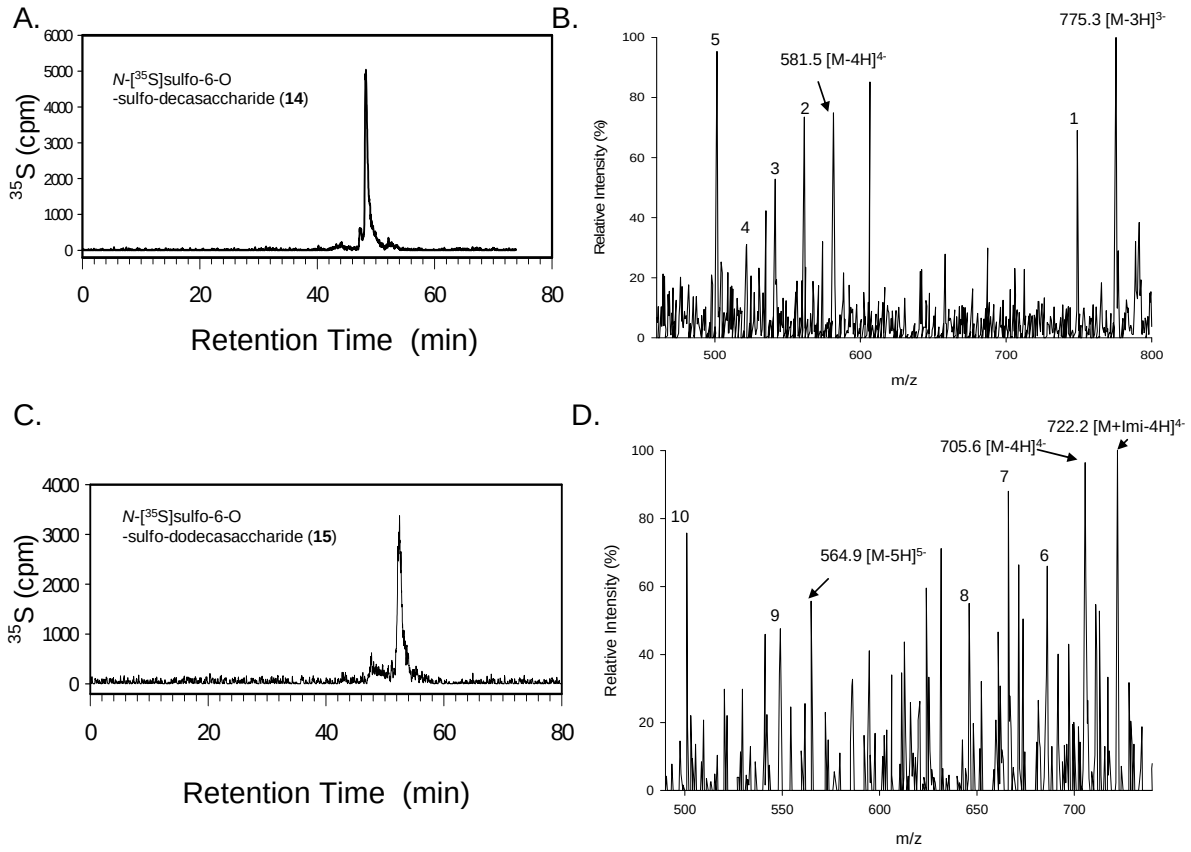

Fig 44. Structural characterization of decasaccharide **14** and dodecasaccharide **15**. Panel A shows the HPLC chromatogram of ^{35}S-labeled decasaccharide **14** using a DEAE-HPLC column. Panel **B** shows the MS spectrum of decasaccharide **14**. The MS analysis is conducted by ESI-MS in negative mode. The decasaccharide was purified by DEAE-HPLC, the purified decasaccharide was dialyzed against 20 mM ammonium acetate prior to the MS analysis. Additional molecular ions are labeled as 1 through 5, where 1 is 748.9 $[M\text{-}SO_3\text{-}3H]^{3-}$; 2 is 561.5 $[M\text{-}SO_3\text{-}4H]^{4-}$; 3 is 541.4 $[M\text{-}2SO_3\text{-}4H]^{4-}$; 4 is 521.8 $[M\text{-}3SO_3\text{-}4H]^{4-}$; 5 is 501.5 $[M\text{-}4SO_3\text{-}4H]^{4-}$. Panel **C** shows the HPLC chromatogram of ^{35}S-labeled dodecasaccharide **15** using a DEAE-HPLC column. Panel **D** shows the MS spectrum of dodecasaccharide **15**. The MS analysis is conducted by ESI-MS in negative mode. The decasaccharide was purified by DEAE-HPLC, the purified decasaccharide was dialyzed against 20 mM ammonium acetate prior to the MS analysis. Additional molecular ions are labeled as 6 through 10, where 6 is 686.1 $[M\text{-}SO_3\text{-}4H]^{4-}$; 7 is 666.1 $[M\text{-}2SO_3\text{-}4H]^{4-}$; 8 is 646.0 $[M\text{-}3SO_3\text{-}4H]^{4-}$; 9 is 549.0 $[M\text{-}SO_3\text{-}5H]^{5-}$; 10 is 501.0 $[M\text{-}4SO_3\text{-}5H]^{5-}$.

Preparation of oligosaccharides binding to AT

Next, we prepared oligosaccharides capable of binding to antithrombin (AT). The AT-binding correlates to HS anticoagulant activity. We previously demonstrated that an AT-binding HS does not require the presence of IdoUA or 2-*O*-sulfo-iduronic acid residues, which simplified the synthesis of AT-binding HS. However, the minimum length and the precise structure of this novel AT-binding domain were not known. We hypothesized that the preparation of decasaccharide **16** and dodecasaccharide **17** should provide insights on the structural requirement for this AT-binding site. Incubation of oligosaccharides **14** and **15** with 3OST1 and 3OST5 in the presence of [^{35}S]PAPS afforded ^{35}S-labeled decasaccharide **16** and dodecasaccharide **17**. The ^{35}S-labeled decasaccharide **16** and dodecasaccharide **17** were purified by DEAE-HPLC. Using a site-specific [^{35}S]sulfo-labeled technique followed by disaccharide analysis (Figure 45-50), we proved the structure of decasaccharide **16** to be (GlcUA-GlcNS3S6S)$_4$-GlcUA-AnMan (as shown in Figure 45) and dodecasaccharide **17** to be (GlcUA-GlcNS3S6S)$_5$-GlcUA-AnMan (as shown in Figure 48).

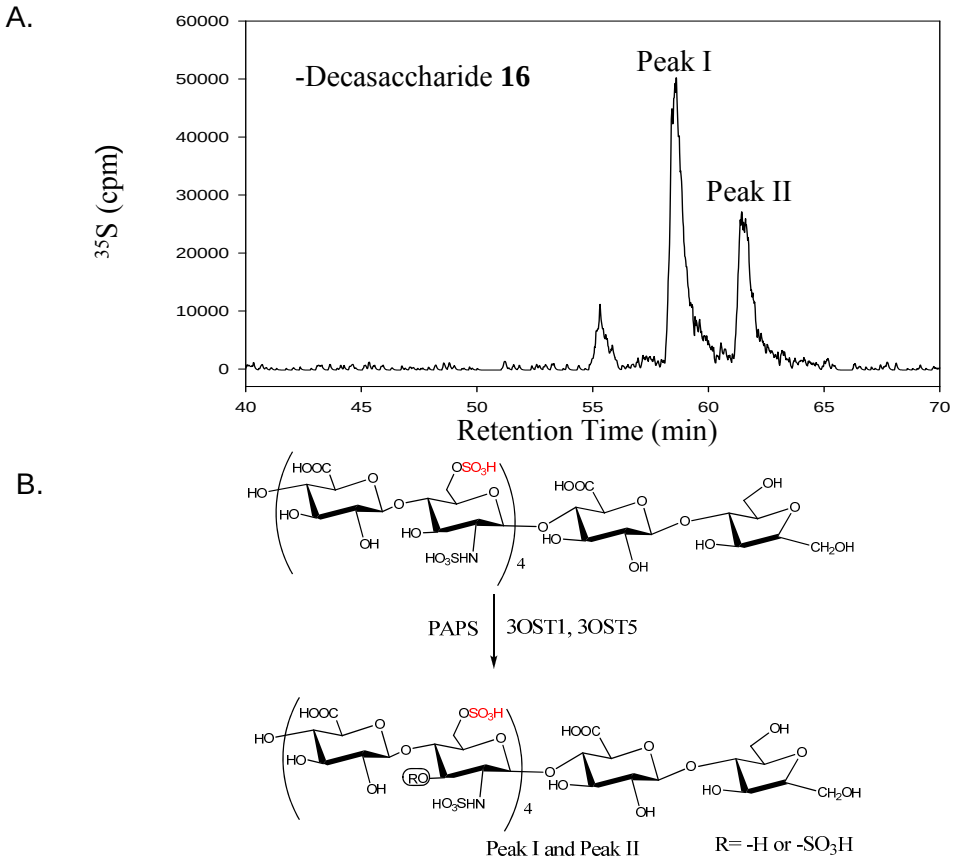

Fig 45. Preparation of 3-*O*-sulfo decasaccharide **16**. Panel **A** shows the HPLC chromatogram of 6-*O*-[^{35}S]sulfo-labeled decasaccharide **16** using a DEAE-HPLC column. The decasaccharide was prepared by incubating decasaccharide **14** with 3OST1 and 3OST5 as depicted in Panel **B**. Two major products, designated as Peak I and Peak II, were observed. Both components were purified and subjected to disaccharide analysis. The 6-*O*-[^{35}S]sulfo group was colored in red to indicate the site of radioactive sulfate.

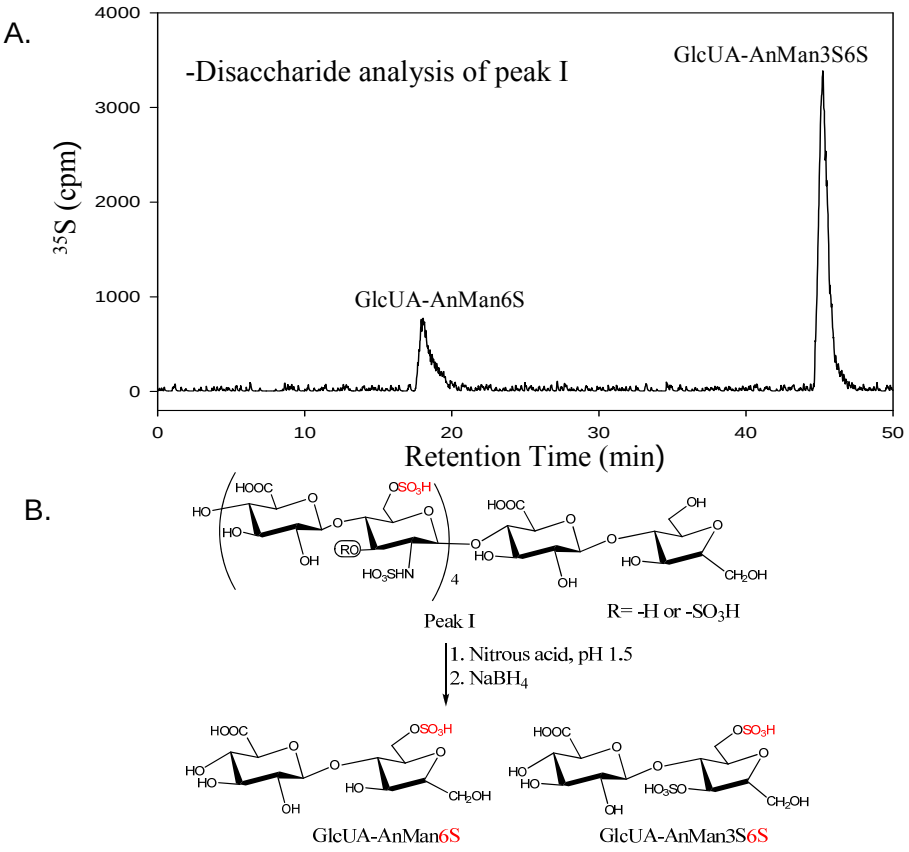

Fig 46. Determination of the structures of peak I for decasaccharide **16**. Panel **A** shows the HPLC chromatogram of the disaccharide analysis of Peak I using a C_{18} column under RPIP-HPLC conditions. Two ^{35}S-labeled disaccharides, including GlcUA-AnMan6S and GlcUA-AnMan3S6S, were observed. The data suggest that Peak I is a partially 3-*O*-sulfated decasaccharide. Because the molar ratio of those two disaccharides was 1: 3.4, we concluded that Peak I carries only three 3-*O*-sulfo groups. Panel **B** shows the reaction involved in the disaccharide analysis of Peak I. The 6-*O*-[^{35}S]sulfo group was colored in red to indicate the site of radioactive sulfate. To improve the clarity, nonradioactively labeled disaccharides resulted from nitrous acid degradation was not indicated.

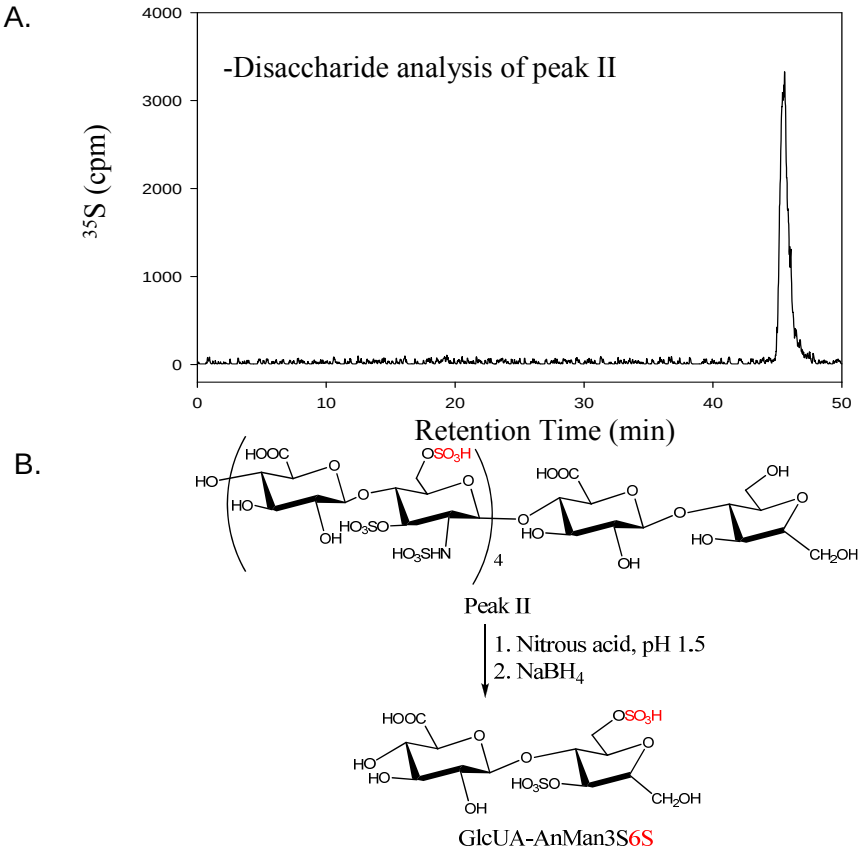

Fig 47. Determination of the structures of peak II for decasaccharide **16**. Panel **A** shows the HPLC chromatogram of the disaccharide analysis of Peak II using a C_{18} column under RPIP-HPLC conditions. Only a single ^{35}S-labeled disaccharide (GlcUA-AnMan3S6S) was observed, suggesting that Peak II is a fully 3-*O*-sulfo decasaccharide. Peak II was therefore designated as decasaccharide **16** for the antithrombin-binding study as described in the text. Panel **B** shows the reaction involved in the disaccharide analysis of Peak II. The 6-*O*-[^{35}S]sulfo group was colored in red to indicate the site of radioactive sulfate. To improve the clarity, nonradioactively labeled disaccharides resulted from nitrous acid degradation was not indicated.

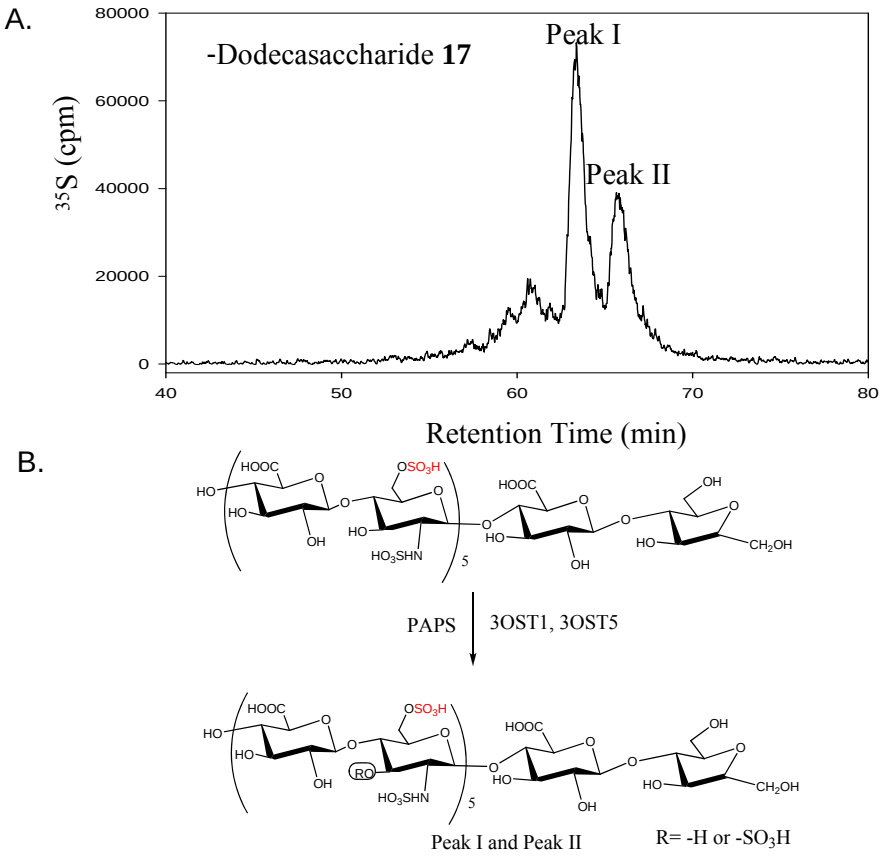

Fig 48. Preparation of 3-*O*-sulfo dodecasaccharide **17**. Panel **A** shows the HPLC chromatogram of 6-*O*-[^{35}S]sulfo-labeled dodecasaccharide **17** using a DEAE-HPLC column. The dodecasaccharide was prepared by incubating dodecasaccharide **15** with 3OST1 and 3OST5 as depicted in Panel **B**. Two major products, designated as Peak I and Peak II, were observed. Both components were purified and subjected to disaccharide analysis. We noted that the resolution of Peak I and II was not base-line separation as we obtained for the decasaccharide (Figure 45). The 6-*O*-[^{35}S]sulfo group was colored in red to indicate the site of radioactive sulfate.

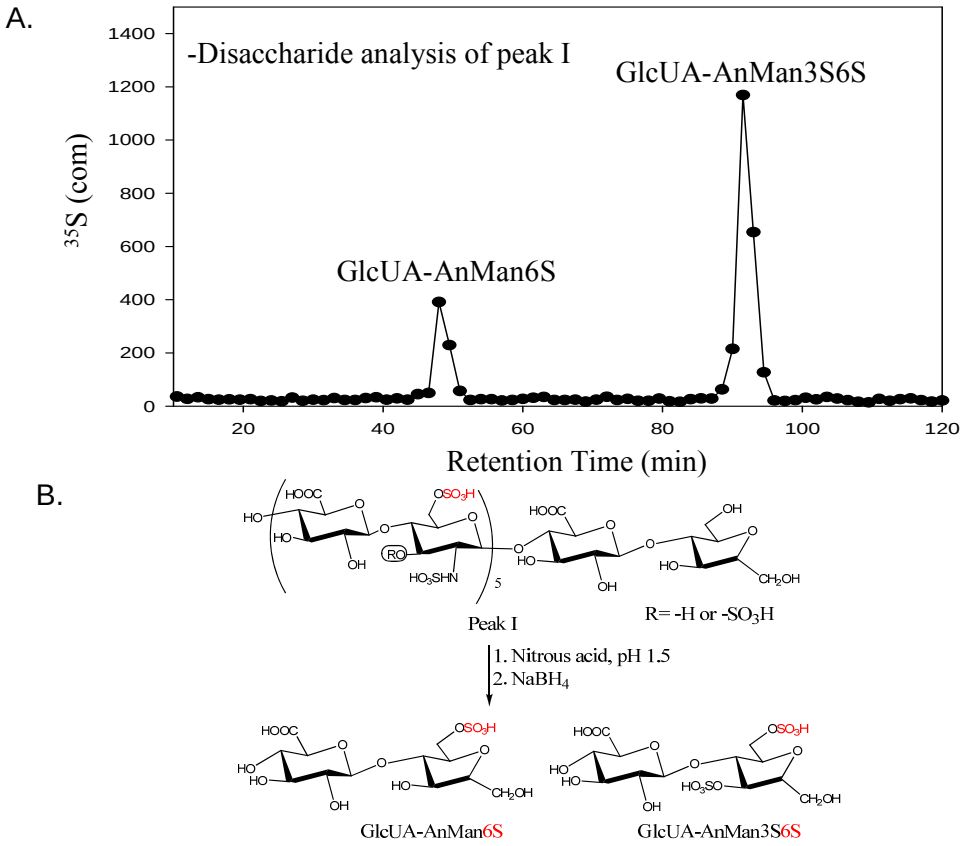

Fig 49. Determination of the structures of peak I for dodecasaccharide **17**. Panel **A** shows the HPLC chromatogram of the disaccharide analysis of Peak I using a C_{18} column under RPIP-HPLC conditions. Two ^{35}S-labeled disaccharides, including GlcUA-AnMan6S and GlcUA-AnMan3S6S, were observed. The data suggest that Peak I is a partially 3-*O*-sulfated dodecasaccharide. Because the molar ratio of those two disaccharides was 1: 3.7, we concluded that Peak I carries only four 3-*O*-sulfo groups. Panel **B** shows the chemical reaction involved in the disaccharide analysis of Peak I. The 6-*O*-[^{35}S]sulfo group was colored in red to indicate the site of radioactive sulfate. To improve the clarity, nonradioactively labeled disaccharides resulted from nitrous acid degradation was not indicated.

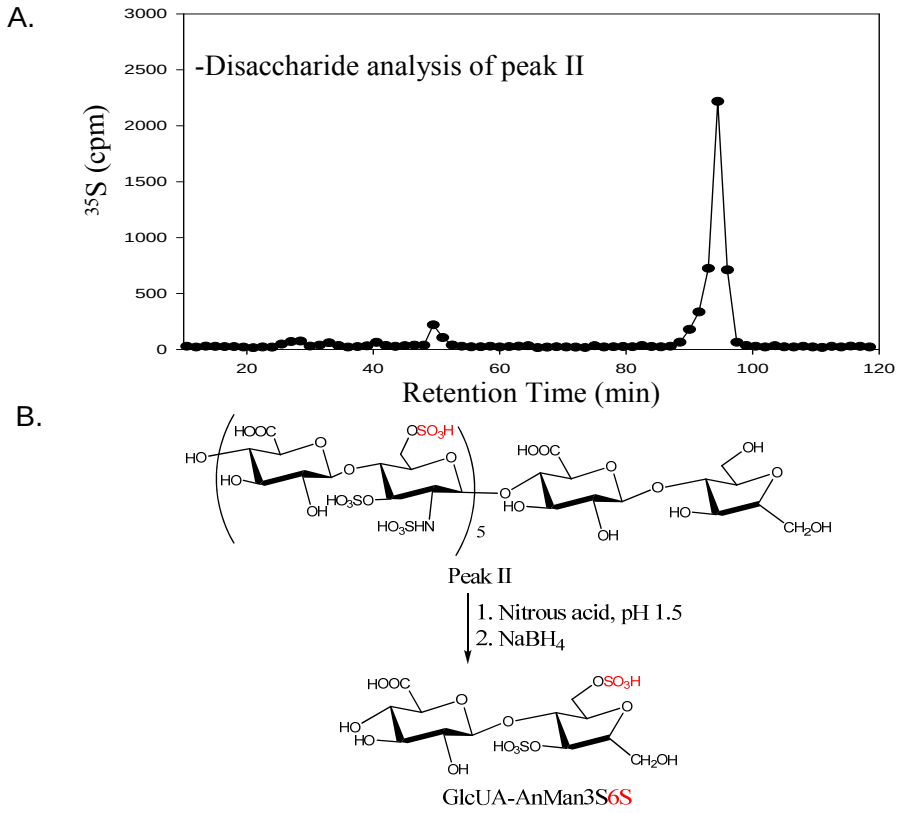

Fig 50. Determination of the structures of peak II for dodecasaccharide **17**. Panel **A** shows the HPLC chromatogram of the disaccharide analysis of Peak II using a C_{18} column under RPIP-HPLC conditions. Predominantly a single ^{35}S-labeled disaccharide (GlcUA-AnMan3S6S) with very small amount of GlcUA-AnMan6S was observed, suggesting that Peak II is a fully 3-*O*-sulfo dodecasaccharide. The reason for the small amount of GlcUA-AnMan6S was likely due to the contamination of Peak I, provided that the base-line separation of Peak I and II was not achieved. Peak II was therefore designated as dodecasaccharide **17** for the antithrombin-binding study as described in the main text. Panel **B** shows the reaction involved in the disaccharide analysis of Peak II. The 6-*O*-[^{35}S]sulfo group was colored in red to indicate the site of radioactive sulfate. To improve the clarity, nonradioactively labeled disaccharides resulted from nitrous acid degradation was not indicated.

The AT-binding affinities

The AT-binding affinities of oligosaccharides **15**, **16** and **17** were determined (Table 6). Dodecasaccharide **17** showed a dissociation constant (K_d) of 145 nM, close to that of a full length HS polysaccharide (57 nM) (124). The K_d value measured for decasaccharide **16**

was 515 nM, showing considerably weaker binding to AT, clearly demonstrating the size-dependency for HS binding to AT. Dodecasaccharide **9**, having no 3-*O*-sulfo groups, exhibited a K_d of >100 μM. These results confirmed the critical role of 3-*O*-sulfo groups for AT-binding. While the dodecasaccharide **17** binds AT with lower affinity than does the commercial pentasaccharide drug, Arixtra, improvement of dodecasaccharide binding affinity to AT may be possible by modifying its sequence through the appropriate placement of GlcNAc residues.

Table 6. The binding affinity of oligosaccharides to AT

Substrates	Proposed structure	K_d(nM)
16	$(GlcUA\text{-}GlcNS3S6S)_4$-GlcUA-AnMan	515 ± 40
17	$(GlcUA\text{-}GlcNS3S6S)_5$-GlcUA-AnMan	145 ± 24
15	$(GlcUA\text{-}GlcNS6S)_5$ -GlcUA-AnMan	>100,000
Arixtra[2]	GlcNS6S-GlcUA-GlcNS3S6S-IdoUA2S-GlcNS6S-OMe	33
Recomparin[3]	Polysaccharide, no defined structure	57

1. The binding affinity of the oligosaccharides to AT was determined using affinity co-electrophoresis.
2. The ^{35}S-labeled Arixtra was prepared as described previously.
3. The binding affinity of Recomparin to AT was taken from our previous publication.

Section 3. Conclusion

The current study demonstrates the feasibility of a total synthesis of structurally defined HS dodecasaccharides with AT-binding activity using a chemoenzymatic approach. This method is capable of synthesizing oligosaccharides with different sulfation patterns and structures by transferring UDP-sugars onto an easily prepared disaccharide acceptor. Advances in analytical methods will be required to expand our synthesis to a greater and more structurally complex variety of defined oligosaccharide structures. This study demonstrated the viability of synthesis structurally defined large HS oligosaccharide with

biological functions. Synthetic HS oligosaccharides could be employed to interrogate the structure and activity relationship in the new field of HS glycomics. These results also open a possibility to prepare novel HS-based anticoagulant drugs as well as other HS-based therapeutic agents.

Chapter VI SOLID PHASE SYNTHESIS OF HS

Section 1. Introduction

This chapter describes the attempt for enzyme-based synthesis on a solid support. The method would provide advantages over solution-phase synthesis: First, the oligosaccharide is immobilized; so sample loss during subsequent manipulations is minimal. Second, large excesses of reagents could be used to drive reactions to completion. Third, if a cleavable linker is present in the capture molecule, the processed oligosaccharide can be released into solution in a small volume for further analysis. Here, our research effort will focused on immobilizing a disaccharide on the solid support and examine the ability of glycotransferase KifA and pmHS2 to alternatively incorporate GlcNAc and GlcUA residues, from UDP-GlcNAc and UDP-GlcUA to the nonreducing ends of the immobilized disaccharide.

Considering enzymes are large molecules, one must be careful for choosing the support for solid-phase synthesis. For the porous support, the material should have pores large enough to accommodate these macromolecules and should be hydrophilic to allow good compatibility in water, or the solid support should be rigid therefore the enzyme will not be entrapped (168, Figure 51). Therefore, two different solid supports have been investigated: polyethylene glycol-polyacrylamide resin (PEGA) which swells in both organic and aqueous solvents and has functional amino groups incorporated in the range of 0.4 mmol g^{-1}; and

controlled-pore glass (CPG), which comprises rigid particles having pores of size >1400 Å and near 60 μmol g^{-1} incorporated amino groups.

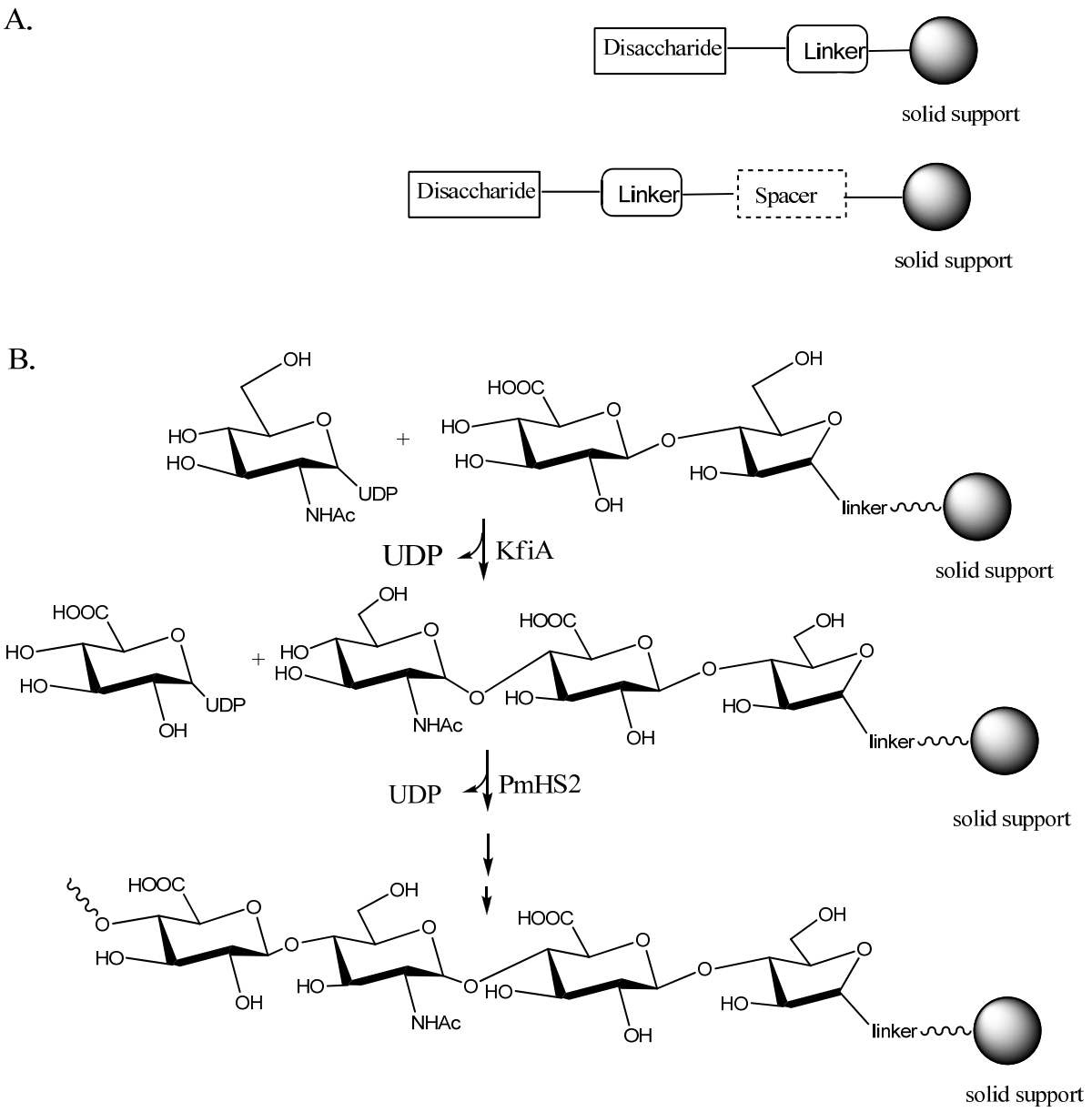

Fig 51. Solid phase HS oligosaccharide synthesis. Panel **A** shows the disaccharide will be immobilized to solid phase through a linker or optionally through a spacer molecule. Panel **B** shows the glycotransferases KfiA and pmHS2 will transfer a GlcNAc or GlcUA moiety to the solid phase to build up HS oligosaccharides.

Section 2. Solid phase synthesis

Preparation of Resins **1** and **2**

Guillaumie and coworkers has reported to successfully immobilize oligosaccharide from pectin onto PEGA support via a hydroxylamine or hydrazide terminated group (169). Both resins were prepared (Resin **1** and **2**) followed this report. Briefly, to prepare hydroxylamine resin **1**, reactions were carried out in a 10 mL plastic column equipped with a scintered Teflon filter. Amino PEGA resin (600 mg, wet) was initially washed with DMF (3 × 1 mL), 10% DIPEA in DMF (3 × 1 mL), and DMF (3 × 1 mL). 1.5 mL DMF containing N^{μ}-Boc-aminooxy acetic acid (N^{μ}-Boc-Aoa-OH, 20 mg, 0.1 mmol), benzotriazol-1-yloxy)tripyrrolidinophosphonium hexafluorophosphate (PyBOP, 27 mg, 0.1 mmol), 1-hydroxybenzotriazole (HOBt, 14 mg, 0.1 mmol) and DIPEA (35 μL, 0.2 mmol) was then added to the resin. After the column was shaken at room temperature for overnight, the reagents were removed by suction and washed with DMF (3 × 1 mL) and CH_2Cl_2 (4 × 1 mL). A qualitative ninhydrin test was used to monitor the reaction by examining the remaining level of primary amino group. After confirming the occupation of primary amine was completed, the removal of Boc groups was accomplished by treatment with 50% TFA in CH_2Cl_2 for 3 hour at room temperature (Figure 52). The resin was washed with CH_2Cl_2 (4 × 1 mL), DMF (3 × 1 mL) and CH_2Cl_2 (3 × 1 mL) respectively. A qualitative ninhydrin test was used to indicate the reaction was completed. The same procedure was used to prepare CPG resin.

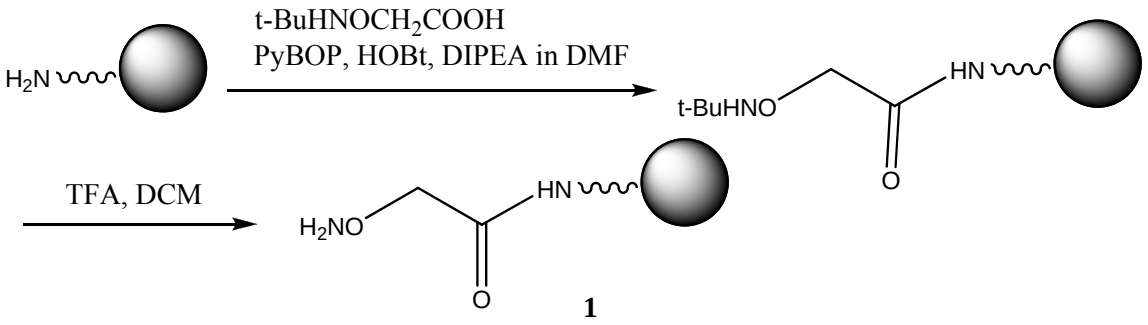

Fig 52. Preparation of hydroxylamine resin **1**.

To prepare the hydrazide-terminated resin **2**, reactions were carried out in a 10 mL plastic column equipped with a scintered Teflon filter. Amino PEGA resin (400 mg, wet) was initially washed with DMF (3 × 1 mL). DMF solution (1 mL) containing succinic anhydride (20 mg, 0.12 mmol) and *O*-(benzotriazol-1-yl)-*N*, *N*, *N*', *N*'-tetramethyluronium tetrafluoroborate (TBTU, 40 mg, 0.12 mmol) DIPEA (30 μL, 0.18 mmol) was then added to the resin and the column was shaken at room temperature for overnight. The reagents were removed by suction and the resin was washed with DMF (3 × 1 mL) and MeOH (4 × 1 mL). A qualitative ninhydrin test was used to monitor the reaction by examining the remaining level of primary amino group. After the quench of the primary amino group, half of the resin was washed with DMF (3 × 1 mL) to remove the methanol. DMF solution (400 μL) containing TBTU (19 mg, 60 μmol), DIPEA (9 μL, 60 μmol) and hydrazine monohydrate (3 μL, 60 μmol) was added to the resin. After overnight coupling at room temperature, solvents and unreacted compounds were removed by suction, and the resin was washed with DMF (4 × 1 mL) and MeOH (4 × 1 mL), respectively (Figure 53). Again, the modification of the primary amine on the surface was confirmed by ninhydrin test.

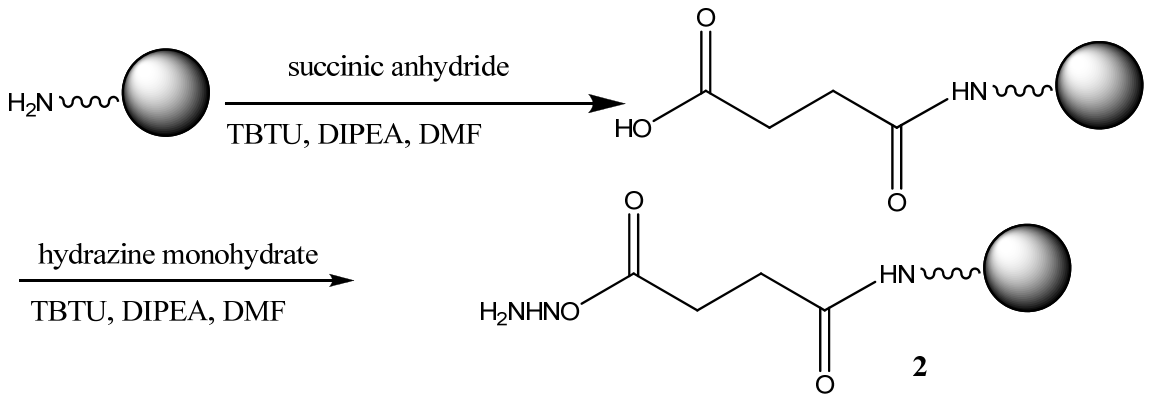

Fig 53. Preparation of hydrazide resin **2**.

Preparation of cleavable linker **33** and spacer **34**

A cleavable linker is essential for recovering after the completion of the synthesis for further analysis. Recently, Ole Hindsgaul and co-workers have developed a technique named solid-phase oligosaccharide tagging (SPOT), they showed that PEGA or CPG beads functionalized with hydroxylamine group could be used to capture oligosaccharide from solution (170). In order to immobilize the oligosaccharide to the solid support, the authors synthesized a benzyl hydroxylamine capture groups attached through a cleavable ester linkage to a solid support, optionally through a spacer molecule. The linker could be removed by treatment of base. Based on this discovery, with the protocol and linker **33** samples from Hindsgaul's lab, our lab synthesized the same linker **33** and spacer **34** (Figure 54) followed the procedures as reported (170).

A.

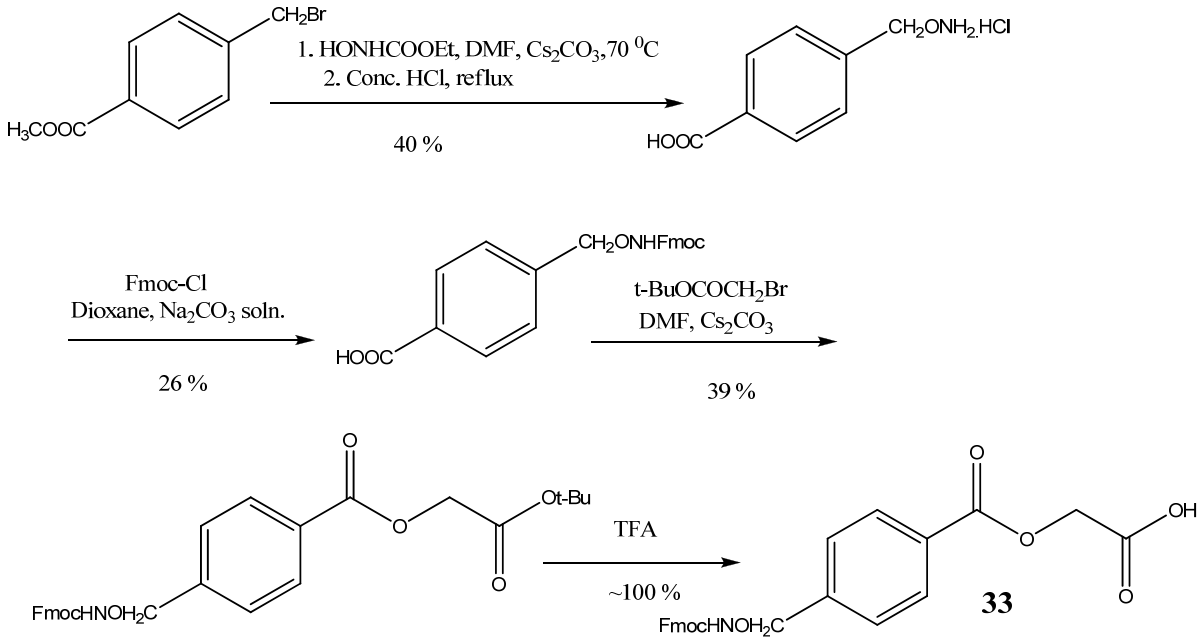

B.

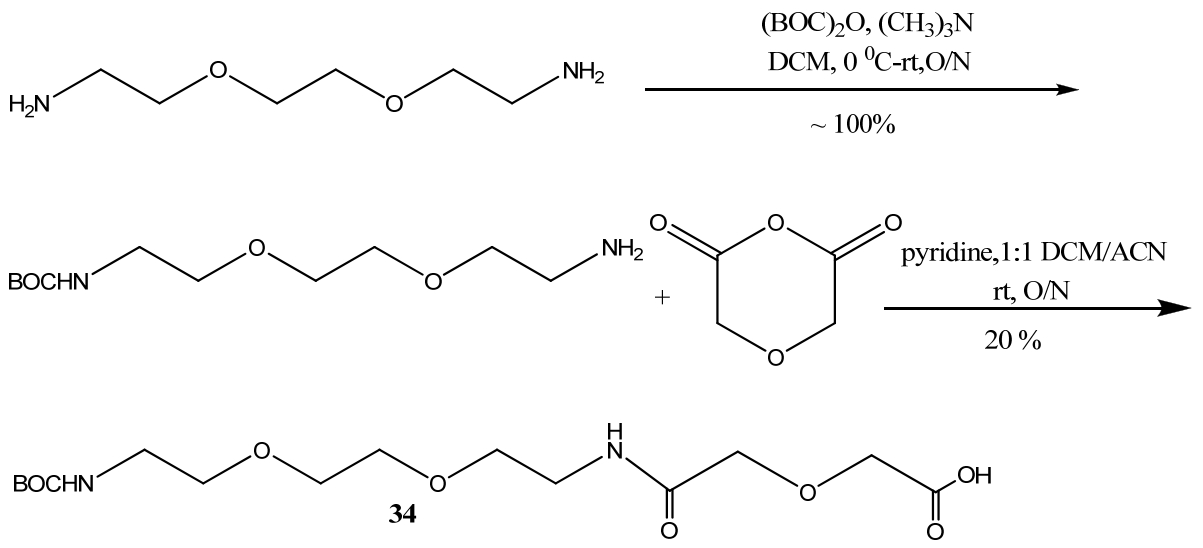

Fig 54. Total Synthesis of cleavable Linker **33** and Spacer **34**. Panel **A** shows the total synthesis of linker **33**. Panel **B** shows the total synthesis of spacer **34**.

Preparation of cleavable resin **3**

The linker **33** was installed on the solid support followed the literature (170). Briefly, reactions were carried out in a 10 mL plastic column equipped with a scintered Teflon filter. Amino PEGA resin (50 mg) swelled in methanol was initially washed with DMF (3 × 1 mL) to ensure complete removal of the methanol. Linker **33** (22 mg, 50 μmol), TBTU (17 mg, 50 μmol) and DIPEA (14 μL, 80 μmol) was mixed in 600 μL DMF and left for pre-activate for 5 mins. The solution mixture was then added to the resin. After the beads were shaken at room temperature for 3 hours, the reagents were removed by suction and washed with CH_2Cl_2 (5 × 4 mL). After confirming the occupation of primary amine was completed by A qualitative ninhydrin test, the Fmoc protection groups was removed by treatment with 20% piperidine in DMF for 1 hour at room temperature followed by extensive washes with DMF (5 × 4 mL) and CH_2Cl_2 (7 × 4 mL). The resin was dried under high vacuum for 24 hours to give final PEGA resin **3**. The linker could be removed by treatment of 1 M LiOH at room temperature for 1 hour (Figure 55).

Installation of spacer

The spacer **34** was installed on the solid support followed the literature (170). The CPG resin (720 mg) was washed was washed with DMF (3 × 2 mL), swollen in MeOH (1 × 10 mL), and then washed with DMF (3 x 1 mL), 10% DIPEA in DMF (3 × 1 mL) and DMF (3 × 1 mL). The beads were incubated with a mixture of spacer **34** (60 mg, 0.12 mmol), TBTU (38 mg, 0.12 mmol) and DIPEA (20 μL, 0.12 mmol) in DMF (3 mL) overnight at 37 °C. The resin was then washed with DMF (3 x 2 mL), CH_2Cl_2 (3 × 2 mL), and treated with 50% Ac_2O in pyridine for 30 min at room temperature to quench the remaining amino groups.

A qualitative ninhydrin test was used to monitor the reaction by examining the remaining level of primary amino group. The bead was then washed with CH_2Cl_2 (3 × 2 mL), DMF (3 × 2mL), and CH_2Cl_2 (3 × 2 mL), respectively. Removal of Boc groups was accomplished by treatment with 50% TFA in CH_2Cl_2 for 1 hour at room temperature and treated with 50% TFA in CH_2Cl_2 for 1 hour at room temperature. The resin was washed with CH_2Cl_2 (3 × 2 mL), DMF (3 × 2mL), respectively and the completion of the reaction was monitored by a qualitative ninhydrin test. The coupling of spacer, Ac_2O-pyriding, and TFA treatment were repeated to install the second spacer (Figure 56). The linkers was linked to the spacer followed the same procedure as described above.

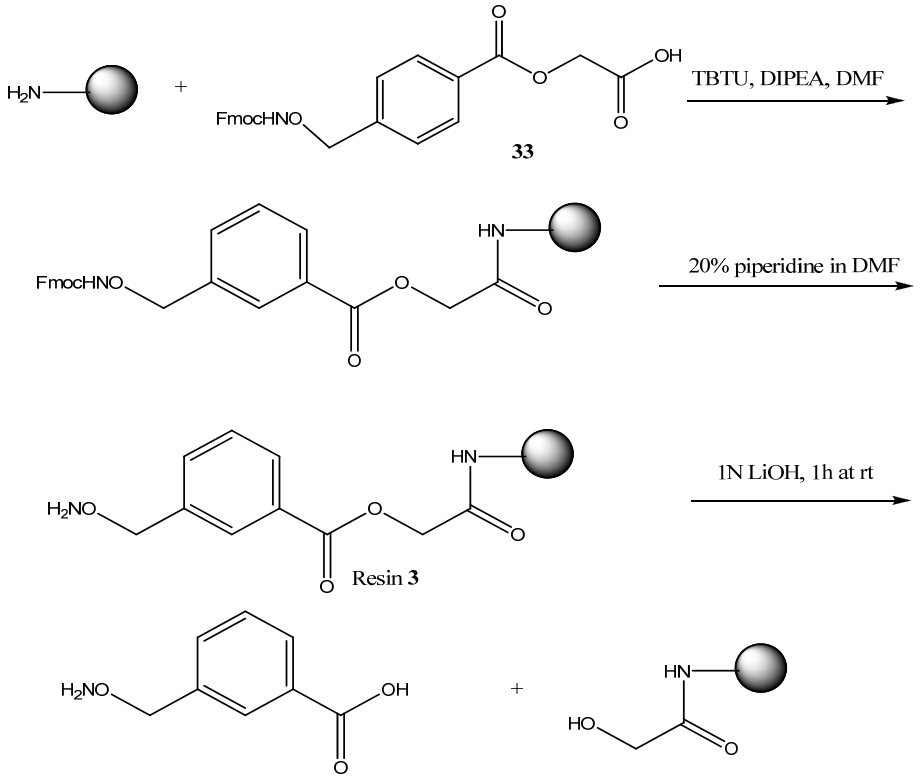

Fig 55. Preparation of cleavable hydroxylamine resin **3**. After the installation of the linker **33**, it could be cleaved by 1 M LiOH.

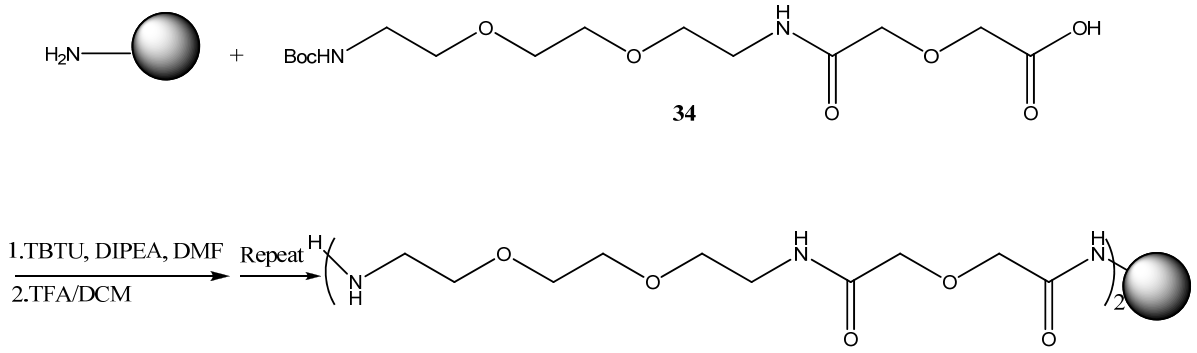

Fig 56. Installation of spacer **34**.

Immobilization of disaccharide to the solid support

To immobilize the disaccharide to the solid support, we have examined the optimal conditions for the capture of disaccharide for two different resins. Disaccharide (GlcUA-AnMannose **2)** was prepared from 10 mg heparosan, which was mixed with 140,000 cpm ^{14}C-labeled heparosan for calculation of coupling capacity. For PEGA beads, 1:1 DMF/H_2O 40 °C, and reaction for >12 h was found to be optimal. Capping was achieved with 50 % acetic anhydride in MeOH (1 hour) and reduction was achieved with $NaBH_3CN$ (1 hour). For CPG beads, incubation overnight at 55 °C in aqueous phosphate buffer (NaH_2PO_4, pH 5.0) proved to be optimal for the capture process (Figure 57). The coupling capacity was calculated based on the incorporation of [^{14}C] counts. Coupling capacity for disaccharide was about 0.3 μg /mg (CPG) or 0.18 μg/mg (PEGA).

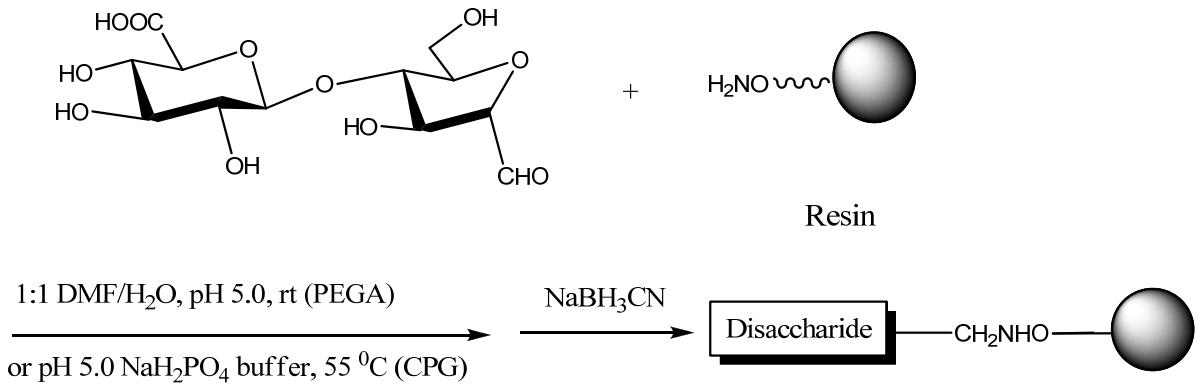

Fig 57. Immobilization of disaccharide to solid support.

Solid phase KfiA assay

A typical KfiA assay was in solution (400 µL) containing 25 mM Tris (pH 7.2), 10 mM $MnCl_2$, 1% triton, 0.1 mg KfiA and 35,000 cpm [^{3}H]-UDP-GlcNAc. The reaction mixture incubated with 4 µmol resin for overnight. After washed with reaction buffer, the resin was taken to examine the remaining radioactivity. The yield is calculated based on the incorporation of [^{3}H] counts. Although GlcNAc could be transferred to disaccharide immobilized on the solid phase, the yield is very low compare to solution phase. PEGA is only about 1~2% yield while CPG has a better yield, which is about 28%. This study indicated that solid phase synthesis might not be a viable approach to build up HS oligosaccharides.

Section 3. Conclusion

In this study, we successfully prepared three different resins which could immobilize disaccharide (GlcUA-AnMannose **2**) into the solid support. Although the disaccharide could

be immobilized to two different solid supports with reasonable capacity, and KfiA could successfully transfer a GlcNAc into the immobilized disaccharide, demonstrating the viability of solid phase HS synthesis, the low efficiency limited the further application of this technique to build up HS oligosaccharide, this either due to the reason that enzyme is entrapped at the solid surface or enzyme is difficult to recognize the substrate on the solid surface. Further study need to investigate the possibility to synthesized the HS oligosaccharides on the solid surface.

Chapter VII CONCLUSION

HS is a unique class of macromolecule that is widely expressed on the cell surface and in the extracellular matrix. HS is involved in numerous biological processes, including blood coagulation, wound healing, embryonic development, regulation of tumor growth, and assisting viral and bacterial infections. Thus, HS is a molecule with a high density of information and significant potential for therapeutic applications. Heparin, an analog of HS, is a commonly used anticoagulant drug with annual sales close of up to $4 billion worldwide. However, the crisis of heparin drug in 2008 indicated that the heparin supply chain is vulnerable; a substitute for heparin with reduced side effects still remains a high priority. Understanding the mechanism employed by HS to regulate a specific biological process could improve the pharmacological drug properties of anticoagulant heparin and aid the development of HS or heparin-based therapeutic agents with anticancer and antiviral activities.

The current study demonstrates the feasibility of a total synthesis of structurally defined HS oligosaccharides using a chemoenzymatic approach. This method is capable of synthesizing oligosaccharides with different sulfation patterns and structures by transferring UDP-sugars onto an easily prepared disaccharide acceptor. A key advancement enzymatic synthesis of these oligosaccharides involves the utilization of an unnatural UDP-donor that allows the controlled placement of GlcNS and GlcNAc residues throughout the oligosaccharide back bone. In Chapter III, an octasaccharide library with different

GlcNS/GlcNAc pattern was synthesized, proving the feasibility to control GlcNS/GlcNAc patterning. In Chapter IV, hexasaccharides with different 6-*O*-sulfation patterns were synthesized, indicating the viability of this approach to control the subsequent positioning of *O*-sulfo groups through GlcNS/GlcNAc patterning and demonstrating that oligosaccharides synthesized via this approach can be recognized by the substrate specificity of the OSTs. In Chapter V, we prepared different *N*-sulfo, *O*-sulfo deca, nonadeca and dodecasaccharide and found a novel dodecasaccharide with AT-binding activity. This study demonstrated the opportunity to prepare novel HS-based anticoagulant drugs as well as other HS-based therapeutic agents. In Chapter VI, we examined the viability to build up HS oligosaccharide on a solid support. While we demonstrated the viability of solid phase HS synthesis, the low efficiency limited further application of this method.

Further studies should focus on developing a more refined protocol to position the remaining modifications, such as 2-*O*- and 3-*O*-sulfation, as well as, incorporation of the IdoUA residue. Also, improvement of binding affinity to AT may be possible by modifying HS sequence through the appropriate placement of GlcNAc residues. Therefore, several dodecasaccharides with different GlcNS and GlcNAc patterning should be prepared. Furthermore, the tagged oligosaccharides of different sizes will be prepared to discover the minimum size of tagged oligosaccharides required to exhibit both anti-IIa and anti-Xa activities.

While this method is fully capable of synthesizing large libraries of diverse HS oligosaccharide structures, it is currently limited by the time and effort required for the full structural characterization of the resulting oligosaccharide products. Advances in analytical

methods, especially MS and MS/MS will be required to expand our synthesis to a greater and more structurally complex variety of defined oligosaccharide structures.

Overall, this dissertation advanced our understanding of HS biosynthesis. Most importantly, the results will not only allow us to investigate novel synthesis of anticoagulant drugs but also lead to a general method for preparation of structurally more defined HS structures with various other biological functions and help develop novel heparin/HS based therapeutic agents.

APPENDIX

Curriculum Vitae

Renpeng Liu
Division of Medicinal Chemistry and Natural Products
Eshelman School of Pharmacy
University of North Carolina-Chapel Hill
Chapel Hill, NC 27510
Email: renpengl@email.unc.edu
Tel: 919-962-0065

Personal Information

Place of Birth: Wuhan, Hubei, P. R. China
Gender: Male

Education

Bachelor of Science in Chemistry
Wuhan University — June 2002

Master of Science in Chemistry — June 2005
Department of chemistry, The Ohio State University-Columbus

Ph. D.
Medicinal Chemistry and Natural Products, UNC-Chapel Hill — June 2005-Current

TA&RA Experiences

College of Molecular Science and Chemistry, Wuhan University — June 2001-June 2002

Research Associate

Department of Chemistry, The Ohio State University-Columbus — July 2002 – June 2005

Teaching Associate

Medicinal Chemistry and Natural Products, UNC-Chapel Hill — June 2005-Current

Research Associate

Research Experiences

Developing DNA cross-linking agents as anti-cancer drug	June 2001-June 2002
Organic synthesis of antibacterial drug	July 2002-June 2005
Chemoenzymatic synthesis of heparan sulfate	Current

Publications

1. A Potent, Water-Soluble and Photoinducible DNA Cross-Linking Agent

Wang, P.; **Liu, R.;** Wu, X.; Ma, H.; Cao, X.; Zhou, P; Zhang, J.; Weng, X.; Zhang, X.-L.; Qi, J.; Zhou, X.; Weng, L.; *J. Am. Chem. Soc.;* **(Communication); 2003;** 125(5); 1116-1117.

The significance of this paper was highlighted in *Heart Cut* (2003, March 17) and this *Heart Cut* highlight was again mentioned in the collection *Best of Heart Cut in 2003* (2003, November 24)

2. Insight into Preference of Peptide Deformylase for Fe^{2+} over Zn^{2+} as the Catalytic Metal

Jain, R.; Hao, B.; **Liu, R-P.;** Chan, M. K.; *J. Am. Chem. Soc.;* **(Communication); 2005**; 127(13); 4558-4559.

3. Enzymatic Synthesis of Heparin

Liu, R.; Liu, J. in *Sustainable Biotechnology -Sources of Renewable Energy* (Singh, Om V.; Harvey, Steven P. Eds.) Springer (Book Chapter).

4. Chemoenzymatic Design of Heparan Sulfate Oligosaccharides

Liu, R.*; Xu, Y*.; Chen, M.; Weïwer, M.; Zhou, X.; Bridges, A. S.; DeAngelis, P. L.; Zhang, Q.; Linhardt, R. J.; Liu, J. Submitted. (* Both authors contributed equally to this work)

Award

UNC Graduate School Merit Scholar	2005-2006

REFERENCES

1. Howell, W. H., and Holt, E. (1918) Two new factors in blood coagulation-heparin and pro-antithrombin *Am J Physiol* **47,** 328-41.

2. Linhardt, R. J. (2003) 2003 Claude S. Hudson Award address in carbohydrate chemistry. Heparin: structure and activity *J Med Chem* **46,** 2551-64.

3. Liu, J., and Pedersen, L. C. (2007) Anticoagulant heparan sulfate: structural specificity and biosynthesis *Appl Microbiol Biotechnol* **74,** 263-72.

4. Capila, I., and Linhardt, R. J. (2002) Heparin-protein interactions *Angew Chem Int Ed* **41,** 390-412.

5. Fuster, M. M., and Esko, J. D. (2005) The sweet and sour of cancer: glycans as novel therapeutic targets *Nat Rev Cancer* **5,** 526-42.

6. Parish, C. R. (2006) The role of heparan sulphate in inflammation *Nat Rev Immunol* **6,** 633-43.

7. Bishop, J., Schuksz, M., and Esko, J. D. (2007) Heparan sulphate proteoglycans fine-tune mammalian physiology *Nature* **446,** 1030-7.

8. Esko, J. D., and Lindahl, U. (2001) Molecular diversity of heparan sulfate *J Clin Invest* **108,** 169-73.

9. Rosenberg, R. D., Showrak, N. W., Liu, J., Schwartz, J. J., and Zhang, L. (1997) Heparan sulfate proteoglycans of the cardiovascular system. Specific structures emerge but how is synthesis regulated? *J Clin Invest* **99,** 2062-70.

10. Bernfield, M., Gotte, M., Park, P. W., Reizes, O., Fitzgerald, M. L., Lincecum, J., and Zako, M. (1999) Functions of cell surface heparan sulfate proteoglycans *Ann Rev Biochem* **68,** 729-77.

11. Liu, J., and Thorp, S. C. (2002) Cell surface heparan sulfate and its roles in assisting viral infections *Med Res Rev* **22,** 1-25.

12. Liu, D., Shriver, Z., Venkataraman, G., Shabrawi, Y. E., and Sasisekharan, R. (2002) Tumor cell surface heparan sulfate as cryptic promoters or inhibitors of tumor groth and metastasis *Proc Natl Acad Sci* **99,** 568-73.

13. Liu, R., and Liu, J. (2010) Enzymatic synthesis of heparin in *Sustainable Biotechnology -Sources of Renewable Energy* (Singh, Om. V.; Harvey, Steven. P. Eds.) Springer, Netherlands 259-77.

14. Esko J. D., and Selleck, S. B. (2002) Order out of chaos: assembly of ligand binding sites in heparan sulfate *Annu Rev Biochem* **71,** 435-71.

15. Chapman, E., Best M. D., Hanson, S. R., and Wong, C-H. (2004) Sulfotransferases: structure, mechanism, biological activity, inhibition, and synthetic utility *Angew Chemie Int Ed* **42,** 3526-48.

16. Gallagher, J. T. (2001) Heparan sulfate: growth control with a restricted sequence menu *J Clin Invest* **108,** 357-61.

17. Toida, T., Yoshida, H., Toyoda, H., Koshiishi, T., Imanari, T., Hileman, R. E., Fromm, J. R., and Linhardt, R. J. (1997) Structural differences and the presence of unsubstituted amino groups in heparan sulfates from different tissues and species *Biochem J* **322,** 499-506.

18. Liu, J., Shriver, Z., Pope, R. M., Thorp, S. C., Duncan, M. B., Copeland, R. J., Raska, C. S., Yoshida, K., Eisenberg, R. J., Cohen, G., Linhardt, R. J., and Sasisekharan, R. (2002) Characterization of a heparan sulfate octasaccharide that binds to herpes simplex viral type 1 glycoprotein D *J Biol Chem* **277,** 33456-67.

19. Powell, A. K., Fernig, D. G., and Turnbull, J. E. (2002) Fibroblast growth factor receptors 1 and 2 interact differently with heparin/heparan sulfate: implications for dynamic assembly of a ternary signaling complex *J Biol Chem* **277,** 28554-28563.

20. Mikhailov, D., Young, H. C., Linhardt, R. J., and Mayo, K. H. (1999) Heparin dodecasaccharide binding to platelet factor-4 and growth-related protein-alpha: induction of a partially folded state and implications for heparin-induced thrombocytopenia *J Biol Chem* **274,** 25317-25329.

21. Shukla, D., Liu, J., Blaiklock, P., Shworak, N. W., Bai, X., Esko, J. D., Cohen, G. H., Eisenberg, R. J., Rosenberg, R. D., and Spear, P. G. (1999) A novel role for 3-O-sulfated heparan sulfate in herpes simplex virus 1 entry *Cell* **99,** 13-22.

22. Peterson, S., Frick, A., and Liu, J. (2009) Design of biologically active heparan sulfate and heparin using an enzyme-based approach *Nat Prod Rep* **26,** 610-27.

23. Slaughter, T. F., and Greenberg, C. S. (1997) Heparin-associated thrombocytopenia and thrombosis: implications for perioperative management *Anesthesiology* **83,** 667-75.

24. Kishimoto, T. K., Viswanathan, K., Ganguly, T., Elankumaran, S., Smith, S., Pelzer, K., Lansing, J. C., Sriranganathan, N., Zhao, G., Galcheva-Gargova, Z., Al-Hakim, A., Bailey, G. S., Fraser, B., Roy, S., Rogers-Cotrone, T., Buhse, L., Whary, M., Fox, J., Nasr, M., Dal Pan, G. J., Shriver, Z., Langer, R. S., Venkataraman, G., Austen, K. F., Woodcock, J., and Sasisekharan, R. (2008) Contaminated heparin associated with adverse clinical events and activation of the contact system *N Engl J Med* **358,** 2457-67.

25. Guerrini, M., Beccati, D., Shriver, Z., Naggi, A., Viswanathan, K., Bisio, A., Capila, I., Lansing J. C., Guglieri, S., Fraser, B., Al-Hakim, A., Gunay, N. S., Zhang, Z., Robinson, L., Buhse, L., Nasr, M., Woodcock, J., Langer, R., Venkataraman, G., Linhardt, R. J., Casu, B., Torri, G., and Sasisekharan, R. (2008) Oversulfated chondroitin sulfate is a contaminant in heparin associated with adverse clinical events *Nat Biotechnol* **26,** 669-75.

26. Zhang, Z., Weïwer, M., Li, B., Kemp, M. M., Daman, T. H. and Linhardt, R. J. (2008) Oversulfated chondroitin sulfate: impact of a heparin impurity, associated with adverse clinical events, on low-molecular-weight heparin preparation *J Med Chem* **51,** 5498-501.

27. WuDunn, D., and Spear, P. G. (1989) Initial interaction of herpes simplex virus with cells is binding to heparan sulfate *J Virol* **63,** 52-8.

28. Trybala, E., Bergstro¨m, T., Svennerholm, B., Jeansson, S., Glorioso, J. C., and Olofsson, S. (1994) Location of a functional site on herpes simplex virus type 1 glycoprotein C involved in binding to cell surface heparan sulfate *J Gen Virol* **75,** 743-52.

29. Liu, J., Shriver, Z., Blaiklock, P., Yoshida, K., Sasisekharan, R., and Rosenberg, R. D. (1999) Heparan sulfate D- glycosaminyl 3-O-sulfotransferase-3A sulfates N-unsubstituted glucosamine residues *J Biol chem* **274,** 38155-62.

30. Herold, B. C., WuDunn, D., Soltys, N., and Spear, P. G. (1991) Glycoprotein C of herpes simplex virus type 1 plays a principal role in the adsorption of virus to cells and in infectivity *J Virol* **65,** 1090-8.

31. Callahan, L. N., Phelan, M., Mallinson, M., and Norcross, M. A. (1991) Dextran sulfate blocks antibody binding to the principal neutralizing domain of human immunodeficiency virus type 1 without interfering with gp120-CD4 interactions *J Virol* **65,** 1543-50.

32. Nara, P. L., Garrity, R. R., and Goudsmit, J. (1991) Neutralization of HIV-1: a paradox of humoral proportions *FASEB J* **5,** 2437-55.

33. Roderiquez, G., Oravecz, T., Yanagishita, M., Bou-Habib, D. C., Mostowski, H., and Norcross, M. A. (1995) Mediation of human immunodeficiency virus type 1 binding by interaction of cell surface heparan sulfate proteoglycans with the V3 region of envelope gp120-gp41 *J Virol* **69,** 2233-9.

34. Crublet, E., Andrieu, J-P., Romain, R., Vivès, R. R., and Lortat-Jacob, H. (2008) The HIV-1 envolope gp120 features four heparan sulfate binding domains,including the co-receptor binding site *J Biol Chem* **283,** 15193-200.

35. Rider, C. C., Deirdre, R., Coombe, D. R., Harrop, H. A., Hounsell, E. F., Bauer, C., Feeney, J., Mulloy, B., Mahmood, N., Hay, A., and Parish, C. R. (1994) Anti-HIV-1 activity of chemically modified heparin: correlation between binding to V3 loop of gp120 and inhibition of cellular HIV-1 infection in vitro *Biochemistry* **33,** 6974-80.

36. Ceballos, A., Lenicov, F. R., Sabatté, J., Rodrígues, C. R., Cabrini, M., Jancic, C., Raiden, S., Donaldson, M., Pasqualini Jr., R. A., Marin-Briggiler, C., Vazquez-Levin, M., Capani, F., Amigorena, S., and Geffner, J. (2009) Spermatozoa capture HIV-1 through heparan sulfate and efficiently transmit the virus to dendritic cells *J Exp Med* **206,** 2717-33.

37. Tyagi, M., Rusnati, M., Presta, M., and Giacca, M., (2001) Internalization of HIV-1 Tat requires cell surface heparan sulfate proteoglycans *J Biol Chem* **276,** 3254-61.

38. Gatignol, A., and Jeang, K. T. (2000) Tat as a transcriptional activator and a potential therapeutic target for HIV-1 *Adv Pharmacol* **48,** 209-27.

39. Ray, P. E., Xu, L., Rakusan, T., and Liu, X. H. (2004) A 20-year history of childhood HIV-associated nephropathy *Pediatr Nephrol* **19,** 1075–92.

40. Rusnati, M., Tulipano, G., Spillmann, D., Tanghetti, E., Oreste, P., Zoppetti, G., Giacca, M., and Presta M. (1999) Multiple interactions of HIV-I Tat protein with size-defined heparin oligosaccharides *J Biol Chem* **274,** 28198-205.

41. Zhang, X., Ibrahimi, O. A., Olsen, S..K., Umemori, H., Mohammadi, M., and Ornitz, D. M. (2006) Receptor specificity of the fibroblast growth factor family. The complete mammalian FGF family *J Biol Chem* **281,** 15694–700.

42. Kwan, C. P., Venkataraman, G., Shriver, Z., Raman. R., Liu, D., Qi, Y., Varticovski. L., and Sasisekharan, R. (2001) Probing fibroblast growth factor dimerization and role of heparin-like glycosaminoglycan in molecular dimerization and signaling *J Bio Chem* **276,** 23421-9.

43. Schlessinger, J., Plotnikov, A. N., Ibrahimi, O. A., Eliseenkova, A.V., Yeh, B. K., Yayon, A., and Linhardt, R. J. (2000) Crystal structure of a ternary FGF-FGFR-heparin complex reveals a dual role for heparin in FGFR binding and dimerization *Mol Cell* **6,** 743-50.

44. Pellegrini, L., Burke, D. F., Delft, F. V., Mulloy, B., and Blundell, T. L. (2000) Crystal structure of fibroblast growth receptor ectodomain bound to ligand and heparin *Nature* **407,** 1029-34.

45. Luster, A. D. (1998) Chemokines-chemotactic cytokines that mediate inflammation *N Engl J Med* **338,** 436-45.

46. Parish, C. R. (2005) Heparan sulfate and inflammation *Nat Immunol* **6** 861-2.

47. Lever, R., and Page, C. (2002) Novel drug development opportunities for heparin *Nat Rev Drug Discov* **1**, 140–148.

48. Witt, D. P., and Lander, A. D. (1994) Differential binding of chemokines to glycosaminoglycan subpopulation *Curr Biol* **4**, 394-400.

49. Middleton, J., Neil, S., Wintle, J., Clark-Lewis, J., Moore, H., Lam, C., Auer, M., Hub, E., and Rot, A. (1997) Transcytosis and surface presentation of IL8 by venular endothetial cell *Cell* **91,** 385-95.

50. Kuschert, G. S. V., Coulin, F., Power, C. A., Proudfoot, A. E. I., Hubbard, R. E., Hoogewerf, A. J., and Wells, T. N. C. (1999) Glycosaminoglycans interact selectively with chemokines and modulate receptor binding and cellular response *Biochemistry* **38**, 12959-68.

51. Wang, L., Fuster, M., Sriramarao, P., and Esko, J. D. (2005) Edothelial heparan sulfate deficiency impairs L-selectin- and chemokine-mediated neutrophil trafficking during inlammatoray responses *Nat Immunol* **6,** 902-10.

52. Wang, L., Brown, J. R., Varki, A., and Esko, J. D. (2002) Heparin's anti-inflammatory effects require glucosamine 6-*O*-sulfation and are mediated by blockade of L- and P-selectins *J Clin Invest* **110,** 127-36.

53. Tagalakis, V., Blostein, M., Robinson-Cohen, C., and Kahn, S. R. (2007) The effect of anticoagulants on cancer risk and survival: systematic review *Cancer Treatment Rev* **33,** 358-68.

54. Altinbas, M., Coskun, H. S., Er, O., Ozkan, M., Eser, B., Unal, A., Cetin, M., and Soyuer, S. (2004) A randomized clinical trial of combination chemotherapy with and without low-molecular-weight heparin in small cell lung cancer *J Thromb Haemost* **2,** 1266-71.

55. Seeholzer, N., Thurlimann, B., Koberle, D., Hess, D., and Korte, W. (2007) Combining chemotherapy and low-molecular weight heparin for the treatment of advanced breast cancer: results on clinical response, transforming growth factor-beta 1 and fibrin monomer in a phase II study *Blood Coagulation and Fibrinolysis* **18,** 415-23.

56. Freeman, C., and Parish, C. R. (1998) Human platelet heparanase: purification, characterization and catalytic activity *Biochem J* **330**, 1341–50.

57. Pikas, D. S., Li, J.-P., Vlodavsky, I., and Lindahl, U. **(**1998) Substrate specificity of heparanases from human hepatoma and platelets *J Biol Chem* **273**, 18770–7.

58. Vlodavsky, I. , Friedmann, Y., Elkin, M., Aingorn, H., Atzmon, R., Ishai-Michaeli, R., Bitan, M., Pappo, O., Peretz, T., Michal, I., Spector, L., and Pecker, I. (1999) Mammalian heparanase: gene cloning, expression and function in tumor progression and metastasis *Nat Med* **5**, 793–802.

59. Toyoshima, M., and Nakajima, M. (1999) Human heparanase purification, characterization, cloning, and expression *J Biol Chem* **274**, 24153–60.

60. Simizu, S., Ishida, K., and Osada, H., (2004) Heparanase as a molecular target of cancer chemotherapy *Cancer Sci* **95**, 553–8.

61. Eutick, M. www.progen.com.au, 2008.

62. Mousa, S. A., Linhardt, R. J., Francis, J. L., and Amirkhosravi, A. (2006) Anti-metastatic effect of a non-anticoagulant low-molecular-weight heparin versus the standard low-molecular-weight heparin, enoxaparin. *Thromb Haemost* **96,** 816-21.

63. Martel, N., Lee, J., and Wells, P. S. (2005) Risk for heparin-induced thrombocytopenia with unfractionated and low-molecular-weight heparin thromboprophylaxis: a meta-analysis *Blood* **106,** 2710-5.

64. Ahmed, I., Majeed, A., and Powell, R. (2007) Heparin induced thrombocytopenia: diagnosis and management update *Postgrad Med J* **83,** 575–82.

65. Warkentin, T. E. (2006) Think of HIT *Hematology Am Soc Hematol Educ Program* **2006**, 408–14.

66. Ibel, K., Poland, G. A., Baldwin, J. P., Pepper, D. S., Luscombe, M., and Holbrooke, J. J. (1986) Low-resolution structure of the complex of human blood platelet factor 4 with heparin determined by small-angle neutron scattering *Biochim Biophys Acta* **870,** 58-63.

67. Stringer, S. E. and Gallagher, J. T. (1997) Specific binding of the chemokineplatalet factor 4 to heparan sulfate *J Biol Chem* **272,** 20508-14.

68. Mikhailov, D., Young, H.C., Linhardt, R.J., and Mayo, K.H. 1999. Heparin Dodecasaccharide Binding to Platelet Factor-4 and Growth-related Protein-alpha *J. Biol. Chem.* 274:25317-25329.

69. Marshall, S. E. Luscombe, M., Pepper, D. S., and Holbrooke, J. J. (1984) The interaction of platelet factor 4 with heparins of different chain length *Biochim Biophys Acta* **797,** 34-9.

70. Maccarana, M., and Lindahl, U. (1993) Mode of interaction between platelet factor 4 and heparin *Glycobiology* **3,** 271-7.

71. Petitou, M., Herault, L. P., Bernat, A., Driguez, P. A., Duchaussoy, P., Lormeau, J. C. and Herbert, J. M. (1999) Synthesis of thrombin-inhibiting heparin mimetics without side effects *Nature* **398,** 417-22.

72. Petitou, M., and van Boeckel, C. A. A. (2004) A synthetic antithrombin III binding pentasaccharide is now a drug! what comes next? *Angew Chem Int Ed* **43,** 3118-33.

73. Bauer, K. A., Hawkins, D. W., Peters, P. C., Petitou, M., Herbert, J. M., van Boeckel, C. A. A. and Meuleman, D. G. (2002) Fondaparinux, a synthetic pentasaccharide: the first in a new class of antithrombotic agents-the selective factor Xa inhibitors *Cardiovasc Drug Rev* **20,** 37-52.

74. Sinaÿ, P., Jacquinet, J. C., Petitou, M., Duchaussoy, P., Lederman, I., Choay, J., and Torri, G. (1984) Total synthesis of a heparin pentasaccharide fragment having high affinity for antithrombin III *Carbohydr Res* **132,** C5-C9.

75. Aikawa, J.-i., Grobe, K., Tsujimoto, M., and Esko, J. D. (2001) Multiple isozymes of heparan sulfates/heparin GlcNAc *N*-deacetylase/GlcN *N*-sulfotransferase: structure and activity of the fourth member, NDST4 *J Biol Chem* **276,** 5876-82.

76. Habuchi, H., Tanaka, M., Habuchi, O., Yoshida, K., Suzuki, H., Ban, K., and Kimata, K. (2000) The occurance of three isoforms of heparan sulfate 6-*O*-sulfotransferase having different specificities for hexuronic acid adjacent to the targeted *N*-sulfoglucosamine *J Biol Chem* **275,** 2859-68.

77. Gotting, C., Kuhn, J., Zahn, R., Brinkmann, T., and Kleesiek, K. (2000) Molecular cloning and expression of human UDP-D-xylose:proteoglycan core protein β-D-xylosyltransferase and its first isoform XT-II *J Mol Biol* **304,** 517-28.

78. Zhang, L., David, G., and Esko, J. D. (1995) Repetitive Ser-Gly sequences enhance heparan sulfate assembly in proteoglycans *J Biol Chem* **270,** 27127-35.

79. Almeida, R., Levery, S. B., Mandel, U., Kresseparallel, H., Schwientek, T., Bennett, E. P., and Clausen, H. (1999) Cloning and expression of a proteoglycan UDP-galactose:β-xylose β1,4-galactosyltransferase I: the seventh member of human β4galactosyltransferase gene family *J Biol Chem* **274,** 26165-71.

80. Bai, X., Zhou, D., Brown, J. R., Crawford, B. E., Hennet, T., and Esko, J. D. (2001) Biosynthesis of linkage region of glycosaminoglycan: cloning and activity of a galactosyltransferase II, the sixth member of the β1, 3-galactosyltransferase family *J Biol Chem* **276,** 48189-95.

81. Kim, B. T., Kitagawa, H., Tamura, J., Saito, T., Kusche-Gullberg, M., Lindahl, U., and Sugahara, K., (2001) Human tumor suppressor EXT gene family member EXTL2 and EXTL3 encode α1, 4-acetylglucosaminyltransferases that are likely involved in heparan sulfate/heparin biosynthesis *Proc Natl Acad Sci* **98,** 7176-81.

82. McCormick, C., Leduc, Y., Martindale, D., Mattison, K., Esford, L. E., Dyer, A. P., and Tufaro, F. (1998) The putative tumour suppressor EXT1 alters the expression of cell-surface heparan sulfate *Nat Genet* **19,** 158-61.

83. Lind, T., Tufaro, F., McCormick, C., Lindahl, U., and Lidholt, K. (1998) The putative tumor suppressors EXT1 and EXT2 are glycotransferases required for the biosynthesis of heparan sulfate *J Biol Chem* **273,** 26265-8.

84. Strickens, D., Zak, B. M., Rougier, N., Esko, J. D. and Werb, Z. (2005) Mice deficient in ext2 lack heparan sulfate and develop exostoses *Development* **132,** 5055–68.

85. Lin, X., Wei, G., Shi, Z., Dryer, L., Esko, J. D., Wells, D. E. and Matzuk, M. M. (2000) Disruption of gastrulation and heparan sulfate biosynthesis in EXT1-deficient mice *Dev Biol* **224,** 299–311.

86. Gallagher, J. T. (2001) Heparan sulfate: growth control with a restricted sequence menu *J Clin Invest* **108,** 357-61.

87. Duncan, M. B., Liu, M., Fox, C., and Liu, J. (2006) Characterization of the N-deacetylase domain from the heparan sulfate *N*-deacetylase/*N*-sulfotransferase 2 *Biochem Biophys Res Commun* **339,** 1232-7.

88. Kakuta, Y., Sueyoshi, T., Negishi, M., and Pedersen, L. C. (1999) Crystal structure of the sulfotransferase domain of human heparan sulfate *N*-deacetylase/*N*-sulfotransferase 1 *J Biol Chem* **274,** 10673-6.

89. Bame, K. J., and Esko, J. D. (1989) Undersulfated heparan sulfate in a chinese hamster ovary cell mutant defective in heparan sulfate *N*-sulfotransferase *J Biol Chem* **264,** 8059-65.

90. Fan, G., Xiao, L., Cheng, L., Wang, X., Sun, B., and Hu, G. (2000) Targeted disruption of NDST-1 gene leads to pulmonary hypoplasia and neonatal respiratory distress in mice *FEBS Lett* **467,** 7-11.

91. Wang, L., Fuster, M., Sriramarao, P., and Esko, J. D. (2005) Edothelial heparan sulfate deficiency impairs L-selectin- and chemokine-mediated neutrophil trafficking during inlammatoray responses *Nat Immunol* **6,** 902-10.

92. Forsberg, E., Pejler, G., Ringvall, M., Lunderius, C., Tomasini-Johansson, B., Kusche-Gullberg, M., Eriksson, I., Ledin, J., Hellman, L., and Kjellen, L. (1999) Abnormal mast cells in mice deficient in a heparin-synthesizing enzyme *Nature* **400,** 773-6.

93. Pallerla, S. R., Lawrence, R., Lewejohann, L., Pan, Y., Fischer, T., Scholomann, U., Zhang, X., Esko, J. D. and Grobe, K. (2008) Altered heparan sulfate structure in mice with deleted NDST3 gene function *J Biol Chem* **283,** 16885–94.

94. Hagner-McWhirter, A., Lindahl, U., and Li, J. (2000) Biosynthesis of heparin/heparan sulphate: mechanism of epimerization of glucuronyl C-5 *Biochem J* **347,** 69–75.

95. Conrad, H. E. (1998) *Heparin-binding proteins*. San Diego, CA: Academic Press.

96. Rong, J., Habuchi, H., Kimata, K., Lindahl, U., and Kusche-Gullberg, M. (2001) Substrate specificity of the heparan sulfate hexuronic acid 2-*O*-sulfotransferase *Biochemistry* **40,** 5548-55.

97. Hagner-McWhirter, A., Li, J., Oscarson, S., and Lindahl, U. 2004. Irreversible glucuronyl C5-epimerization in the biosynthesis of heparan sulfate. *J. Biol. Chem.* 279:14631-14638.

98. Li, J. P., Gong, F., Hagner-McWhirter, A., Forsberg, E., Abrink, M., Kisilevsky, R., Zhang, X., and Lindahl, U. (2003) Targeted disruption of a murine glucuronyl C5-epimerase gene results in heparan sulfate lacking L-iduronic acid and in neonatal lethality *J Biol Chem* **278,** 28363-6.

99. Cadwallader A. B., and Joseph, H. Y. (2007) Combinatorial expression patterns of heparan sulfate sulfotransferases in zebrafish: III 2-*O*-sulfotransferase and C5-epimerases *Dev Dyn* **236,** 581–86.

100. Bethea, H. N., Xu, D., Liu, J., and Pedersen, L. C. (2008) Redirecting the substrate specificity of heparan sulfate 2-*O*-sulfotransferase by structurally guided mutagenesis *Proc Natl Acad Sci* **105,** 18724-9

101. Bullock, S. L., Fletcher, J. M., Beddington, R. S., and Wilson, V. A. (1998) Renal agenesis in mice homozygous for a gene trap mutation in the gene encoding heparan sulfate 2-sulfotransferase *Genes Dev* **12,** 1894–1906.

102. Merry, C. L., and Wilson, V. A. (2002) Role of heparan sulfate-2-*O*-sulfotransferase in the mouse *Biochim Biophys Acta* **1573,** 319–27.

103. Wilson, V. A., Gallagher, J. T., and Merry, C. L. (2003) Heparan sulfate 2-*O*-sulfotransferase (*Hs2st*) and mouse development *Glycoconj J* **19,** 347–54.

104. Gorsi, B., and Stinger, S. (2007) Tinkering with heparan sulfate sulfation to steer development *Trends Cell Biol* **17,** 173–7.

105. Smeds, E., Habuchi, H., Do, A.-T., Hjertson, E., Grundberg, H., Kimata, K., Lindahl, U., and Kusche-Gullberg, M. (2003) Substrate specificities of mouse heparan sulphate glucosaminyl 6-*O*-sulfotransferases *Biochem J* **372,** 371-80.

106. Habuchi, H., Nagai, N., Sugaya, N., Atsumi, F., Stevens, R. L., and Kimata, K. (2007) Mice deficient in heparan sulfate 6-*O*-sulfotransferase-1 exhibit defective heparan sulfate biosynthesis, abnormal placentation, and late embryonic lethality *J Biol Chem* **282,** 15578–88.

107. Ashikari-Hada, S., Habuchi, H., Kariya, Y., Itoh, N., Reddi, A. H., and Kimata, K. (2004) Characterization of growth factor-binding structures in heparin/heparan sulfate using an octasaccharide library *J Biol Chem* **279,** 12346-54.

108. Edavettal, S. C., Lee, K. A., Negishi, M., Linhardt, R. J., Liu, J., and Pedersen, L. C. (2004) Crystal structure and mutational analysis of heparan sulfate 3-*O*-sulfotransferase isoform 1 *J Biol Chem* **279,** 25789-97.

109. Moon, A., Edavettal, S. C., Krahn, J. X., Munoz, E. M., Negishi, M., Linhardt, R .J., Liu, J., and Pedersen, L. C. (2004) Structural analysis of the sulfotransferase (3-OST-3) involved in the biosynthesis of an entry receptor of herpes simplex virus 1 *J Biol Chem* **279,** 45185-93.

110. Xu, D., Moon, A., Song, D., Pedersen, L. C., and Liu, J. (2008) Engineering sulfotransferases to modify heparan sulfate *Nat Chem Biol* **4,** 200-2.

111. HajMohammadi, S., Enjyoji, K., Princivalle, M., Christi, P., Lech, M., Beeler, D. L., Rayburn, H., Schwartz, J. J., Barzegar, S., de Agostini, A. I., Post, M. J., Rosenberg, R. D., and Shworak, N. W. (2003) Normal levels of anticoagulant heparan sulfate are not essential for normal hemostasis *J Clin Invest* **111,** 989–99.

112. Hodson, N., Griffiths, G., Cook, N., Pourhossein, M., Gottfridson, E., Lind, T., Lidholt, K., and Roberts, I. S. (2000) Identification that KfiA, a protein essential for the biosynthesis of the Escherichia coli K5 capsular polysaccharise, is an alpha-UDP-GlcNAc glycosyltransferase: the formation of a membrane-assocaited K5 biosynthetic complex requires KfiA, KfiB, and KfiC *J Biol Chem* **275,** 27311-5.

113. Chen, M., Bridges, A., and Liu, J. (2006) Determination of the substrate specificities of *N*-acetyl-D-glucosaminyl transferase *Biochemistry* **45,** 12358-65.

114. Deangelis, P. L., and White, C. L. (2002) Identification and molecular cloning of a heparosan synthase from pasteurella multocida types D *J Biol Chem* **277,** 6852-7.

115. Deangelis, P. L., and White, C. L. (2004) Identification of a distinct, cryptic heparosan synthase from pasteurella multocida types A, D, and F *J Bacteriol* **186,** 8529-32.

116. de Kort, M., Buijsman, R.C., and van Boeckel C.A. Synthetic heparin derivatives as new anticoagulant drugs *Drug Discov Today* **10,** 769-79.

117. Harenberg, J. (2009) Deveolpment of idraparinux and idrabiotaparinux for anticoagulant therapy *Thromb Haemost* **102,** 811-5.

118. Herbert, J. M., Hérault, J. P., Bernat. A., Savi, P., Schaeffer, P., Driguez, P. A., Duchaussoy, P. and Petitou, M. (2001) SR123781A, a synthetic heparin mimetic *Thromb Haemost* **85,** 852-60.

119. Baleux, F., Loureiro-Morais, L., Hersant, Y., Clayette, P., Arenzana-Seisdedos, F., Bonnaffé, D., and Lortat-Jacob, H. (2009) A synthetic CD4-heparan sulfate glycoconjugate inhibits CCR5 and CXCR4 HIV-1 attachment and entry *Nat Chem Biol* **5,** 743-8.

120. Lindahl, U., Li, J., Kusche-Gullberg, M., Salmivirta, M., Alaranta, S., Veromaa, T., Emies, J., Roberts, I., Taylor, C., Oreste, P., Zoppetti, G., Naggi, A., Torri, G., and Casu, B. (2005) Generation of "neoheparin" from E. Coli K5 capsular polysaccharide *J Med Chem* **48,** 349-52.

121. Balagurunathan, K., Beeler, D. L., Lech, M., Wu, Z. L., and Rosenberg, R. D. (2003) Chemoenzymatic synthesis of classical and non-classical anticoagulant heparan sulfate polysaccharides *J Biol Chem* **278,** 52613-21.

122. Kuberan, B., Beeler, D. L., Lawrence, R., Lech, M., and Rosenberg, R. D. (2003) Rapid two-step synthesis of mitrin from heparosan: a replacement for heparin *J Am Chem Soc* **125,** 12424-5.

123. Chen, J., Avci, F. Y., Muñoz, E. M., McDowell, L. M., Chen, M., Pedersen, L. C., Zhang, L., Linhardt, R. J. and Liu, J. (2005) Enzymatic redesigning of biological active heparan sulfate *J Biol Chem* **280,** 42817-25.

124. Chen, J., Jones, C. L., and Liu, J. (2007) Using an enzymatic combinatorial approach to identify anticoagulant heparan sulfate structures *Chem Biol* **14,** 986-93.

125. Burkart, M. D., Izumi, M., Chapman, E., Lin, C., and Wong, C-H. (2000) Regeneration of PAPS for the enzymatic synthesis of sulfated oligosaccharides *J Org Chem* **65,** 5565-74.

126. Das, S. K., Mallet, J. M., Esnault, J., Driguez, P. A., Duchaussoy, P., Sizun, P., Herault, J. P., Herbert, J. M., Petitou, M., and Sinaÿ, P. (2001) Synthesis of conformationally locked L-iduronic acid derivatives: direct evidence for a critical role of the skew-boat 2S0 conformer in the activation of antithrombin by heparin *Chemistry* **7,** 4821-34.

127. Kuberan, B., Lech, M. Z., Beeler, D. L., Wu, Z. L. and Rosenberg, R. D. (2003) Enzymatic synthesis of antithrombin III−binding heparan sulfate pentasaccharide *Nature Biotech* **21,** 1343-6.

128. Copeland, R. J., Balasubramaniam, A., Tiwari, V., Zhang, F., Bridges, A., Linhardt , R. J., Shukla, D., and Liu, J. (2008) Using a 3-O-sulfated heparan sulfate octasaccharide to inhibit the entry of herpes simplex virus type 1 *Biochemistry* **47,** 5774-83.

129. Montgomery, R. I., Warner, M. S., Lum, B. J., and Spear, P. G. (1996) Herpes simplex virus-1 entry into cells mediated by a novel member of the TNF/NGF receptor family *Cell* **87,** 427-36.

130. Pertel, P. E., Fridberg, A., Parish, M. L., and Spear, P. G. (2001) Cell fusion induced by herpes simplex virus glycoproteins gB, gD, and gH-gL requires a gD receptor but not necessarily heparan sulfate *Virology* **279,** 313-24.

131. Sismey-Ragatz, A. E., Dixy, E. G., Otto, N. J., Rejzek, M., Field, R. A., and Deangelis, P. L. (2007) Chemoenzymatic synthesis with distinct pasteurella heparosan synthases: monodisperse polymers and unnatural structures *J Biol Chem* **282,** 28321-7.

132. Weïwer, M., Sherwood, T., Green, D. E., Chen, M., DeAngelis, P. L., Liu, J., and Linhardt, R. J. (2008) Synthesis of uridine 5'-diphosphoiduronic acid: a potential substrate for the chemoenzymatic synthesis of heparin *J Org Chem* **73,** 7631-7.

133. Galliher, P. M., Cooney, C. L. Langer, R., and Linhart, R. J. (1981) Heparinase production by Flavobacterium heparinum *Appl Environ Microbiol* **41,** 360–5.

134. Linker, A., and Hovingh, P. (1972) Isolation and characterization of oligosaccharides obtained from heparin by the action of heparinase *Biochemistry* **11,** 563–8.

135. Xu, D., Tiwari, V., Xia, G., Clement, C., Shukla, D., and Liu, J. (2005) Characterization of heparan sulfate 3-*O*-sulfotransferase isoform 6 and its role in assisting the entry of herpes simplex virus, type 1 *Biochem J* **385,** 451-9.

136. Pervin, A., Al-Hakim, A., and Linhardt, R. J. (1994) Separation of glycosaminoglycan-derived oligosaccharides by capillary electrophoresis using reverse polarity *Anal Biochem* **221,** 182-8.

137. Linhardt, R. J., Turnbull, J. E., Wang, H. M., Loganathan, D., and Gallagher, J. T. (1990) Examination of the substrate specificity of heparin and heparan sulfate lyases *Biochemistry* **29,** 2611–7.

138. Desai, U. R., Wang, H. M., and Linhardt, R. J. (1993) Specificity studies on the heparin lyases from Flavobacterium heparinum *Biochemistry* **32,** 8140–5.

139. Shively, J. E., and Conrad, H. E. (1976) Formation of anhydrosugars in the chemical depolymerization of heparin *Biochemistry* **15,** 3932–42.

140. Pope, M., Raska, C., Thorp, S. C., and Liu, J. (2001) Analysis of heparan sulfate oligosaccharides by nanoelectrospray ionization mass spectrometry *Glycobiology* **11,** 505-13.

141. Thanawiroon, C., Rice, K. G., Toida, T., and Linhardt, R. J. (2004) LC/MS sequencing approach for highly sulfated heparin-derived oligosaccharides *J Biol Chem* **279,** 2608-15.

142. Saad, O. M., and Leary, J. A., (2005) Heparin sequencing using enzymatic digestion and ESI-MSn with HOST: a heparin/HS oligosaccharide sequencing tool *Anal Chem* **77,** 5902-11.

143. Zhang, Z., Xie, J., Liu, J., and Linhardt, R. J. (2008) Tandem MS can distinguish hyaluronic acid from N-acetylheparosan. *J Am Soc Mass Spectrom* **19,** 82-90.

144. Wolff, J. J., Laremore, T. N., Aslam, H., Linhardt, R. J., (2008) Electron-induced dissociation of glycosaminoglycan tetrasaccharides *J Am Soc Mass Spectrom* **19,** 1449-58.

145. Hricovíni, M., Guerrini, M., Bisio, A., Torri, G., Naggi, A., and Casu, B. (2002) Active conformations of glycosaminoglycans. NMR determination of the conformation of heparin sequences complexed with antithrombin and fibroblast growth factors in solution *Semin Thromb Hemost* **28,** 325-34.

146. Hricovíni, M., Guerrini, M., Bisio, A., Torri, G., Petitou, M., and Casu, B. (2001) Conformation of heparin pentasaccharide bound to antithrombin III *Biochem J* **359,** 265-72.

147. Guerrini, M., Agulles, T., Bisio, A., Hricovini, M., Lay, L., Naggi, A., Poletti, L., Sturiale, L., Torri, G., and Casu, B. (2002) Minimal heparin/heparan sulfate sequences for binding to fibroblast growth factor-1 *Biochem Biophys Res Commun* **292,** 222-30.

148. Guglier, S., Hricovíni, M., Raman, R., Polito, L., Torri, G., Casu, B., Sasisekharan, R., and Guerrini, M. (2008) Minimum FGF2 binding structural requirements of heparin and heparan sulfate oligosaccharides as determined by NMR spectroscopy *Biochemistry* **47,** 13862-9.

149. Zhang, Z., McCallum, S. A., Xie, J., Nieto, L., Corzana, F., Jiménez-Barbero, J., Chen, M., Liu, J., and Linhardt, R. J. (2008) Solution structures of

chemoenzymatically synthesized heparin and its precursors *J Am Chem Soc* **130,** 12998-3007.

150. Linhardt, R. J., Dordick, J. S., Deangelis, P. L., and Liu, J. (2007) Enzymatic synthesis of glycosaminoglycan heparin *Semin Thromb Hemost* **33,** 453-65.

151. Leiting, B., Pryor, K. D., Eveland, S. S., and Anderson, M. S. (1998) One-day enzymatic synthesis and purification of UDP-*N*-[1-14C]acetyl-glucosamine *Anal Biochem* **256,** 185-91.

152. Sala, R. F., MacKinnon, S. L., Palcic, M. M., and Tanner, M. E. (1998) UDP-*N*-trifluoroacetylglucosamine as an alternative substrate in *N*-acetylglucosaminyltransferase reactions *Carbohydr Res* **306,** 127-36.

153. Wolfrom, M. L., and Conigliaro, P. J. (1969) Trifluoroacetyl as an *N*-protective group in the synthesis of purine nucleosides of 2-amino-2-deoxy saccharides *Carbohydr Res* **11,** 63-76.

154. Shworak, N. W., Liu, J., Fritze, L. M., Schwartz, J. J., Zhang, L., Logear, D., and Rosenberg, R. D. (1997) Molecular cloning and expression of mouse and human cDNAs encoding heparan sulfate D-glucosaminyl 3-*O*-sulfotransferase *J Biol Chem* **272,** 28008-19.

155. Cooper, A. B., Wright, J. J, Ganguly, A. K., Desai, J., Loebenberg, D., Parmegiani, R., Feingold, D. S., and Sud, I. J. (1989) Synthesis of 14-α-aminomethyl substituted lanosterol derivatives; inhibitors of fungal ergosterol biosynthesis *J Chem Soc Chem Commun* **14,** 898 – 900.

156. Domon, B., and Costello, C. E. (1988) A systematic nomenclature for carbohydrate fragmentations in FAB-MS/MS spectra of glycoconjugates *Glycoconj J* **5**, 397-409.

157. Lee, M. K., and Lander, A. D. (1991) Analysis affinity and structural selectivity in the binding of proteins to glycosamineglycans: Development of a sensitive electrophoretc approach *Proc Natl Acad Sci* **88,** 2768-72.

158. Zhang, W. (2004) Fluorous tagging strategy for solution-phase synthesis of small molecules,peptides and oligosaccharides *Curr Opin Drug Discov Devell* **7(6),** 784-97.

159. Zhang, W. (2004) Fluorous synthesis of heterocyclic systems *Chem Rev* **104,** 2531–56.

160. Curran, D. P.; Luo, Z. Y. (1999) Fluorous synthesis with fewer fluorines (light fluorous synthesis): separation of tagged from untagged products by solid phase extraction with fluorous reverse-phase silica gel *J Am Chem Soc* **121,** 9069-72.

161. Curran, D. P., Zhang, Q., Lu, H., and Gudipati, V. (2006) Characterization and analysis of a twenty-eight member stereoisomer library of murisolins and their mosher ester derivatives. *J Am Chem Soc* **128,** 9943–56.

162. Luo, Z., Zhang, Q., Oderaotoshi, Y., and Curran, D. P. (2001) Fluorous mixture synthesis: a fluorous-tagging strategy for the synthesis and separation of mixtures of organic compounds *Science* **291,** 1766–9.

163. Zhang, Q., Lu, H., Richard, C. R., and Curran, D. P. (2004) synthesis of sixteen stereoisomers of murisolin, murisolin A and 16,19-cis-murisolin by fluorous mixture synthesis *J Am Chem Soc* **126,** 36-7.

164. Zhang, Q., Rivkin, A., and Curran, D. P. (2002) Quasiracemic synthesis: concepts and implementation with a fluorous tagging strategy to make both enantiomers of pyridovericin and mappicine *J Am Chem Soc* **124,** 5774–81.

165. Curran, D. P. (2008) Fluorous tags unstick messy chemical biology problems *Science* **321,** 1645-5.

166. Ko, K.-S., Jaipuri, F. A., and Pohl, N. L. (2005) Fluorous-based carbohydrate microarrays *J Am Chem Soc* **127,** 13162-3.

167. Brittain, S. M., Ficarro, S. B., Brock, A., and Peters, E. (2005) Enrichment and analysis of peptide subsets using fluorous affinity tags and mass spectromerty *Nat Biotechnol* **23,** 463-8.

168. Sears, P., and Wong, C. H. (2001) Toward automated synthesis of oligosaccharides and glycoproteins *Science* **291,** 2344-50.

169. Guillaumie, F., Thomas, O., and Jensen, K. J. (2002) Immobilization of pectin fragments on solid supports: novel coupling by thiazolidine formation *Bioconjugate Chem* **13,** 285-94.

170. Lohse, A,, Martins, R., Jorgensen, M. R., Hindsgaul, O. (2006) Solid-phase oligosaccharide tagging (SPOT): validation on glycolipid-derived structures *Angew Chem Int Ed Engl* **45,** 4167-72.